EVALUATION OF AQUIFER STORAGE RECOVERY IN THE SANTEE LIMESTONE/BLACK MINGO AQUIFER NEAR CHARLESTON, SOUTH CAROLINA, 1993-95

By Bruce G. Campbell, Kevin J. Conlon, June E. Mirecki, *and* Matthew D. Petkewich

---

U.S. GEOLOGICAL SURVEY

Water-Resources Investigations Report 96-4283

Prepared in cooperation with the

CHARLESTON COMMISSIONERS OF PUBLIC WORKS

Columbia, South Carolina
1997

U.S. DEPARTMENT OF THE INTERIOR
BRUCE BABBITT, Secretary

U.S. GEOLOGICAL SURVEY
Gordon P. Eaton, Director

For addtional information write to:

District Chief
U.S. Geological Survey
Stephenson Center-Suite 129
720 Gracern Road
Columbia, SC 29210-7651

Copies of this report can be purchased from:

U.S. Geological Survey
Branch of Information Services
Box 25286
Denver, CO 80225-0046

CONTENTS

FIGURES

TABLES

Multiply	By	To obtain
	Length	
inch (in.)	25.4	centimeter
foot (ft)	0.3048	meter
mile (mi)	1.609	kilometer
	Area	
square foot (ft^2)	0.09290	square meter
square mile (mi^2)	2.590	square kilometer
	Volume	
gallon (gal)	3.785	liter
million gallon (Mgal)	3,785	cubic meter
	Flow	
foot per day (ft/d)	0.3048	meter per day
square foot per day (ft^2/d)	0.09290	square meter per day
gallon per minute (gal/min)	3.785	liter per minute
gallon per day (gal/d)	0.00112	acre-foot per year
	Pressure	
pounds-force per square inch (lbf/in^2)	6.895	kilopascal

Temperature: In this report, temperature is given in degrees Celsius (^oC), which can be converted to degrees Fahrenheit (^oF) by the following equation:

$$^oF = 1.8 \times (^oC) + 32$$

Sea Level: In this report, "sea level" refers to the National Geodetic Vertical Datum of 1929--a geodetic datum derived from a general adjustment of the first-order level nets of the United States and Canada, formerly called Sea Level Datum of 1929.

Chemical concentration: In this report, chemical concentration in water is expressed in metric units as milligrams per liter (mg/L) or micrograms per liter (µg/L).

Transmissivity: The standard unit for transmissivity is cubic foot per day per square foot times foot of aquifer thickness $[(ft^3/d)/ft^2]$ ft. In this report, the mathematically reduced form, foot squared per day (ft^2/d), is used for convenience.

Specific conductance is given in microsiemens per centimeter at 25 degrees Celsius (µS/cm at 25 ^oC).

ACRONYMS

ASR	aquifer storage recovery
CCPW	Charleston Commissioners of Public Works
DIC	dissolved inorganic carbon
MCL	maximum contaminant level
MODFLOW	a MODular three-dimensional finite-difference ground-water FLOW model
NETPATH	an interactive code for interpreting NET geochemical reactions from chemical and isotopic data along a flow PATH
PHREEQE	pH-REdox-EQuilibrium Equations
PVC	polyvinyl chloride
RMSE	root-mean-square-error
SL/BM	Santee Limestone/Black Mingo
SMCL	secondary maximum contaminant level
TDS	total dissolved solids
USEPA	U.S. Environmental Protection Agency
USGS	U.S. Geological Survey

Additional Abbreviations:

bls	below land surface
d	day
d^{-1}	per day
hr	hour
H	head
I	ionic strength
LPZ	lower-production zone
Ma	million years before present
mg/kg	milligram per kilogram
min	minute
mmol	millimolar
mmol/kg	millimolar per kilogram
pH	hydrogen-ion activity
Q	well discharge rate
Q_c	critical rise level
SI	saturation index
T_{col}	transmissivity along a model column
T_{row}	transmissivity along a model row
UPZ	upper-production zone
µm	micron, micrometer
>	greater than
<	less than
≤	less than or equal to

EVALUATION OF AQUIFER STORAGE RECOVERY IN THE SANTEE LIMESTONE/BLACK MINGO AQUIFER NEAR CHARLESTON, SOUTH CAROLINA, 1993-95

By Bruce G. Campbell, Kevin J. Conlon, June E. Mirecki, *and* Matthew D. Petkewich

Abstract

The feasibility of using aquifer storage recovery for storing potable drinking water for emergency use was tested in Charleston, South Carolina, during 1993-95. Thirteen injection, storage, and recovery cycles were conducted to evaluate the hydrologic and geochemical characteristics of the Tertiary Santee Limestone/Black Mingo confined aquifer. The Santee Limestone/Black Mingo aquifer at the pilot-scale aquifer storage recovery site is characterized by carbonate rock-type solution openings, fracture-dominated semiconsolidated sandstone, and interlayered crystalline limestone. The aquifer is confined by the underlying Black Creek confining unit and the overlying Santee Limestone/Black Mingo confining unit.

The pilot-scale site consisted of two wells and was designed to test the use of aquifer storage recovery technology. Treated surface water from the city of Charleston distribution system was injected into the Santee Limestone/Black Mingo aquifer, stored for various lengths of time, and recovered. Treated surface water is characterized by low ionic strength and low concentrations of dissolved ions. The native aquifer water is characterized by comparatively high ionic strength and high concentrations of chloride, sodium, bicarbonate, and sulfate. Testing at the pilot-scale site indicated that hydraulic conductivity and porosity of the aquifer increased over the duration of several aquifer storage and recovery cycles. Recovery and injection rates increased during the course of the testing indicating possible dissolution of the carbonate sediments. Two aquifer tests were completed at the pilot-scale site and the drawdown data were evaluated using analytical and numerical methods to estimate Santee Limestone/Black Mingo aquifer properties. Using analytical methods, transmissivities of 190 and 220 feet squared per day and storage coefficients of 4.0×10^{-4} and 5.5×10^{-4} were estimated. Using numerical methods, a transmissivity of 130 feet squared per day and a storage coefficient of 1.0×10^{-4} were estimated.

Geochemical model codes NETPATH and PHREEQE were used to simulate water-quality changes resulting from storage and recovery of treated surface water during aquifer storage recovery cycles 4 through 9 and 11. Geochemical reactions that influenced the treated surface-water quality included dissolution of calcite, dolomite, gypsum, halite, and amorphous silica from aquifer material, and ingassing of dissolved carbon dioxide. Mixture percentages of waters (treated surface water and Santee Limestone/Black Mingo aquifer water) withdrawn during recovery stages were estimated using PHREEQE. Groundwater samples collected early during recovery consisted of 1 to 7 percent Santee Limestone/Black Mingo aquifer water. Ground-water samples consisted of approximately 100 percent Santee Limestone/Black Mingo aquifer water following withdrawal of 80 to 90 percent of the total injected volume.

The U.S. Geological Survey modular groundwater flow model (MODFLOW) was used to simulate water-level changes at ten proposed injection sites on the Charleston, South Carolina, peninsula. The hydrogeologic framework used to design the model area was composed of two aquifers with an intervening confining unit. The modeled area corresponded to 115,000 feet by 158,000 feet and was discretized into 11,248 model cells of variable size. The ten proposed injection/recovery sites were located on public property with access to water mains. Eight observation sites were selected to monitor the changes in water levels during various simulated injection tests. The injection rates were constrained to maintain a potentiometric surface for the Santee Limestone/Black

Mingo aquifer at or below land-surface altitude of the observation sites. Simulation results indicated that a simultaneous injection rate of approximately 22 gallons per minute at each of the ten proposed injection sites did not raise the potentiometric surface of the aquifer above land surface and would allow the storage of 116 million gallons of treated surface water per year.

INTRODUCTION

Charleston, S.C., is located at the confluences of the Ashley, Cooper, and Wando Rivers near the Atlantic Ocean in the lower Atlantic Coastal Plain (fig. 1). The area is characterized by wide estuaries bordered by extensive salt marshes, typical of coastal topography of low relief. The city is vulnerable to hurricanes and coastal flooding as demonstrated in 1989 during Hurricane Hugo (Purvis, 1989). The Charleston area also is subject to earthquakes. In 1886, the city was heavily damaged by the largest earthquake to strike the eastern United States in recorded history (Bollinger, 1977). The area is also subject to occasional hard freezes, such as one in December 1989, which caused major disruptions in water-distribution service. One of the consequences of these disasters for the city of Charleston was the loss of potable water-transmission capacity, especially in the historic peninsula section of the city. This area of the city is served by aging water mains that are subject to breakage.

In 1992, the Charleston Commissioners of Public Works (CCPW) began seeking a cost-effective and location-specific method to store part of their treated surface water in the peninsula area for emergency use. The major concern of the CCPW is that demand may exceed capacity during extraordinary circumstances, such as an earthquake, for the Charleston peninsula section of their service area (fig. 1).

One possible strategy for increasing water storage capacity in this part of the city is to construct an aquifer storage recovery (ASR) system. The concept of an ASR system is to place water in short- or long-term storage by injecting it underground for later recovery and to supplement, or replace other water supplies during periods of high demand. Pyne (1995) defines aquifer storage recovery as the storage of water in a suitable aquifer through a well during times when water is available, then recovering the water from the same well when it is needed. Because ASR technology does not involve construction of above-ground storage facilities, the technology is potentially extremely cost-effective. Also, the peninsula section of Charleston is completely urbanized and bounded by water on three sides with essentially no place to construct large above-ground tanks.

The Charleston area is underlain by a number of geohydrologic units that potentially can be utilized for an ASR system (fig. 2). A series of Cretaceous aquifers are the most productive in the area. However, their depth (800 to 2,200 ft below land surface (bls)), relatively high water temperatures (up to 37 °C), and expensive well-construction costs limit their potential usefulness for an ASR system. The Santee Limestone/Black Mingo (SL/BM) aquifer contains several permeable zones that are more accessible (380 to 450 ft bls in the study area), contain water of moderately good quality and lower temperature (about 21 °C), and are suitable for inexpensive open-hole well construction. For these reasons, the SL/BM aquifer is considered the most promising for applying ASR technology.

In order to design a usable and cost-effective ASR system, a number of hydrologic and geochemical factors must be considered. Of particular importance are chemical reactions induced by the injected treated surface water that may limit the quantity or quality of water stored in the aquifer. The U.S. Geological Survey (USGS), in cooperation with CCPW designed, constructed, and tested a pilot-scale ASR system. This system was used to monitor the hydrologic and water-quality changes that were induced by the injection of treated surface water. The source of the treated surface water is primarily the Edisto

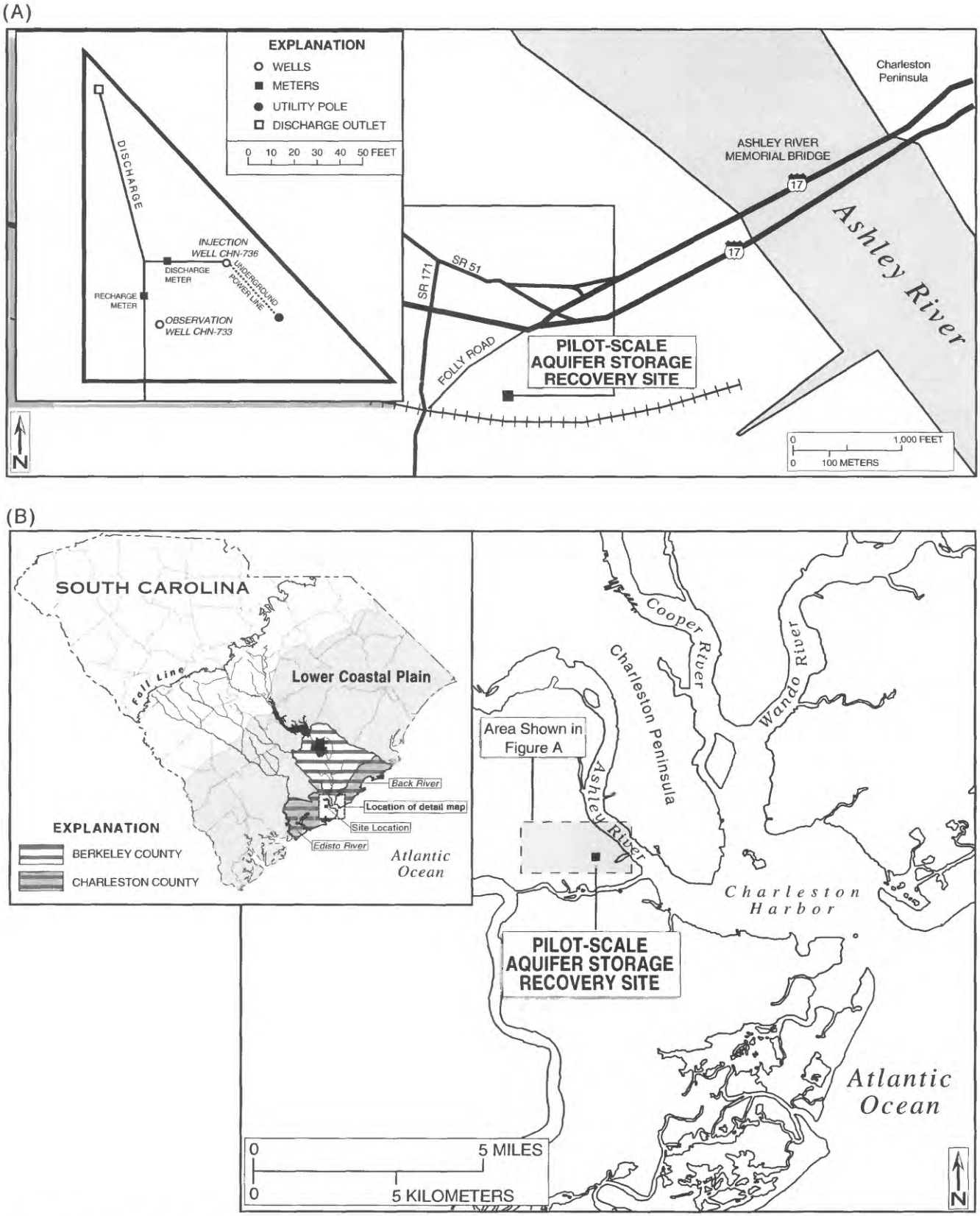

Figure 1. Study area (A) and location of pilot-scale aquifer storage recovery site (B), Charleston, South Carolina.

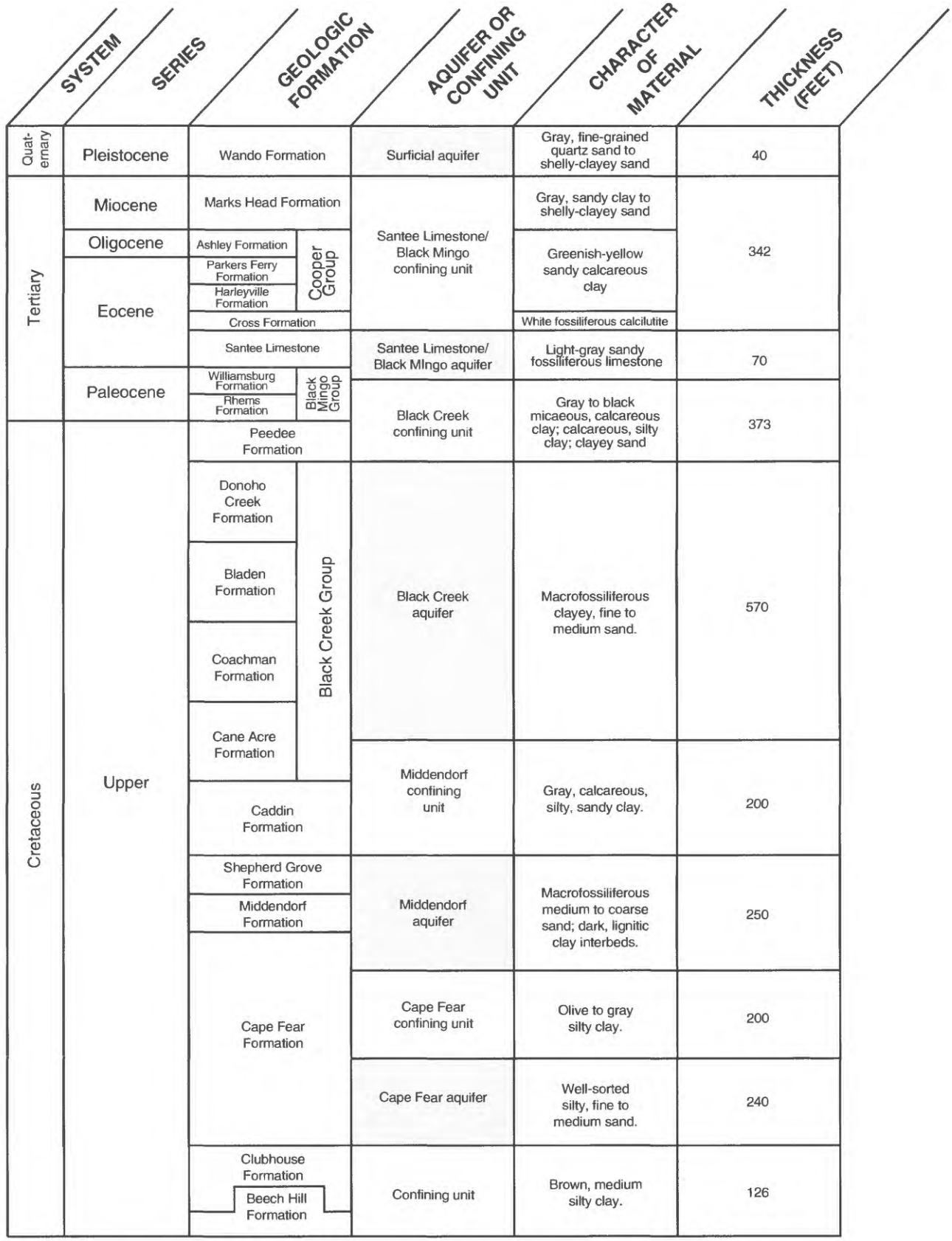

Figure 2. Generalized stratigraphic and geohydrologic column for Charleston, South Carolina.

River with the Back River serving as a secondary source of supply (Charleston Commissioners of Public Works, written commun., 1996) (fig. 1).

Purpose and Scope

This report provides a quantitative evaluation of ASR technology applied to the SL/BM aquifer at the pilot-scale site and describes the major geochemical reactions and processes and hydraulic changes that occurred during storage of treated surface water in the SL/BM aquifer and its subsequent recovery. The estimated effects of geochemical processes on stored water quality are described in terms of comparisons of stored water quality with Federal drinking water standards. The evaluation of a proposed system of ASR wells located at ten sites on the Charleston peninsula using computer simulations of ground-water flow is also described. The report also assesses the ability of the SL/BM aquifer to store large quantities of potable water for emergency use in the Charleston area.

The scope of the report includes discussions of test drilling, well installation, wireline coring, examination of the cores and geophysical logging. Continuous water-levels and specific-conductance data were collected from an observation well. Some of these data are presented in the report and all of the data is available in the USGS WATSTORE database. Water-quality samples were collected from each injection, storage, and recovery cycle and analyzed to determine major and minor cations and anions, field parameters, and dissolved gases. These data are available in the USGS database WATSTORE. Aquifer tests were conducted to estimate aquifer and confining unit hydraulic characteristics. These data are available in the USGS South Carolina District office files. Numerical models were used to estimate water-quality changes and ground-water levels. Input and output files for these models are archived in the USGS South Carolina District office. This report discusses findings made from 1993 to 1995.

Acknowledgments

The assistance of Steve Kinard, John Cook, Harry Wilson, and Pete Copleston, Charleston Commissioners of Public Works, in the collection of hydrologic data is gratefully acknowledged. Dixie Fanning, Charleston Commissioners of Public Works, provided results of chemical analyses of numerous ground-water samples. John Barton, U.S. Geological Survey, provided valuable assistance during sampling and data-collection activities at the pilot-scale site. Larry Harrelson, U.S. Geological Survey, coordinated two aquifer tests at the pilot-scale site. Clay Duffie and Melvin Bennett, Mount Pleasant Waterworks and Sewer Commission, provided geologic and hydrologic data related to the SL/BM aquifer in the Mount Pleasant area.

DATA-COLLECTION AND ANALYTICAL METHODS

The methods used to evaluate the SL/BM aquifer for potential ASR use are discussed in the following sections. Ground-water flow and geochemical modeling also are discussed.

Test-Well Installation and Sampling

A production well (CHN-736) and an observation well (CHN-733) (fig. 1) were drilled using hydraulic rotary methods at the pilot-scale site. These wells and associated equipment were used to inject treated surface water into the SL/BM aquifer and recover and monitor native ground water, and mixtures of the two waters. A continuous core was recovered from the observation well bore using wire-line coring technology. Borehole geophysical logs were collected from both wells and used to interpret the site hydrogeology. The observation well was fitted with satellite-telemetry equipment to monitor water-level stage and specific conductance at 5-min intervals at two depths within the well. Ground-water sampling

was accomplished through the use of a submersible pump in the production well and a double check-valve bailer in the observation well.

Determination of Aquifer and Confining-Unit Properties

The transmissivity and storage coefficient of the SL/BM aquifer and vertical hydraulic conductivity of the overlying confining unit were estimated using standard analytical procedures (Lohman, 1979) and the USGS Modular Groundwater Flow Model (MODFLOW) developed by McDonald and Harbaugh (1988). The model was used to derive hydraulic characteristics by calibrating a simulated SL/BM aquifer system to the results of an aquifer test at the pilot-scale site. MODFLOW was also used to estimate the lateral anisotropy of the confined SL/BM aquifer and leakage from the surficial aquifer through the overlying confining unit during pumping at the pilot-scale site.

Geochemical Sample Collection

Ground-water geochemical composition was determined during the recovery phase of ASR cycles by continuously monitoring the hydrogen-ion activity (pH), temperature, and specific conductance of ground water at the observation well (CHN-733), and by analyzing groundwater samples collected at discrete stratigraphic intervals. Down-hole profiles of specific conductance were performed prior to sampling in order to estimate the position of the permeable zones (and hence target sampling horizons) in the SL/BM aquifer. Before any ASR tests were performed, background concentrations of major and trace dissolved water-quality constituents and field parameters (pH, alkalinity, specific conductance) were measured in samples collected during the initial pumping test from the production well.

To determine water-quality changes that resulted from ASR testing, samples were collected from discrete stratigraphic intervals in the observation well using a specially designed double check-valve bailer (fig. 3). The 10-ft long bailer was constructed of 1 1/4-in. diameter polyvinyl chloride (PVC) pipe and fitted with one-way check valves at each end. The bailer was attached to a stainless-steel aircraft cable (marked in feet) and was lowered or raised within the well by a winch. To sample ground water, the bailer was lowered rapidly into the water column in the observation well. The check valves opened as the bailer was lowered and allowed the water to flow through and out of the PVC pipe. When the target depth was reached, the descent of the bailer was stopped abruptly, causing the check valves to close. The winch was then reversed and the bailer was recovered from the well with the water sample.

Ground-water samples obtained using the double check-valve bailer were split into three subsamples immediately after withdrawal from the well. The subsamples were analyzed for these constituents: 1) dissolved gases; 2) dissolved inorganic carbon (DIC), field alkalinity, dissolved chloride, and pH; and 3) major and trace dissolved constituents and nutrients.

The initial subsample was analyzed for dissolved gases, including dissolved oxygen, methane, total trihalomethanes, dissolved chlorine, and hydrogen sulfide (H_2S) during selected ASR cycles. Dissolved oxygen concentrations were measured in bailer samples using a Hach Company (1989) colorimetric method. Dissolved methane and total trihalomethane gases were analyzed using gas chromatography methods in the South Carolina District laboratory (methane) or the CCPW laboratory (total trihalomethanes). Dissolved hydrogen sulfide and chlorine gases were measured at the well head using Hach Company (1989) colorimetric methods. To permit the collection of samples containing dissolved gases, the bailer was fitted with three rubber septa located at the top, middle, and bottom of the bailer (fig. 3). These ports allowed the withdrawal of small water volumes by syringe without exposure to the atmosphere. The syringe was fitted with a 0.45-μm filter to remove suspended solids, and discharged into a pre-cleaned glass

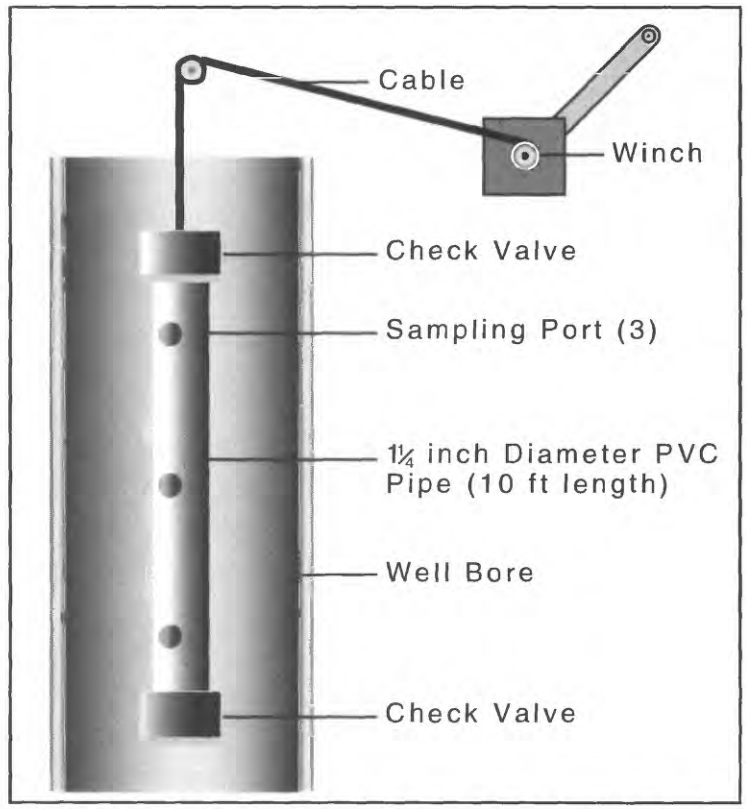

Figure 3. Construction of double check-valve bailer used to sample discrete intervals within the observation well.

vial capped with a crimped rubber septum. This procedure eliminated atmospheric contact with the ground-water sample, which would affect pH, alkalinity, DIC, and dissolved gas concentrations from samples collected at depth. The double check-valve bailer also maintained subsurface pressure conditions as the ground-water sample was brought to the surface.

The second subsample was used for field analyses of pH, specific conductance, dissolved chloride concentration, alkalinity, and laboratory analysis of DIC. Specific conductance and pH were measured using calibrated probes after the subsample was removed from the bailer. Dissolved chloride was measured in the field using Hach Company colorimetric measurements so that water quality could be compared to the secondary maximum contaminant level (SMCL) for chloride (250 mg/L) as recovery progressed. Dissolved inorganic carbonate was measured using ion chromatography methods at the South Carolina District laboratory.

The second subsample was removed from the bailer by lowering a polytetrafluoride tube into the bailer and pumping out the ground-water sample. To determine whether the bailer sampled the desired hydrostratigraphic interval in the observation well, specific conductance values measured in bailer samples were compared to specific conductance values measured at the two specific conductance probes in the observation well. If the specific conductance value of the bailer sample was within the range of the two probes in the observation well, it was retained for analysis. If the sample did not match, it was discarded and the well was resampled. If the ground-water sample passed the specific conductance screening, the third subsample was then used for analysis of major and trace dissolved constituents and nutrients. These analyses were performed using standard USGS methods at the Water Quality Laboratory in Ocala, Fla.

Geochemical and Ground-Water Flow Simulations

Geochemical model codes NETPATH (Plummer and others, 1994) and PHREEQE (pH-REdox-EQuilibrium Equations; Parkhurst and others, 1980) were used to simulate and quantify water-quality changes during the ASR tests. The NETPATH model code was used to interpret water-quality changes resulting from reactions between water and aquifer material in the production zones. NETPATH is an equilibrium geochemical model code that uses the mass-balance approach to specify reactions between initial and final wells along a flowpath. The PHREEQE model code was used to simulate mixture percentages of treated surface water and SL/BM native aquifer water during recovery cycles. PHREEQE is a speciation model code that enables calculation of mixture compositions at equilibrium using forward modeling methods; that is, using reasonable geochemical hypotheses to predict final mixture compositions from well-defined end-members.

A MODFLOW ground-water flow model was developed to evaluate the potential response in the SL/BM aquifer to injection at ten potential ASR sites on the Charleston peninsula. MODFLOW is a modular finite-difference model that simulates ground-water flow in three dimensions. Aquifer and confining unit hydraulic characteristics used in this model were obtained from the analysis of aquifer test results at the pilot-scale site. Boundary conditions used in the model were appropriate to the SL/BM aquifer on the Charleston peninsula and are described in detail later in this report.

GEOLOGIC AND HYDROGEOLOGIC FRAMEWORK

The ASR pilot-scale site is located in the lower Coastal Plain physiographic province and is underlain by Quaternary, Tertiary, and upper Cretaceous sediments with a total combined thickness of about 2,500 ft. These depositional units are composed of terrigenous and carbonate sediments that unconformably overlie Precambrian and Paleozoic basalt and Triassic-Jurassic red beds and basalts (Gohn and others, 1977). The ASR pilot study was undertaken in the SL/BM aquifer, a Tertiary-age unit of the Coastal Plain sediments. A generalized description of the Tertiary and Quaternary stratigraphy and lithology at the ASR pilot-scale site was based on a continuous core obtained during the drilling of the observation well (CHN-733) (fig. 4). The Tertiary section that occurs beneath the ASR site was subdivided on the basis of lithology, paleontology, and geophysical logs (fig. 5).

Stratigraphy

The Tertiary Black Mingo Group is composed of two upper Paleocene formations (fig. 2): the Williamsburg Formation and the underlying Rhems Formation (Sloan, 1908). The dominant lithology of the Black Mingo Group consists of interbedded sequences of greenish-gray mudstones and dark-gray to black laminated clays. At the pilot-scale ASR site, the upper 50 ft of the Williamsburg Formation consists of the following: interbedded sequences of gray, bioturbated, muddy limestones; gray mudstones and siltstones; carbonate- and silica-cemented sandstones; and white to pale-gray argillaceous sands (fig. 4). The total thickness of the Black Mingo Group penetrated at the pilot-scale site is approximately 130 ft. These sediments were deposited in inner-shelf and marginal-marine depositional environments about 55-million years before present (Ma).

The middle Eocene Santee Limestone unconformably overlies the Williamsburg Formation of the Black Mingo Group (fig. 4). The lower Eocene Fisburne Formation is not present at the pilot-scale ASR site. The Santee Limestone is a light-gray, quartz-rich moldic biosparrudite, and has a thickness of about 10 ft at the pilot-scale ASR site. The upper 5 ft is extensively bioturbated with quartz-, phosphate-, and glauconite-filled burrows. A well-defined phosphatic crust

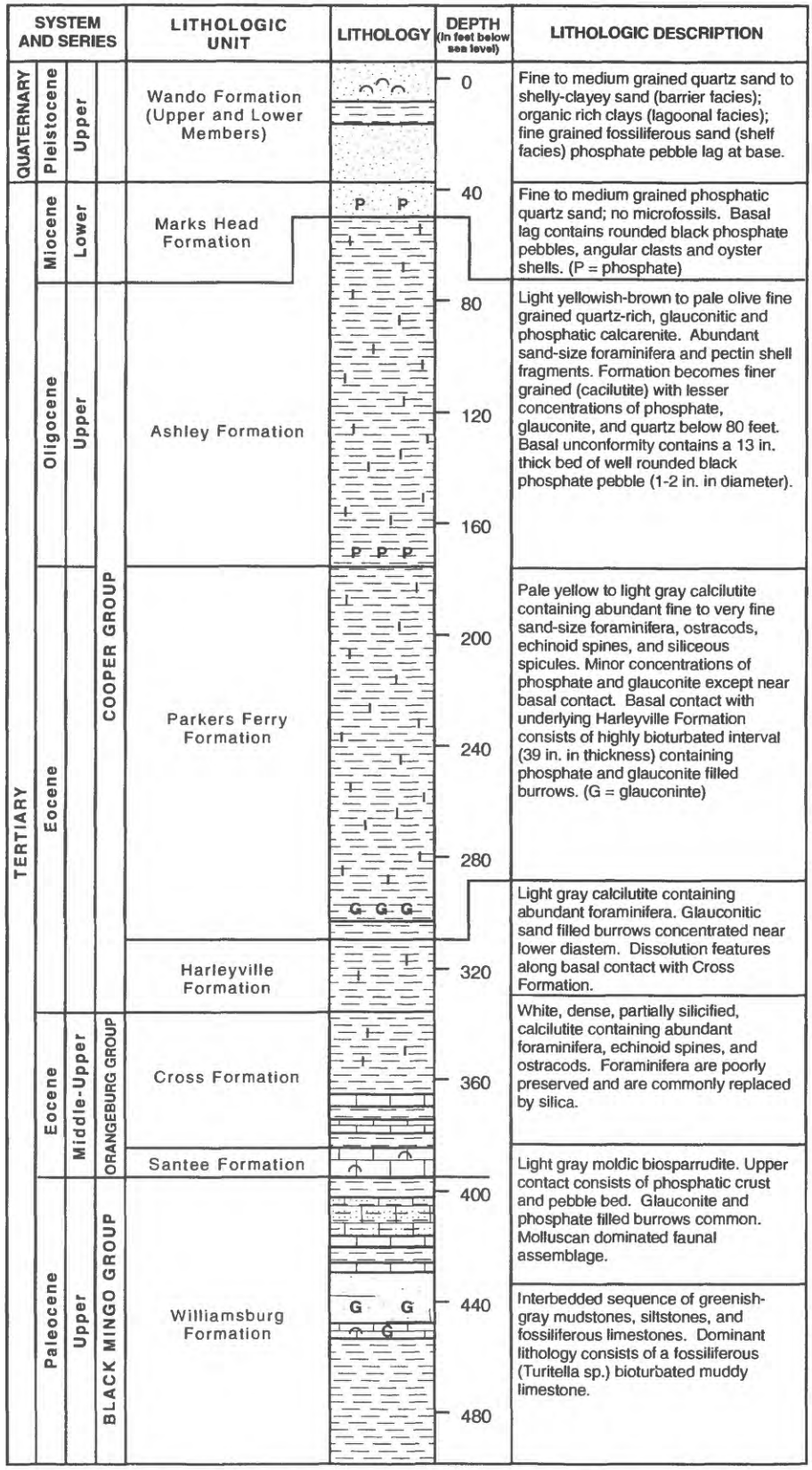

Figure 4. Lithologic log and descriptions of a core and cuttings from observation well CHN-733 at the pilot-scale aquifer storage recovery site, Charleston, South Carolina.

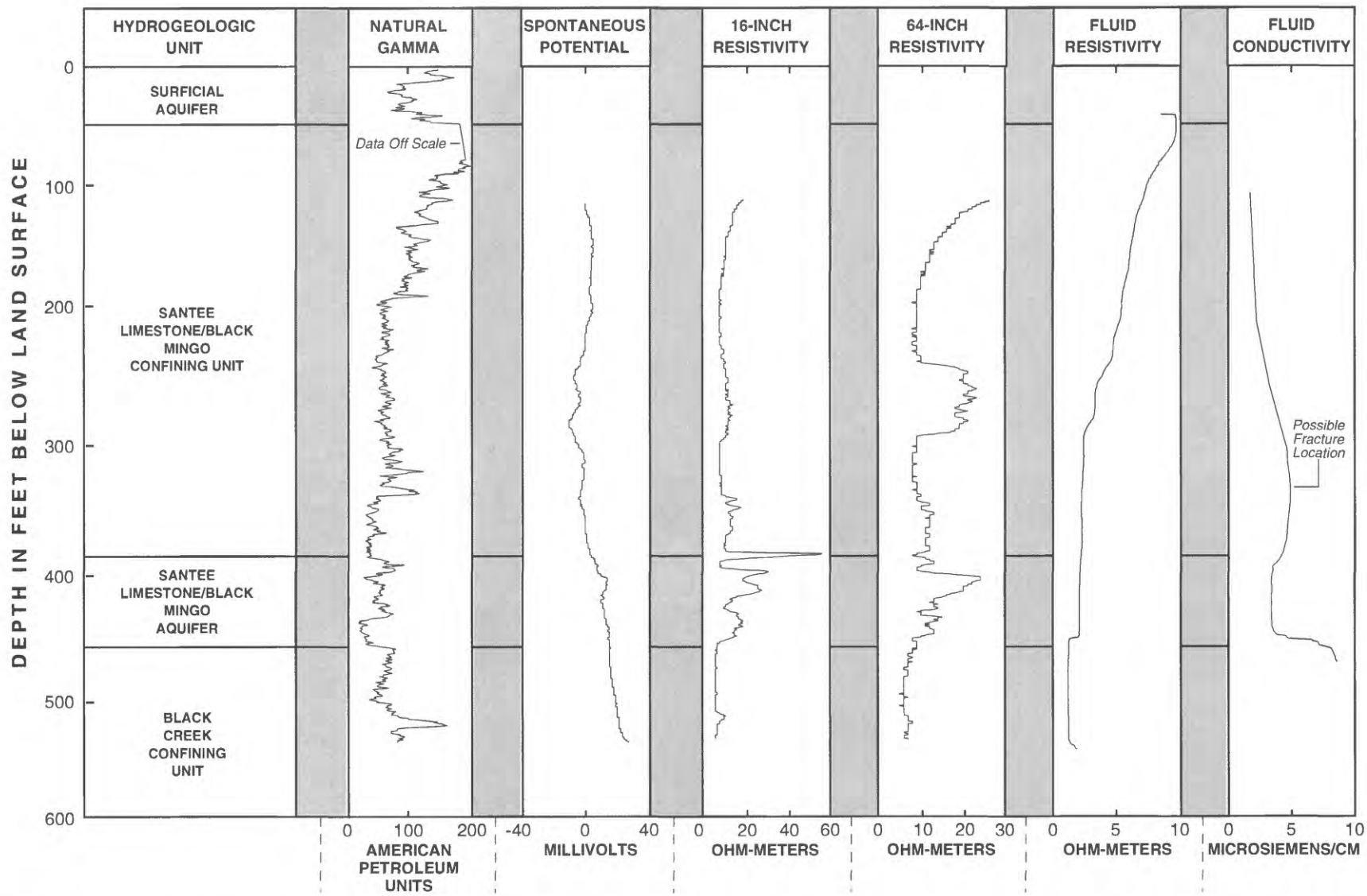

Figure 5. Geophysical logs from observation well CHN-733 at the pilot-scale aquifer storage recovery site, Charleston, South Carolina.

and pebble bed mark the contact with the overlying middle to upper Eocene Cross Formation. The Santee Limestone was deposited in a shallow, open-marine-shelf environment about 45 Ma.

The middle to upper Eocene Cross Formation (fig. 4) is a white, dense, partially silicified calcilutite containing abundant foraminifera, echinoid spines, and ostracods (Fronabarger and others, 1995). Total thickness of the Cross Formation at the pilot-scale site is approximately 50 ft. The sediments were deposited in an outer-continental-shelf environment about 41 Ma.

The Cross Formation is unconformably overlain by the Cooper Group, which consists of the Harleyville, Parkers Ferry, and Ashley Formations (fig. 4) (Ward and others, 1979; Weems and Lemon, 1984). The upper Eocene Harleyville Formation is a compact, phosphatic, light-gray calcilutite containing abundant foraminifera. The total thickness of the Harleyville Formation at the pilot-scale ASR site is approximately 16 ft. Both contacts with the underlying Cross Formation and the overlying Parkers Ferry Formation are defined by extensively bioturbated phosphate- and glauconite-filled burrows. Geophysical logs (fluid resistivity and conductivity) indicate a possible fracture located near the Cross-Harleyville formational contact (fig. 5). The upper Eocene Parkers Ferry Formation is a dense, pale yellow to light gray calcilutite containing abundant echinoid spines and sand-sized foraminifera. The total thickness of the Parkers Ferry Formation at the pilot-scale ASR site is approximately 140 ft. The Harleyville and Parkers Ferry Formations were deposited in an outer-continental-shelf environment about 38 Ma. The Parkers Ferry Formation is unconformably overlain by the upper Oligocene Ashley Formation. The unconformity is well defined by a 13-in.-thick lag deposit of well-rounded black phosphate pebbles. Lithologically, the Ashley Formation is a pale-olive, fine-grained, quartz-rich, glauconitic and phosphatic calcarenite (Fronabarger and others, 1995). Abundant sand-size foraminifera characterize this formation. The total thickness of the Ashley Formation at the pilot-scale ASR site is approximately 126 ft. The Ashley Formation was deposited in outer-continental-shelf to marginal-marine environments about 30 Ma.

The lower Miocene Marks Head Formation lies unconformably on the Ashley Formation at the ASR site. It is an olive-gray to moderate-olive brown, quartz, phosphate sand and attapulgite-rich clay (Abbott and Huddleston, 1980). Rounded, black phosphate pebbles and angular clasts define the basal contact with the underlying Ashley Formation. No microfossils are present in the unit (Fronabarger and others, 1995). The unit is about 7-ft thick at the pilot-scale ASR site and was deposited in a shallow, brackish water lagoonal environment about 18 Ma.

The upper Pleistocene Wando Formation lies unconformably on the Marks Head Formation. The Wando Formation consists of quartz sand to shell-rich, clayey sand, organic-rich clays, and fine-grained, fossiliferous sand overlying a phosphate pebble lag deposit (Fronabarger and others, 1995). The total thickness of the formation at the pilot-scale ASR site is approximately 30 ft. The Wando Formation has a complex depositional history related to late Quaternary-age sea-level changes, and is about 130,000 years old (McCartan and others, 1980; Wehmiller and Belknap, 1982).

Hydrogeology

The South Carolina Coastal Plain can be divided into a series of aquifers and confining units based on their relative permeabilities. Aucott and Speiran (1985a) describe five major Coastal Plain aquifers in the Charleston area. From youngest to oldest, they are: the surficial, Floridan, Black Creek, Middendorf, and Cape Fear aquifers (fig. 2). The surficial aquifer is composed of Quaternary unconsolidated sands of various formations. In Charleston, the Floridan aquifer occurs in the Tertiary limestones and sands of the Santee Limestone and Black Mingo Group, respectively, and has been referred to as the SL/BM aquifer in the Charleston area (Park, 1985). The SL/BM aquifer name is used in this

report. The confined Black Creek, Middendorf, and Cape Fear aquifers are composed of unconsolidated sands of within the respective Cretaceous formations (Campbell and Gohn, 1994).

The focus of this study is the Tertiary limestone and sand aquifer of the Santee Limestone and the Black Mingo Group (fig. 4). Park (1985) and Meadows (1987) indicate that the two geologic units (the Santee Limestone and the upper 100 ft of the Black Mingo Group) respond hydraulically as a single geohydrologic unit. The combined units are characterized by a significant degree of hydraulic connection and little difference in potentiometric levels. The permeable zones of the Santee Limestone and Black Mingo Group are relatively thin (approximately 70 ft) at the pilot-scale ASR site. The SL/BM aquifer is confined above by the SL/BM confining unit corresponding to the Marks Head Formation, the Cooper Group, and the Cross Formation (fig. 4). A distinct freshwater/brackish water interface occurs at the pilot-scale ASR site at approximately 440 ft bls in the SL/BM aquifer. At this interface, specific-conductance values increase from about 3,000 to 8,000 μS/cm (fig. 5). Transmissivity of the SL/BM aquifer varies regionally between 130 and 3,700 ft^2/d (Aucott and Newcome, 1986; Newcome, 1993; Park, 1985). A storage coefficient of $1.0x10^{-4}$ was reported for this aquifer in Berkeley County (Newcome, 1993).

Predevelopment flow (prior to 1960) in the SL/BM aquifer was from northwest to southeast, generally perpendicular to the coastline. Predevelopment water-level altitudes in the SL/BM aquifer in the Charleston area were approximately 25 ft above sea level. Ground-water recharge entered the aquifer at its outcrop area near Orangeburg and Lake Marion, and flowed toward the southeast (fig. 6). Large-scale development of the aquifer began during the 1960's, especially in the area approximately 20-mi northwest of Charleston (fig. 6). Water-level measurements collected in 1982 show a cone of depression in the SL/BM aquifer potentiometric surface (Aucott and Speiran, 1985b). By the early 1990's, extensive development combined with poor hydraulic characteristics resulted in large depressions in the potentiometric surface with the lowest water-level altitudes (approximately -65 ft) in southern Berkeley County. At present (1995), the regional ground-water flow direction of the SL/BM aquifer is reversed from the predevelopment flow direction in the Charleston area and is toward these cones of depression (B.L. Hockensmith, South Carolina Department of Natural Resources, Water Resources Division, written commun., 1993).

EVALUATION OF A PILOT-SCALE AQUIFER STORAGE RECOVERY SYSTEM

A pilot-scale system was designed and installed in the SL/BM aquifer to evaluate ASR feasibility. The pilot-scale ASR site is located just west of the Ashley River, approximately 2-mi west of downtown Charleston (fig. 1).

System Design

The site consists of two wells with open-hole construction: an observation well (CHN-733) and a production/injection well (CHN -736) (fig. 1 and 7). The production/injection well was cased with 10-in. diameter, black carbon steel to 107 ft bls into the Ashley Formation. The remainder of the production/injection well was constructed in two stages as a nominal 8-in. diameter open-hole to 430 ft bls and later drilled to 530 ft bls (fig. 7). After development, the well depth was 509 ft bls as a result of sediment filling the bottom of the hole during the development procedure. The well was equipped with a 10-horsepower submersible pump, which was set at approximately 200 ft bls. A 2-in. diameter, 60 ft long galvanized steel injection line was placed inside the production well to allow for injection of treated surface water. Recovered water was discharged to a sanitary sewer drain located on site. The observation well is a corehole that was drilled

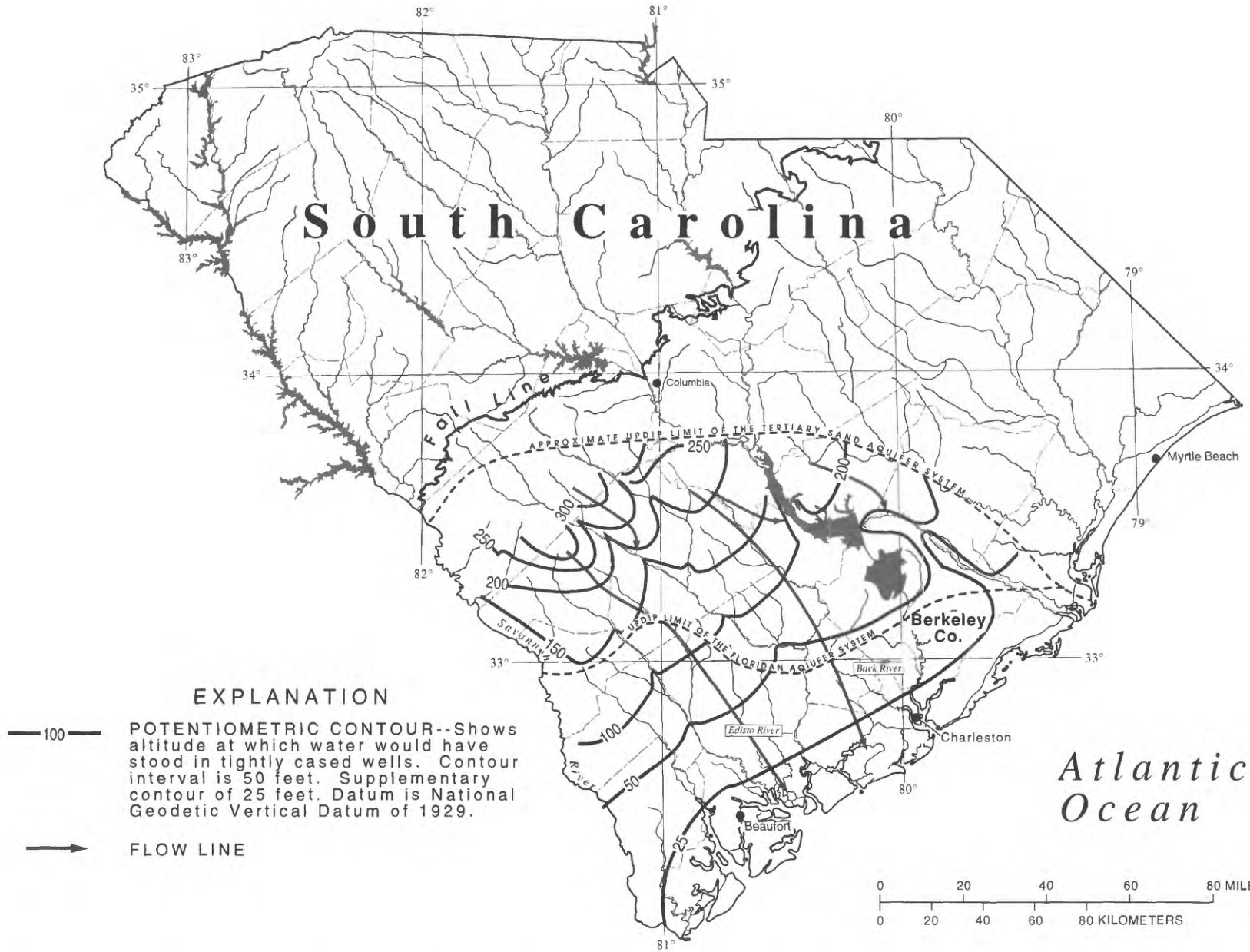

Figure 6. Potentiometric surface of the Floridan aquifer prior to development (Modified from Aucott and Speiran, 1985a).

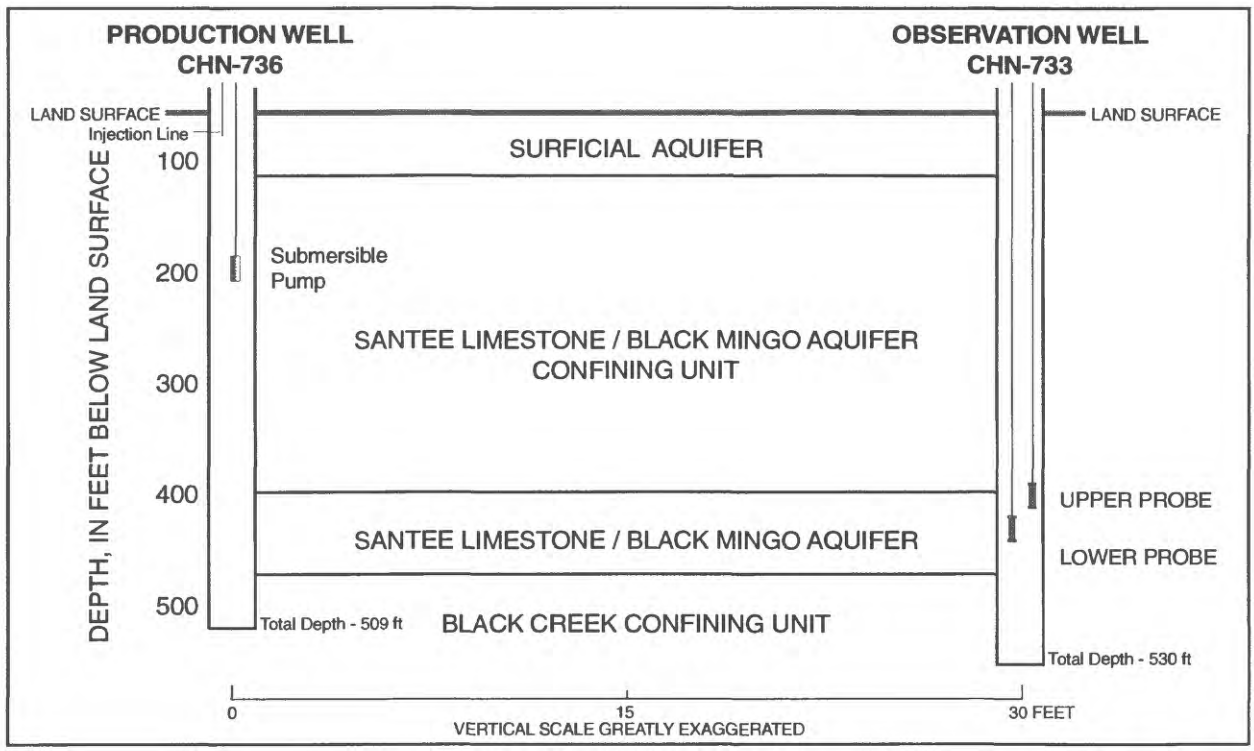

Figure 7. Diagrammatic section showing aquifer storage recovery wells and relative location of monitoring equipment, pump, and injection lines.

and sampled by wireline coring techniques to 428 ft bls and later drilled but not cored to 530 ft bls. The observation well is located approximately 30 ft south of the production well (fig. 1), and was cased with 6-in. diameter polyvinyl chloride (PVC) casing to 60 ft bls into the top of the Ashley Formation of the Cooper Group. The remainder of the well was constructed as a nominal 4.5-in. diameter open hole to 530 ft bls. The well was instrumented with a data-collection platform that recorded water levels and specific conductance at two depths at 5-min intervals. Specific conductance probes were positioned at 400- and 440 ft bls, which monitored the two primary production zones within the SL/BM aquifer at the site (fig. 7).

Water production from the SL/BM aquifer at the pilot-scale ASR site comes from two distinct permeable zones. The upper-production zone (UPZ) occurs in the Santee Limestone from 382 to 401 ft bls, and is characterized by carbonate rock-type solution openings (fig. 5). The lower-production zone (LPZ) occurs in the Black Mingo Group from 430 to 450 ft bls, and is a fracture-dominated, semiconsolidated sandstone with interlayered crystalline limestone. The lower zone is the most productive of the two, producing approximately 80 to 90 percent of the water pumped from the well.

Flow from the UPZ was measured during drilling when the production well (CHN-736) was installed initially to 430 ft bls. Development of the well at the 430-ft depth indicated a well yield of approximately 30 gal/min, which was insufficient for the pilot test. The well was later drilled to 530 ft bls, and production increased to an acceptable rate of 140 gal/min. After the production well was deepened to 530 ft bls and developed, water-level measurements were taken from the production and observation wells. The depth of the observation well was 428 ft bls at this time. The water levels in the two wells were within 1 ft, suggesting a high degree of hydraulic connection between the two zones.

Injection and Recovery Tests

Thirteen cycles of injection, storage, and recovery were conducted between June 1994 and June 1995 at the pilot-scale site. Injection rates, volumes, and recovery data for each ASR cycle are listed in appendix 1.

Injection of treated surface water raised the water level in the SL/BM aquifer from a static level of 30 to 34 ft bls (seasonal range) to the top of the well casing. The water level was held at the top of the well casing (constant head) throughout all cycles after cycle 3. Injection rates and volumes were monitored by a flow meter located on the injection line. Samples of treated surface water were collected periodically at an outlet in the injection line. Water level and specific conductance were measured continuously at the upper- and lower production zones in the observation well during all cycles. After a predetermined volume of water was injected or after a predetermined length of time, injection was terminated and the injected water was stored in the aquifer for a specified length of time. After completion of the storage period, water was recovered from the aquifer through the production well and sampled at the well head as previously described.

A typical injection, storage, and recovery cycle is illustrated by the water-level and specific conductance data collected at the observation well (CHN-733) during cycle 6 (fig. 8). Background water-level and specific conductance data were collected prior to injection. During cycle 6, background conditions are defined by the pre-test data from 0 to 600 min (fig. 8). The water-level altitude was approximately 34 ft bls and the specific conductance values were between approximately 6,000 and 7,000 µS/cm at the upper and lower specific conductance probes, respectively.

Injection of treated surface water, with a specific conductance between 155 and 190 µS/cm, began after 600 min. The water level in the observation well rose immediately to about 25 ft bls, while specific conductance values at the upper- and lower production zones declined. The injection rate decreased over time as resistance to the induced flow of treated surface water in the aquifer increased. The water level in the production well was held constant by periodically decreasing the rate of injection. Pressurizing the production well was avoided due to a casing seal failure during the third injection cycle. Specific conductance values at both probes declined to about 3,000 µS/cm during the injection phase of cycle 6 (fig. 8).

Injection ceased at about 2,000 min into cycle 6, and water levels quickly returned to about 34 ft bls (fig. 8). Treated surface water was stored in the aquifer for 24 hours in this cycle. Specific conductance values in the observation well held constant during storage at approximately 3,500 µS/cm. Recovery was initiated at approximately 3,400 min and proceeded at a rate of 140 gal/min for a duration of 390 min. The water level in the observation well declined to a maximum depth of 65 ft bls. Specific conductance values measured at the two probes changed rapidly because of several factors. A specific-conductance profile was run in the observation well approximately one hour prior to initiating recovery. This process disturbed the freshwater/brackish water interface, and resulted in values of approximately 8,500 µS/cm for about 10 min. Starting and stopping the pump also caused fluctuations in the specific conductance values possibly because of pressure waves that disturbed the vertical position of the freshwater/brackish water interface. As the production well was pumped, specific conductance values gradually increased to about 4,500 µS/cm at both probes. After 390 min, pumping at the production well stopped and water levels in the observation well recovered to 32 ft bls. Specific conductance values gradually rose as SL/BM aquifer water mixed with the treated surface water.

Recovery Efficiency

One important objective of the pilot-scale ASR tests was to determine the recovery efficiency of the system. Recovery efficiency is defined as the percentage of the water stored that

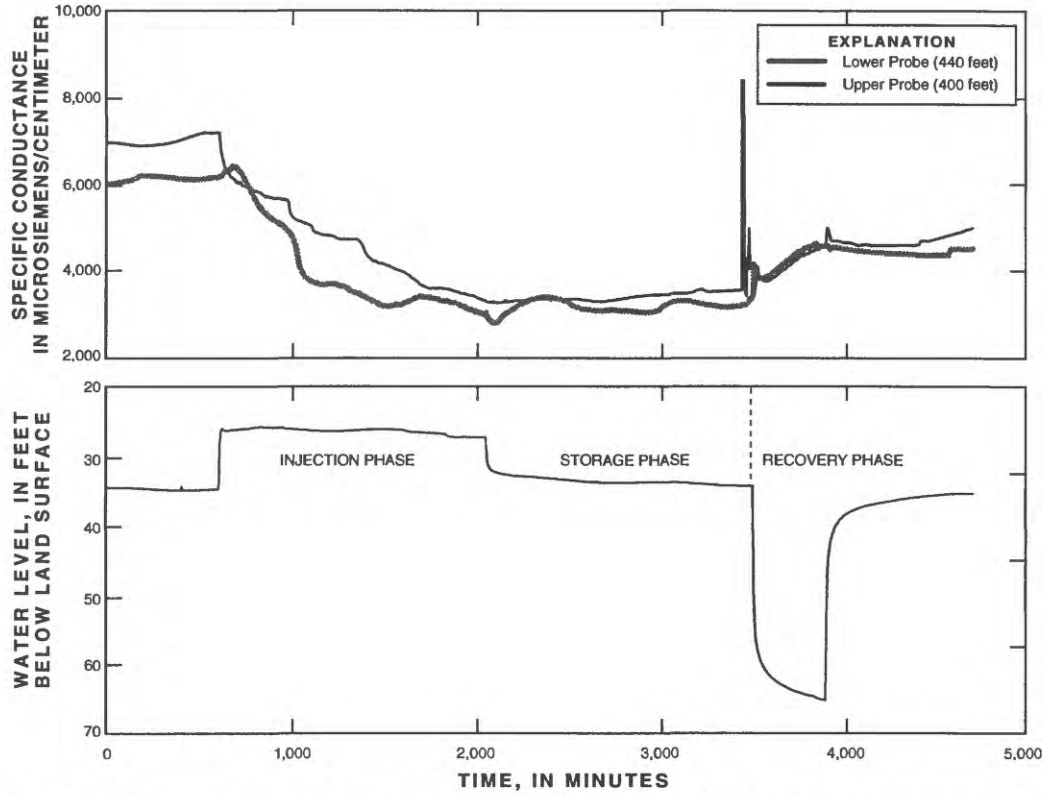

Figure 8. Injection cycle water-level and specific-conductance measurements in observation well CHN-733 during a typical injection, storage, and recovery cycle.

is subsequently recovered and meets a target water-quality criterion (Pyne, 1995). The target water-quality criterion that was used in this study is the U.S. Environmental Protection Agency (USEPA) National Drinking Water Standard, Secondary Maximum Contaminant Level (SMCL) for chloride (250 mg/L) (U.S. Environmental Protection Agency, 1988). Chloride was chosen as the best indicator of recovery efficiency, because it probably behaves conservatively in the carbonate aquifer. Also, chloride concentrations differed significantly between the treated surface water and native-aquifer water. The treated surface water originates from the Edisto River and the Back River reservoir, both sources contain low concentrations of chloride (between 8 and 15 mg/L). In contrast, the SL/BM aquifer water is brackish and contains a relatively high chloride concentration, ranging from 800 to 1,000 mg/L (appendix 2). Recovery efficiencies ranged from 38 percent during cycle 1 to 82 percent during cycle 13 (table 1).

Two types of tests were used to determine whether variations in ASR injection and recovery procedures would influence the recovery efficiency. A discharge-rate test was conducted during cycle 12 to determine whether varying the rate of discharge would increase recovery efficiency. Test 12a was conducted with a discharge rate of 158 gal/min, which resulted in a recovery efficiency of 49 percent. Test 12b was conducted with a discharge rate of 119 gal/min, which also resulted in recovery efficiency rate of 49 percent. Therefore, variation of the recovery phase discharge rate by approximately 40 gal/min had no effect on recovery efficiency at the site.

A buffer-zone test was conducted to determine whether recovery efficiency could be enhanced by creating a zone of mixed treated surface water and native aquifer water. The test was performed by injecting approximately 100,000 gal of treated surface water into the SL/BM aquifer and immediately recovering the water to the point where the SMCL for chloride was exceeded. Injection of treated surface water

Table 1. Recovery efficiencies during aquifer storage recovery cycles 1 through 13, aquifer storage recovery pilot-scale site, Charleston, South Carolina, June 1994 to June 1995

[ASR, aquifer storage recovery; gal, gallons; hr, hours; gal/min, gallons per minute]

ASR cycle number	Dates	Volume injected (gal)	Storage period (hr)	Volume of potable water recovered (gal)	Total volume recovered (gal)	Recovery efficiency (percent)	Average injection rate (gal/min)	Withdrawal rate (gal/min)
1	06/06/94 - 06/07/94	15,132	8	5,789	19,014	38	30	130
2	06/08/94 - 06/09/94	22,492	8	9,964	26,838	44	52	130
4	08/08/94 - 08/09/94	14,832	16	8,088	17,675	55	30	130
5	08/10/94 - 08/11/94	15,536	24	8,821	17,847	57	30	130
6	08/13/94 - 08/15/94	49,966	24	26,746	50,362	54	30	130
7	08/16/94 - 08/19/94	37,355	48	22,809	37,998	61	30	130
8	08/24/94 - 08/30/94	88,406	72	42,195	89,573	48	30	130
9	09/07/94 - 09/17/94	160,154	144	86,186	153,744	54	40	135
10	09/27/94 - 10/12/94	443,302	0	214,205	445,636	48	18	140
11	10/14/94 - 11/02/94	405,424	0	165,009	451,440	41	18	150
				Discharge-rate test				
12a	03/06/95 - 03/07/95	88,211	0	42,845	97,207	49	60	158
12b	03/08/95 - 03/09/95	95,130	0	46,922	105,116	49	60	119
				Buffer-zone test				
13a	03/13/95 - 03/14/95	98,795	0	48,074	50,667	49	60	160
13b	03/14/95 - 03/15/95	106,597	0	66,557	68,809	62	60	160
13c	03/15/95 - 03/17/95	101,915	0	83,768	86,761	82	60	160
13d	03/17/95 -06/02/95	1,048,120	1,488	535,038	555,038	53	60	160

was re-initiated until approximately 100,000 gal of treated surface water was injected again. This recovery-reinjection procedure was repeated three times during cycle 13 and resulted in an increase in the recovery efficiency from 49 to 82 percent. The last phase of this testing resulted in a recovery efficiency of 53 percent as a result of 1,488 hours of storage during cycle 13d.

Hydraulic Characteristics and Trends

Changes in the hydraulic characteristics of the SL/BM aquifer at the pilot-scale site were observed as testing proceeded. The hydraulic connection between the two wells at the site was improved by the injection and recovery of treated surface water. During the testing, at least a single planar preferential flowpath apparently developed between the production well and the observation well.

The changes observed during subsequent ASR tests included increasing injection rates, relatively faster breakthrough of injected water at the observation well, and changes in aquifer characteristics based on test results. Together, these observations indicated a relative increase in the permeability of the SL/BM aquifer due to the cyclic injection and recovery of treated surface water.

Increase in Injection Rates

Injection and recovery rates were increased over the course of the injection-cycle testing (table 1). The injection rates shown in table 1 are average rates for the entire injection cycle. The initial injection rate at the beginning of each injection cycle is shown in table 2. The initial rate increased from 35 gal/min in cycle 1 to 90 gal/min in cycle 12a.

During injection cycles 4 through 7 following the casing-seal failure, the injection rate was maintained at 30 gal/min. During the recovery phase of the 8th cycle, the submersible pump shut down due to a heavy influx of sediment from the aquifer. This was the first indication that the treated surface water, in conjunction with cyclic injection and recovery, was removing and suspending sediments from the aquifer interstices and possibly enhancing the aquifer permeability. After cycle 8, subsequent cycles showed an increase in injection and recovery rates. Following an aquifer test in January 1995, an initial injection rate of 90 gal/min and a recovery rate of 160 gal/min were accomplished during ASR cycles 12 and 13.

Decrease in Breakthrough Arrival Times

A second indication of increasing aquifer permeability was observed in the time required for the treated surface water injected at the production well to reach the observation well. The breakthrough of treated surface water was characterized by decreasing specific conductance measured continuously by probes set in the observation well. The initial 2,000 min of specific conductance data from four injection cycles are presented in figure 9. No clear breakthrough of treated surface water was observed in the observation well during cycles 4 and 6. Specific conductance in the well bore decreased, but did not reach the specific conductance values (155-190 µS/cm) characteristic of the treated surface water. Subsequent ASR cycles 9 and 12a show more definitive breakthrough curves. During cycles 9 and 12a, the treated surface water arrived at the observation well almost immediately, as shown by an abrupt decrease in specific conductance (fig. 9).

The gradual decrease in the specific conductance was caused by the arrival of the mixture of treated surface water and native ground water at the observation well during injection cycles 4 and 6. During cycle 12a, the specific conductance recorded in the observation well late in the test are the same as those of the treated surface water. These data indicated that a preferential pathway possibly had developed during the cyclical testing. This pathway from the observation well to the production well had been subsequently enlarged during later ASR cycles to allow increasingly larger volumes of water to move at a faster

Table 2. Initial injection rates for aquifer storage recovery cycles 1, 4, 9, and 12 at well CHN-736, Charleston, South Carolina

[gal/min, gallons per minute]

Date	Cycle number	Initial injection rate (gal/min)	Recovery rate (gal/min)
June 6, 1994	1	35	130
August 8, 1994	4	38	130
September 7, 1994	9	51	135
March 6, 1995	12a	90	158

rate. In all likelihood, other ground-water flow pathways away from the production well but not intersecting the observation well also were enlarged.

Aquifer-Test Variation

A third indication of increasing aquifer permeability was observed in drawdown and recovery data from two aquifer tests conducted using the wells at the ASR pilot-scale site (fig. 10). An initial aquifer test was performed in May 1994, prior to the first injection. The maximum drawdown observed was 122.8 ft in the production well and 34.2 ft in the observation well. A second test was conducted in January 1995, after the completion of 11 injection and recovery cycles during which approximately 1.25 Mgal of treated surface water had been injected into the aquifer and recovered through the production well. The maximum drawdown in the production and observation well during the January 1995 test was 80.3 ft and 46.6 ft, respectively.

The total drawdown in the production well was less for the second test when compared to the first, even with a higher discharge rate (140 gal/min in May 1994 compared to 160 gal/min in January 1995). The shape of the drawdown curve also differed between the first and second tests. This difference in shape is reflected in the observation well drawdown curves. There is more drawdown in the observation well in January 1995 test than in the May 1994 test. An explanation of this is presented in Freeze and Cherry (1979, p. 320, fig. 8.6) where two aquifers are described: a relatively low transmissivity aquifer and a relatively high transmissivity aquifer and their associated drawdown cones. An observation well located at the same distance from the pumping well, in this case, would experience more drawdown in the high transmissivity aquifer than the low transmissivity aquifer. This is due to the overall difference in the shape of the cone of depression. A similar situation could have developed during the injection and recovery cycles at the pilot-scale ASR site.

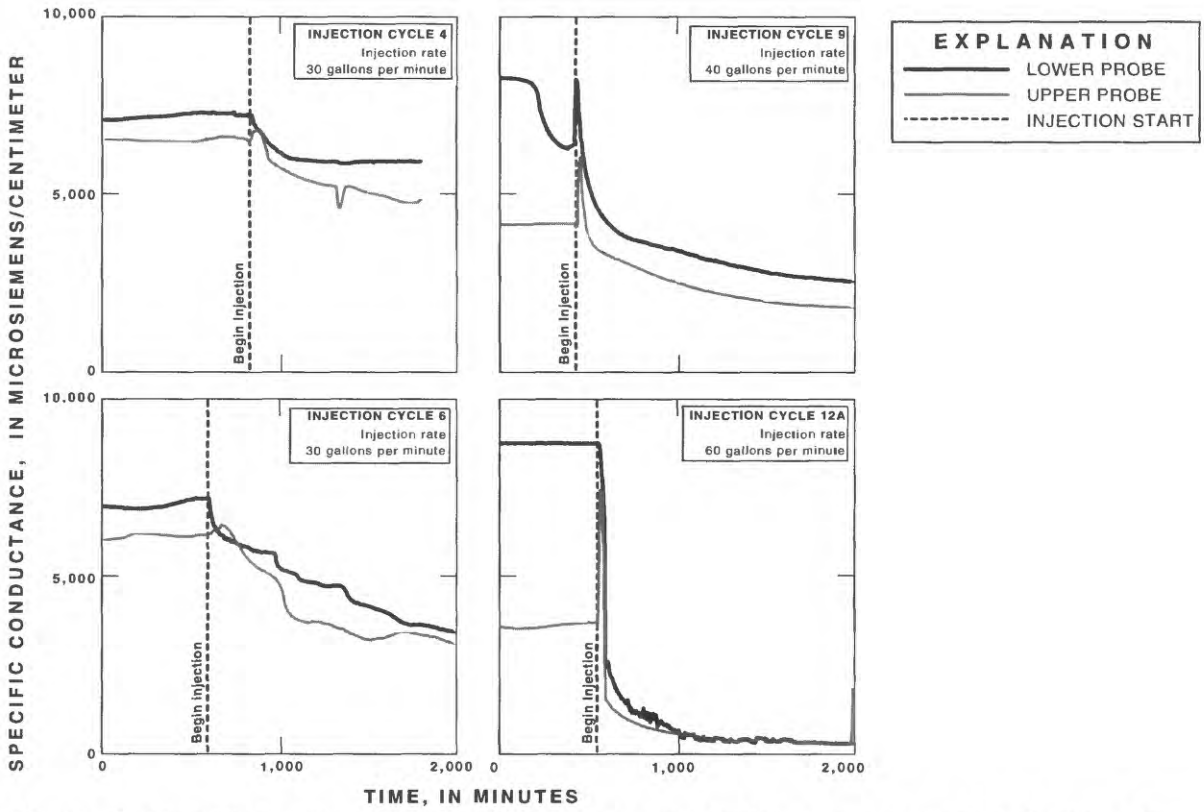

Figure 9. Specific conductance breakthrough curves for injection cycles 4, 6, 9, and 12a at observation well CHN-733.

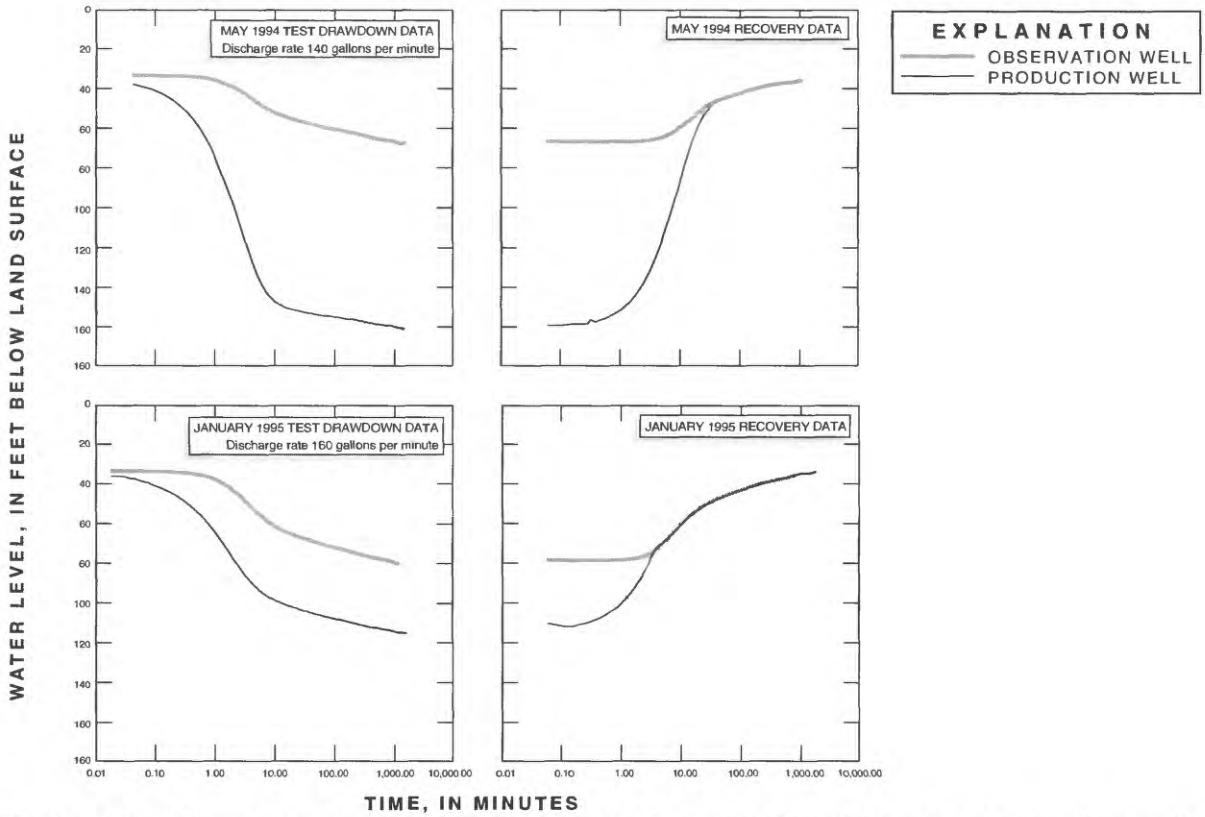

Figure 10. Drawdown and recovery at production well CHN-736 and observation well CHN-733 during two aquifer tests.

A relatively large amount of leakage at 10 min into the drawdown phase of each test was noted during each test. The rate of leakage was enough to cause a subsequent decrease in the rate of drawdown in the wells due to pumping (fig. 10).

Aquifer-Test Analysis

The SL/BM aquifer was tested to estimate hydraulic characteristics at the pilot-scale ASR site. Two aquifer tests were completed and the drawdown and recovery data were evaluated using both analytical and numerical methods. The numerical approach was used to corroborate the analytical results and to aid in the development of a MODFLOW ground-water flow model used to predict aquifer water levels resulting from several ASR scenarios at ten simulated production wells located on the Charleston peninsula.

The aquifer tests were completed at the pilot-scale ASR site in May 1994 and January 1995. The tests consisted of pumping production well CHN-736 at a constant rate, while measuring the drawdown in this well and at observation well CHN-733 using pressure transducers and a data logger. Average pumping rates were 140 and 160 gal/min for the May 1994 and January 1995 aquifer tests, respectively. Water-level data representing background and recovery conditions also were collected.

Analytical results for the May 1994 and January 1995 aquifer tests were obtained using type curves to match the drawdown data for both tests. Initially, analysis of the aquifer-test results was attempted using the Theis method (Lohman, 1979); however, a complete solution was not possible because of the early occurrence of leakage during the two aquifer tests. The Theis method assumes that the confining beds are impermeable and will not transmit water into or out of the confined aquifer. Because leakage into the SL/BM aquifer was evident, aquifer-test results were analyzed using the Hantush-Jacob method for non-steady radial flow in an infinite, leaky confined aquifer (Lohman, 1979). The analytical results for the May 1994 and January 1995 tests agreed closely (table 3). Additionally, the aquifer-test results were analyzed to determine if the source of leakage was from water in storage in one or more of the confining beds using the Hantush modified method (Lohman, 1979). Aquifer-test results did not match the type curves for this method.

The numerical approach consisted of calibrating a quasi-three-dimensional ground-water flow model to the aquifer-test data and simulating an injection, storage, and recovery test to verify calibration. A sensitivity analysis was completed on the calibrated model to determine which input parameters most substantially affected model results.

The USGS three-dimensional, modular, ground-water flow model MODFLOW (McDonald and Harbaugh, 1988) was used to simulate the January 1995 aquifer test. The calibrated model consisted of 2 layers discretized using a variably spaced grid of 9,025 cells over an area of 40,000 ft by 40,000 ft (fig. 11). The model simulated two aquifers: an unconfined surficial aquifer and a deep, confined aquifer separated by a thick, leaky confining unit. The confining unit was not simulated as an active layer, but was modeled using a vertical conductance array between the two aquifers. The top layer of the model corresponded to the surficial aquifer and was assigned a uniform saturated thickness of 40 ft (fig. 11). The conductance array represented the SL/BM confining unit and conductance values assigned to the array were based on a uniform thickness of 342-ft. Ground water in the model was allowed to flow vertically between the two aquifers based on the values of the conductance array and the head distributions assigned to the two layers. The lower layer of the model represented the 70-ft thick SL/BM aquifer at the pilot-scale ASR site.

The model grid was highly discretized in the vicinity of the production and observation wells and was less discretized near the boundaries (fig. 11). The grid was developed to enhance model accuracy by placing more cells in the area

Table 3. Analytical and numerical estimates of the hydraulic characteristics of the Santee Limestone/ Black Mingo aquifer and overlying confining unit, based on the results of the May 1994 and January 1995 aquifer tests, Charleston, South Carolina

[d^{-1}, per day; --, data not available; ft/d, foot per day; ft^{-1}, per foot; ft^2/d, foot squared per day; T_{col}, transmissivity along a model column; T_{row}, transmissivity along a model row]

Property	Analytical results		Numerical results
	May 1994	January 1995	January 1995
Confining unit leakance in d^{-1}	0.04	0.03	--
Confining unit vertical hydraulic conductivity in ft/d	--	--	$5.0x10^{-4}$
Confining unit vertical hydraulic conductivity directly above the production well in ft/d	--	--	10,000
Confining unit specific storage in ft^{-1}	--	--	$5.0x10^{-6}$
Confined aquifer transmissivity in ft^2/d	220	190	130
Confined aquifer storage coefficient	$5.5x10^{-4}$	$4.0x10^{-4}$	$1.0x10^{-4}$
Confined aquifer horizontal anisotropy (T_{col}/T_{row})	--	--	15

where the head changes were the greatest; specifically, near the production well where water was pumped from the lower layer. Model cells in the highly discretized zone were square and corresponded to areas ranging between 1 and 2.25 ft^2. This zone was centered on the production well and extended out radially 30 ft to the observation well. The square cells outside the highly discretized zone gradually increased in size to a maximum side length of 5,920 ft and an area of 1.26 mi^2.

Simulation of ground-water flow requires that the aquifers be enclosed by boundaries that correspond to hydrogeologic features where some characteristic of ground-water flow is defined. The boundaries also may be selected at a distance far enough from the area of interest so that the choice of boundary conditions does not influence the model results. Accordingly, specified-head conditions were assigned to the surficial aquifer and no-flow conditions were assigned along the lateral boundaries and base of the SL/BM aquifer (base of lower layer). The lateral no-flow boundary conditions were assigned at distances far enough from the area of interest to minimize or eliminate any boundary effects on simulation results. Initial head (H) conditions of H = -33.38 ft were assigned to all cells representing the surficial and SL/BM aquifers. These initial-head conditions were equal to the average of the water levels observed in the production and observation wells immediately prior to the January 1995 aquifer test. By assigning equal initial head arrays to both layers, all simulated changes in head can be attributed to the aquifer test.

The ground-water flow model was calibrated to the drawdown and recovery water levels observed during the January 1995 aquifer test using 52 variably spaced time steps and reasonable hydraulic characteristics for the simulated SL/BM aquifer and confining unit. The individual time steps were spaced so that most of the time

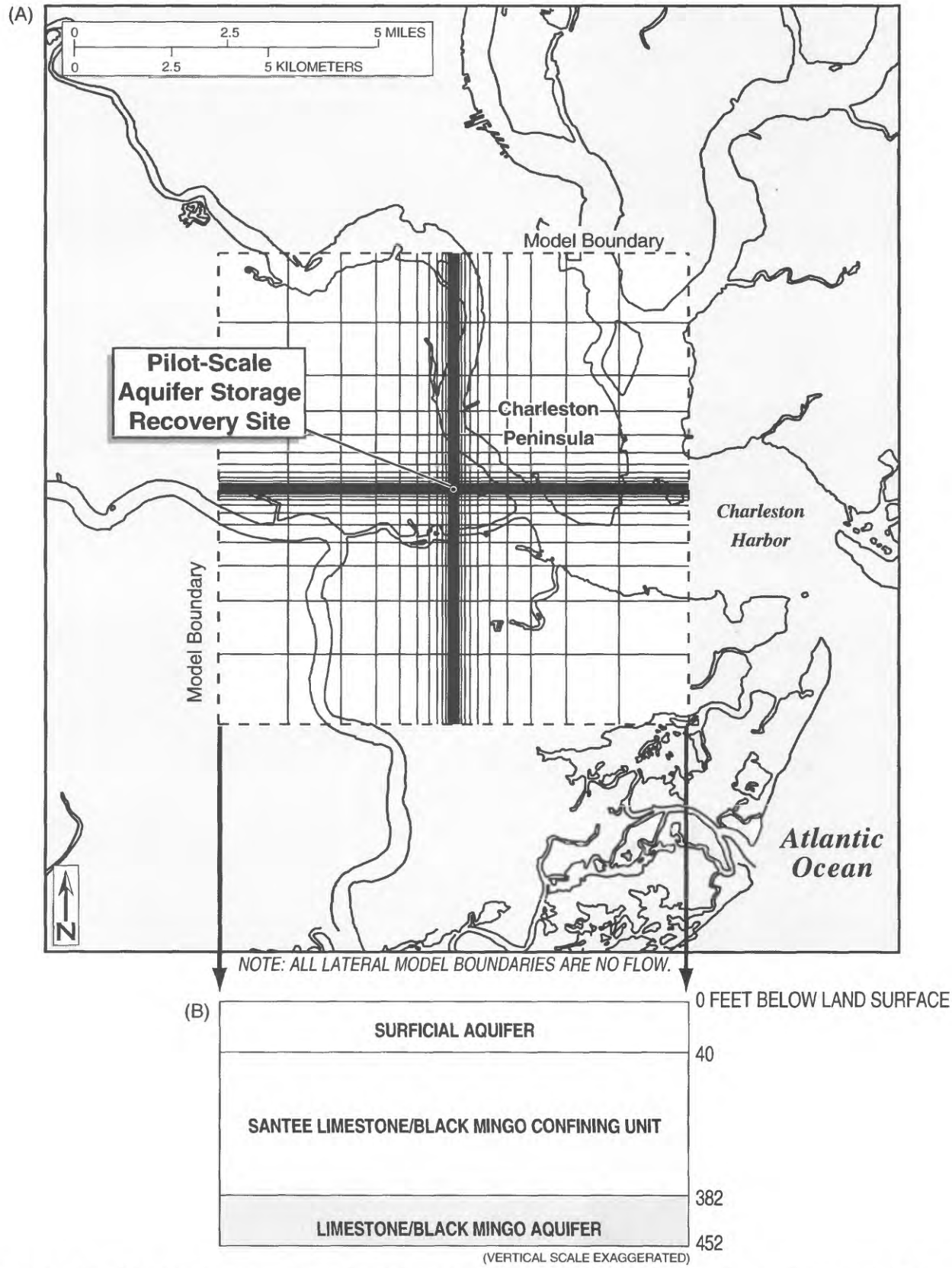

Figure 11. Grid design, location of model boundaries, (A) and vertical descretization (B) of the ground-water flow model used to analyze the January 1995 aquifer test, pilot-scale aquifer storage recovery site, Charleston, South Carolina.

steps occurred early in the simulation during the period of the greatest water-level changes. Initially, all cells in the SL/BM model layer were assigned hydraulic characteristics equal to those determined analytically. The calibration strategy was designed to compare the simulated and observed January 1995 test water levels at the production and observation wells. The hydraulic characteristics of the model layers and the SL/BM confining unit were adjusted by trial and error such that simulation results and observed test water levels agreed as closely as possible. Because of the lack of data that could be used to describe the spatial variability of aquifer and confining unit hydraulic characteristics, any adjustments to hydrologic properties were made uniformly across the model layers. The model was considered calibrated when the simulated water levels at the production and observation wells approximated the observed test water levels (fig. 12). Hydraulic characteristics of the SL/BM aquifer model layer and overlying confining unit determined from model calibration are listed in table 3.

The calibrated ground-water flow model required lower values of transmissivity and storage coefficient than those determined analytically, a high degree of anisotropy in the confined SL/BM aquifer, and a non-uniform SL/BM confining unit vertical hydraulic conductivity (table 3). Simulation was accomplished using the transient-leakage package (Leake and others, 1994) to match the observed drawdown and recovery water levels. Although the model values for transmissivity and storage coefficient are lower than those determined analytically, the values are within the same order of magnitude as the analytical values and compare well to values previously reported for the SL/BM aquifer (Newcome, 1993; Park, 1985). The model required a lateral anisotropy factor (T_{col}/T_{row}) of 15 to match the observed water levels. This high degree of anisotropy could be the result of preferential flow along fractures or solution channels in the Santee Limestone, which happen to intersect the bore of the observation and/or production wells. Model simulations using a lower value of lateral anisotropy required unreasonable values of SL/BM aquifer transmissivity and storage coefficient to match the observed test water levels.

Successful simulation of the January 1995 aquifer test required transient leakage from storage in the SL/BM confining unit. Although analytical results suggested that leakage from confining unit storage was not occurring during the two aquifer tests, accurate simulation results could not be achieved using reasonable values of transmissivity and storage coefficient by simply using the vertical conductance array between the two model layers to control vertical leakage. Simulations that used only the vertical conductance array and did match the observed water levels during the January 1995 aquifer test also required a storage coefficient at least an order of magnitude less than the value determined analytically.

Accurate simulation results also required that a non-uniform vertical hydraulic conductivity distribution be assigned to the SL/BM confining unit. The calibrated model used a vertical hydraulic conductivity of 10,000 ft/d for the portion of the confining unit directly above the production well and a value of 5.0×10^{-4} ft/d above all other cells. This distribution of vertical hydraulic conductivity simulated a confined aquifer that received abundant leakage at the production well, indicating that substantial leakage may have occurred in the vicinity of the production well during the tests. The necessity of simulating increased leakage at the production well to match the observed water levels may be the result of simulating leakage from only one confining unit when other sources of leakage are possible. The leakage observed during the aquifer tests may, by various degrees, result from the SL/BM confining unit, clay interbeds located within the SL/BM aquifer, the Black Creek confining unit, or possibly from a fracture located in the SL/BM confining unit that intersects the open-hole portion of the production well (fig. 5).

The simulated potentiometric response at the lateral model boundaries was evaluated to determine if the assumption of no-flow conditions

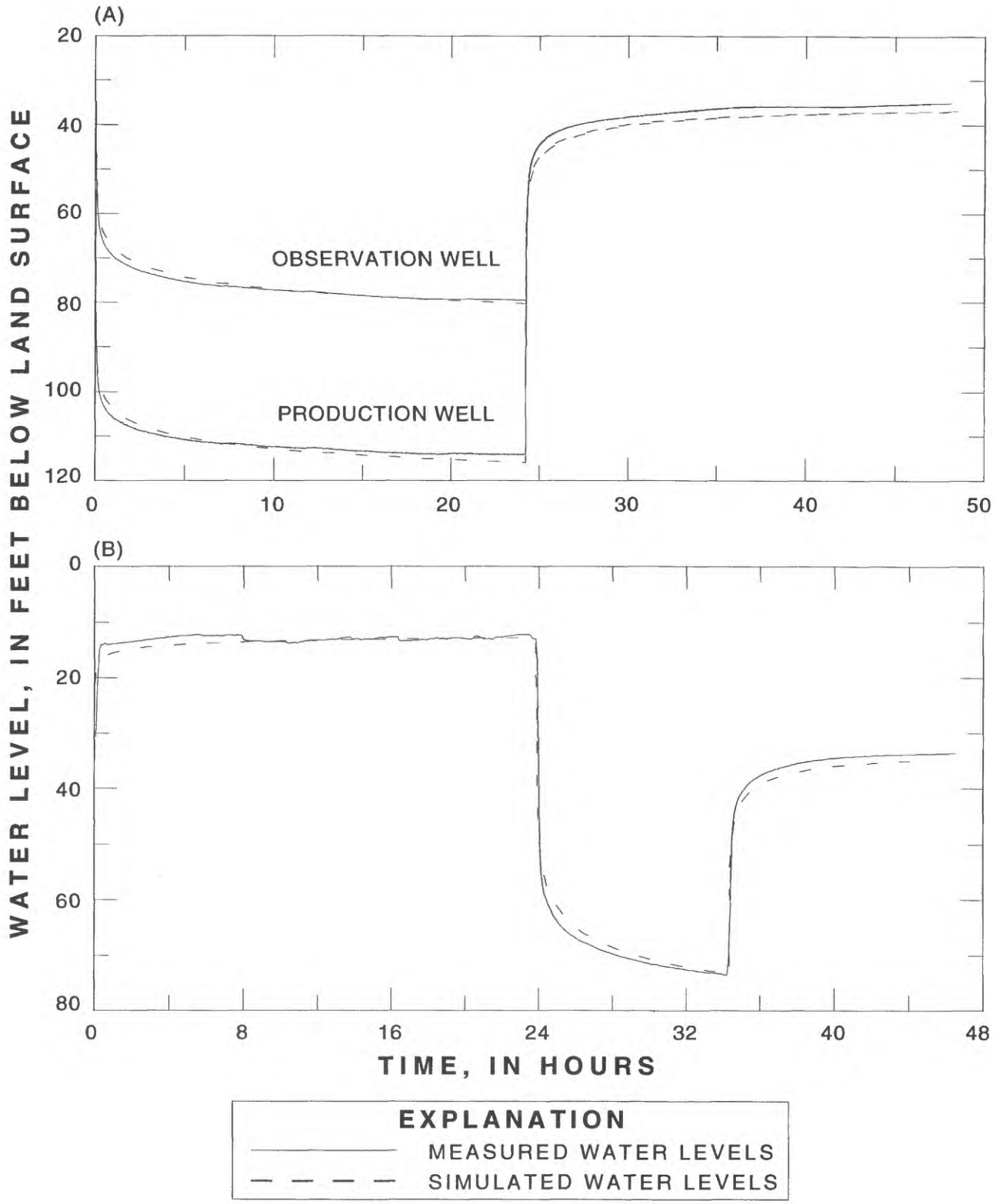

Figure 12. Simulated and measured water levels in production well CHN-736 and observation well CHN-733 during the January 1995 aquifer test (A) and in the observation well during aquifer storage recovery cycle 12 (B) at the pilot-scale aquifer storage recovery site, Charleston, South Carolina.

assigned to the boundaries of the SL/BM aquifer model was appropriate. A maximum simulated head difference of 0.22 ft was produced at the center of the northern and southern model boundaries at the end of the aquifer test. This small response over a model distance of 5,210 ft (the distance between the centers of the last two cells in a row or column) confirmed that no-flow boundaries did not adversely influence the calibrated model results.

Simulated water levels did not accurately match the early drawdown data during the January 1995 aquifer test. Early drawdown represents, in part, the removal of water stored in the well casing and borehole. Because the calibrated model did not actively simulate borehole conditions and instead simulated the removal of all water through the production well directly from the SL/BM aquifer, the model overpredicted drawdown during this early time period. This casing-storage response restricts the use of the first 8 min of aquifer-test drawdown for numerical model calibration. This time interval was estimated by calculating the time required to remove one casing volume of water from the production well at a rate of 160 gal/min.

To determine the level of accuracy of the calibrated model, the simulated water levels were statistically compared to the observed test water levels observed at both wells. Statistical data were compiled for the 20 time steps that simulated the final 1,444 min of the aquifer test. For each time step, the residual or difference between the simulated and observed water level was determined, and the root-mean-square-error (RMSE) of the residuals was calculated for both wells. The RMSE is the square root of the average sum of squares of the residuals, and was calculated using the formula:

$$\mathrm{RMSE} = \sqrt{\frac{1}{N}\sum_{i=1}^{N}(h_s - h_o)^2}, \qquad (1)$$

where

N is the number of residuals;

h_s is the simulated water-level altitude at the center of the cell where the production or observation well is located; and

h_o is the observed water-level altitude in the production or observation well.

The RMSE values determined for the production and observation wells were 1.72 and 1.53 ft, respectively. Because the RMSE value represents the simulation error (at the production and observation wells), lower RMSE values correspond to a more accurate simulation. These low RMSE values indicate that the model adequately simulated the SL/BM aquifer response during the January 1995 aquifer test.

A volumetric budget for the simulation of the drawdown phase of the January 1995 aquifer test is presented in table 4. The table lists, for each designated time step, the volumetric flow rates of water that are exchanged within the model through confining bed storage, constant head leakage, storage, or well discharge. These rates represent the volume of water that each flow component contributed to the overall budget during the listed time step. An average volumetric flow rate for the entire drawdown phase of the test was calculated for each flow component based on cumulative volumes at the end of the last time step and is listed at the bottom of table 4. Budget results indicate that storage in the SL/BM aquifer is the major source of water for discharge at the production well. By the latter part of the test, however, the percentage of water removed from storage in the SL/BM aquifer was decreasing at approximately the same rate that the percentage of water from confining bed storage was increasing. The table also lists the exchange rates of water in the cell where the production well is located. Budget results indicate that almost all constant head leakage from the surficial aquifer to the SL/BM aquifer was exchanged at the production well cell.

Table 4. Simulated volumetric budget for the drawdown phase of the January 1995 aquifer test, Charleston, South Carolina

[All units are in cubic feet per day (ft^3/d), except where noted]

Time step	Total time, hours	INFLOW					OUTFLOW			
		Confining bed storage[1]		Constant head leakage		Aquifer storage	Confining bed storage	Constant head leakage	Aquifer storage	Well discharge[2]
		Total	Cell above production well	Total	Cell above production well					
19	0.004	63	(25)	1,357	(1,357)	29,390	1	1	643	30,800
22	0.009	87	(11)	1,466	(1,466)	29,298	<1	<1	351	30,800
25	0.020	170	(5)	1,570	(1,570)	29,155	<1	2	12	30,800
28	0.045	348	(2)	1,673	(1,673)	28,818	1	<1	167	30,800
31	0.098	717	(1)	1,773	(1,773)	28,329	<1	<1	91	30,800
34	0.22	1,406		1,872	(1,871)	27,550	2	<1	2	30,800
37	0.47	2,477		1,967	(1,967)	26,374	<1	1	<1	30,800
40	1.04	3,654		2,062	(2,061)	25,090	0	1	0	30,800
43	2.29	4,534		2,157	(2,156)	24,110	<1	<1	0	30,800
46	5.02	5,546		2,251	(2,249)	23,003	<1	<1	0	30,800
49	11.03	7,430		2,341	(2,337)	21,029	<1	0	0	30,800
52	24.24	10,544		2,423	(2,415)	17,832	<1	0	0	30,800
Average		7,851	(<1)	2,327	(2,322)	20,623	<1	<1	1	30,800

[1]Number in parentheses () represents the volumetric flow rate at the model cell where the production well is located. The absence of parentheses indicates that the contribution of water to or from the production-well cell is insignificant for the given time step.

[2]All well discharge was from the production-well cell.

Analysis of the volumetric budget produced by the simulation of the January 1995 aquifer test (table 4) indicates the necessity of modeling transient leakage to accurately simulate test results. At the end of this simulation, approximately 34 percent of the water discharging to the production well was contributed from confining bed storage. Although this rate changed over time; for the last 12 time steps (approximately 23 hours of the test), the rate of water entering the SL/BM aquifer from confining bed storage steadily increased from 12 (3,654 ft^3/d) to 34 (10,544 ft^3/d) percent of total water discharged from the production well (30,800 ft^3/d). Minor differences in mass balance between rates of inflow and outflow at specific time steps are the result of numerical approximations used in model calculations and minor contributions to aquifer storage.

A sensitivity analysis was completed to evaluate the relative influence of calibrated model array parameters on model results (table 5). Residuals for the production and observation wells were calculated after increasing or decreasing the calibrated value of a specified model parameter by a small amount. High RMSE values indicated that the model simulations were sensitive to the model parameter, whereas low RMSE values indicated model insensitivity.

The sensitivity analysis indicated that model simulations were most sensitive to changes in the transmissivity, storage coefficient, and anisotropy of the SL/BM aquifer. The model results were moderately sensitive to the vertical hydraulic conductivity of the confining unit directly above the production well. The sensitivity analysis also indicated that model results were not very sensitive to changes in vertical hydraulic conductivity or specific storage of the SL/BM confining unit or to the initial head conditions assigned to the surficial aquifer. The most sensitive calibration parameter in the model was transmissivity of the SL/BM aquifer.

The injection and withdrawal test (cycle 12) that followed the January 1995 aquifer test was simulated using the calibrated model to further confirm model calibration. Data from cycle 12 consist of a continuous record of water levels measured in the observation well during the test, and injection/withdrawal rates and volumes measured during the test. Continuous water levels were not recorded in the production well during this test. During the injection phase of this test, the water level in the SL/BM aquifer was increased 34.61 ft (from 33.04 ft below to 1.57 ft above land surface) and held constant at the well head for 24 hours. After the injection phase, water was withdrawn from the production well at a rate of 155 gal/min. Recovery of the water level in the observation well to static pre-test conditions also was recorded during this test.

The injection, withdrawal, and recovery phases of cycle 12 were simulated using the hydraulic characteristic arrays from the calibrated aquifer test model, 52 variably spaced time steps for each phase of the test, and initial head conditions measured prior to the test. A 5-minute storage phase was simulated following the injection phase using 26 time steps. This amount of time was required in the field to stop injection and begin withdrawal. The initial heads assigned to the confined aquifer were those observed at the observation well immediately preceding this test. The injection phase of the ASR cycle was simulated by establishing specified head conditions (H = 1.57 ft above land surface) at the model cell where the production well was located. The withdrawal phase used the well package of MODFLOW to simulate removal of water from the SL/BM aquifer at 155 gal/min. The recovery phase of the ASR cycle was simulated by removing the stress of pumping at the production well.

Simulated water levels approximated the observed water levels for all phases of ASR cycle 12 (fig. 12). Discrepancies between the simulated and observed water levels during the injection phase were due to injection-rate corrections made in the field to bring the water level in the production well up to the well head. Discrepancies during the withdrawal cycle may be due, in part, to the simulation of withdrawal using a constant rate when variable rates were measured in the field.

Table 5. Results of model sensitivity analysis, January 1995 aquifer test, aquifer storage recovery site, Charleston, South Carolina

[--, no data]

Input parameter	Multiplier	Root mean square error	
		Production well	Observation well
Transmissivity of the Santee Limestone/Black Mingo aquifer	0.75	19.75	8.77
	1.25	14.06	7.43
Storage coefficient of the Santee Limestone/Black Mingo aquifer	0.1	5.06	5.16
	10	10.51	10.93
Anisotropy of the Santee Limestone/Black Mingo aquifer	.75	9.49	3.08
	1.25	8.27	4.00
Vertical hydraulic conductivity of the Santee Limestone/Black Mingo confining unit	.75	1.71	1.49
	1.25	1.73	1.57
Vertical hydraulic conductivity of the Santee Limestone/Black Mingo confining unit directly above the production well	$5.0X10^{-8}$	4.96	2.22
	2	5.84	3.67
Specific storage of the confining unit	0.1	1.71	1.37
	10	2.36	2.57
Initial conditions of the surficial aquifer			
H = -23.38 ft	--	2.18	1.81
H = -38.38 ft	--	1.57	1.41

Simulated recovery water levels approximated observed recovery water levels. The RMSE value determined for the observation well for ASR cycle 12 was 2.70 ft.

A volumetric budget for the simulation of the injection phase of ASR cycle 12 was also compiled (table 6). The cell where the production well was located was modeled as a constant head cell to simulate the injection of water. Budget results indicate that storage in the SL/BM aquifer is the major sink for injected water. By the latter part of this test, however, the percentage of water contributed to storage in the SL/BM aquifer was decreasing at approximately the same rate that the percentage of water contributed to confining bed storage was increasing.

Brackish-Water Upconing

Ground-water withdrawals can induce brackish water to rise in an aquifer where freshwater overlies more saline water. During pumping, if the brackish water rises to or below the critical rise level ($Q \leq Q_c$; where Q is the well discharge rate and Q_c is the critical discharge rate or the rate at which the well will discharge brackish water), the well will continue to discharge freshwater (fig. 13). If the critical pumping rate is exceeded ($Q > Q_c$), the well will discharge brackish water (Reilly and Goodman, 1985). Brackish

Table 6. Simulated volumetric budget for the injection phase of the March 1995 aquifer storage recovery test, Charleston, South Carolina

[All units are in cubic feet per day (ft^3/d), except where noted]

Time step	Total time, hours	INFLOW				OUTFLOW		
		Confining bed storage[1]	Constant head leakage	Constant head[2]		Confining bed storage	Constant head leakage	Aquifer storage
				Total	Cell above production well			
31	0.096	<1	2	16,923	(16,923)	441	<1	16,491
34	0.21	2	<1	16,003	(16,003)	814	<1	15,191
37	0.47	<1	<1	15,190	(15,190)	1,353	<1	13,839
40	1.02	<1	<1	14,458	(14,458)	1,886	<1	12,578
43	2.25	2	0	13,784	(13,784)	2,217	2	11,566
46	4.94	<1	<1	13,179	(13,179)	2,594	1	10,584
49	10.85	<1	<1	12,657	(12,657)	3,354	2	9,301
52	23.83	<1	<1	12,219	(12,219)	4,608	3	7,608
Average		<1	<1	12,816	(12,816)	3,536	2	9,279

[1]Number in parentheses () represents the volumetric flow rate at the model cell where the production well is located. The absence of parentheses indicates that the contribution of water to or from the production-well cell is insignificant for the given time step.

[2]All injection was simulated using a constant head boundary condition in the production-well cell.

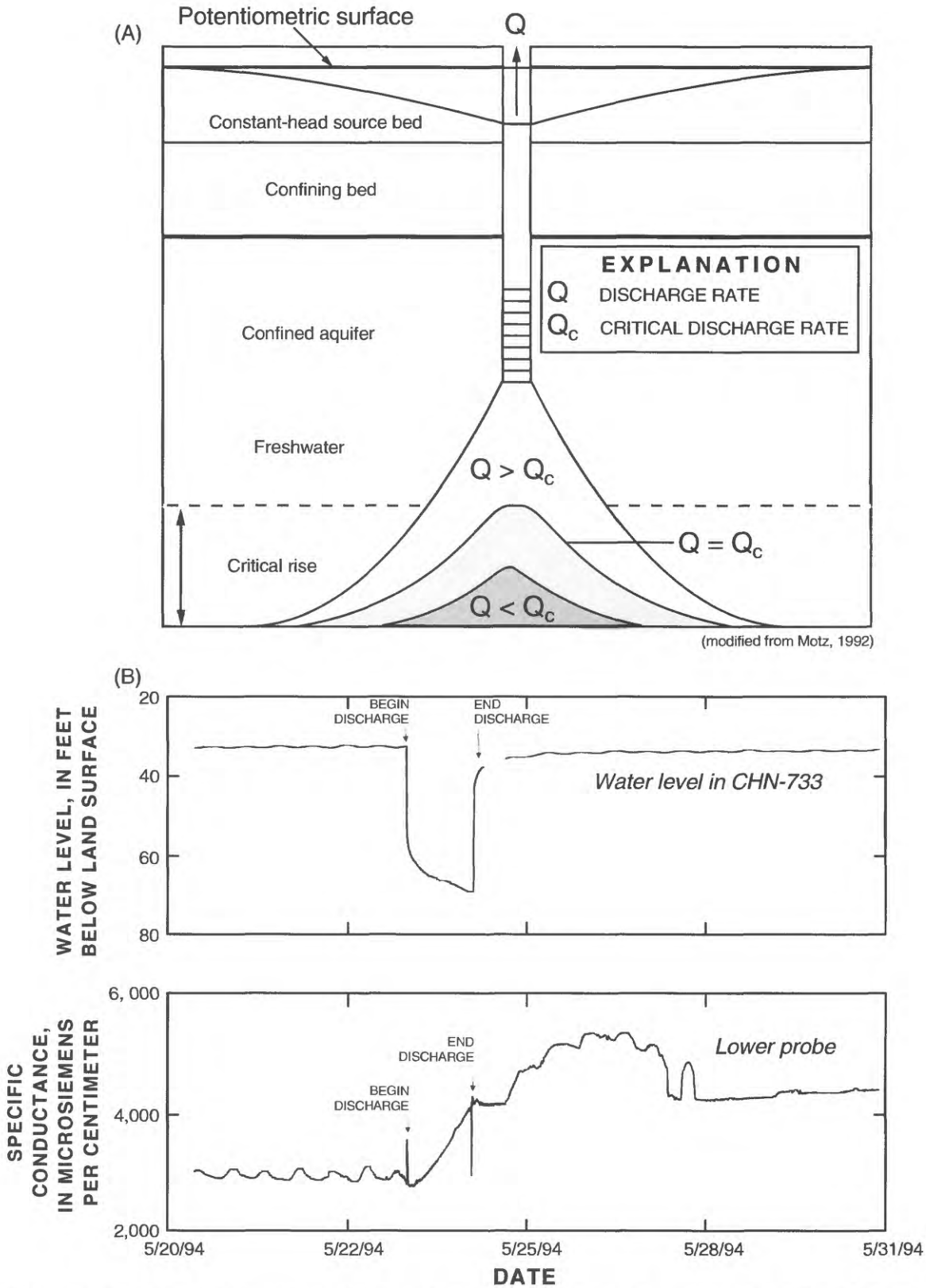

Figure 13. Hypothetical brackish-water upconing due to pumping a well in a leaky confined aquifer (A), and water-level and specific-conductance measurements suggesting brackish-water upconing in observation well CHN-733 (B) (Figure 13A-modified from Motz, 1992).

water upconing has been documented at numerous production well fields, for example in the coastal areas of Massachusetts and Florida (Motz, 1992).

A distinct freshwater/brackish water interface exists in the SL/BM aquifer at the pilot-scale ASR site. Geophysical logging with fluid resistivity and fluid conductivity tools indicated an abrupt change in water quality between 440 and 450 ft bls (fig. 5). At this level, specific conductance increases from 2,000 to 8,500 µS/cm in the production and observation wells. This brackish water is found in the lower part of the SL/BM aquifer at the base of the LPZ.

Upconing can be shown qualitatively by trends in specific conductance measured during a 24-hr aquifer test using probes installed in observation well CHN-733 (fig. 13). Specific conductance measured prior to the May 1994 aquifer test was relatively constant at approximately 2,900 µS/cm at the LPZ specific conductance probe (fig.7). After the aquifer test was initiated, specific conductance values gradually increased to values greater than 5,000 µS/cm at the lower probe. Such increases in specific conductance after aquifer test initiation indicated upconing of brackish water from the SL/BM aquifer. Similarly, increased specific conductance values and major dissolved constituent concentrations were measured during recovery cycles 4 through 9 and 11 at the LPZ probe.

Geochemical Characteristics and Trends

After injection, water-quality characteristics of the treated surface water changed as water reacted with SL/BM aquifer material, and mixed with native ground waters. Water-quality changes are described qualitatively to determine if recovered ground water is potable after storage and recovery. Geochemical model codes were then used to differentiate water-quality changes that occurred during recovery from those that occurred during storage.

Characteristics of the Treated Surface Water and Aquifer Waters

End-member compositions of ground-water samples were defined so that mixing characteristics among treated surface water and native aquifer waters could be interpreted. Water-quality data from the following water samples are compared (fig. 14): injected treated surface water (PI736-66; appendix 2); water from the upper production zone (UPZ), reflecting a source in the Santee Limestone (OB733-3); water from the lower production zone (LPZ), reflecting a source in the SL/BM aquifer (PB736-6); and a composite sample of waters from the upper- and lower-production zones (OB733-4).

These samples were selected for use in geochemical models because they were collected from specific hydrostratigraphic units, or because they probably represented a mixed condition within the open-hole well. The UPZ sample was collected at the observation well from a depth of 430 ft bls, before the LPZ was penetrated. The LPZ sample was collected at the production well head after 24 hours of pumping.

The composite UPZ/LPZ sample was collected during static conditions in the open-hole observation well from a depth of 440 to 450 ft. At this depth, both production zones contributed water to the well. Definition of the composite sample composition is useful because both production zones in the SL/BM aquifer are hydraulically connected. During ASR tests, mixing occurred in the production zones as the result of vertical leakage from the UPZ to the LPZ, from upconing of high specific conductance water at the base of the LPZ during recovery (fig. 13), or from dispersion of injected treated surface water.

The treated surface water is characterized by low ionic strength ($I=0.002$; $I=1/2\ \Sigma(\text{molality})(\text{charge})^2$ for all dissolved ions) (Drever, 1988). Ionic strength is an expression that describes solution composition in terms of ion concentration and valence, and is calculated from dissolved inorganic constituent concentration data. Seawater and brines are characterized by

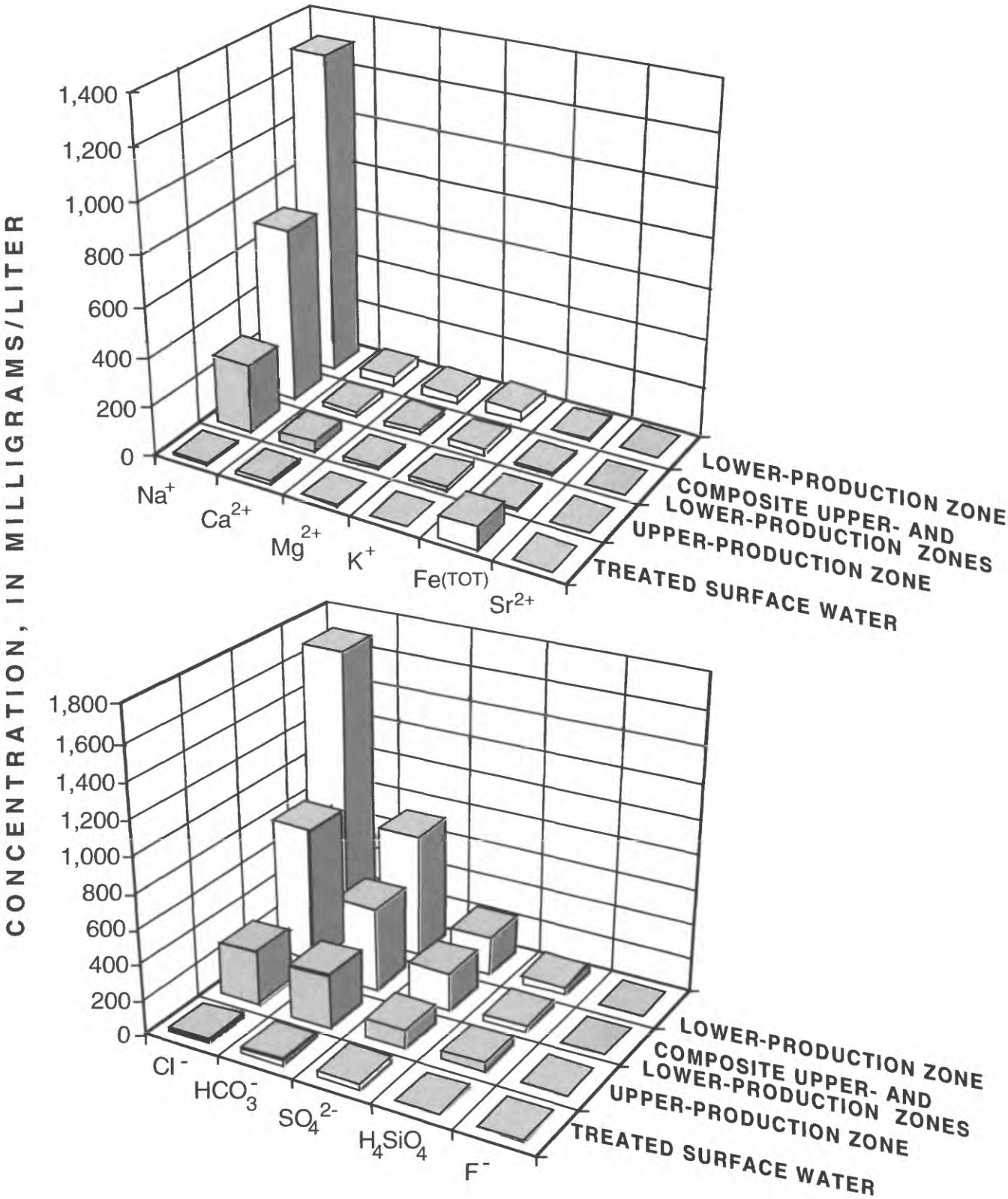

Figure 14. Dissolved inorganic constituent concentrations in ground-water samples from the lower-production zone (sample PB736-6), composite upper- and lower-production zones (sample OB733-4), upper-production zone (sample OB733-3), and treated surface water (OB736-66).

high values of ionic strength (I > 0.8), whereas treated surface water shows low values of ionic strength (I < 0.005).

The treated surface water had the lowest concentrations of all dissolved ions compared to the upper- and lower-production zone samples, with the exception of total dissolved iron. Water from the LPZ is characterized by higher ionic strength (I=0.067), and greater concentrations of chloride, sodium, bicarbonate, and sulfate consistent with its classification as a sodium bicarbonate water (Park, 1985). High ionic strength values are also consistent with high specific conductance values measured in LPZ samples. Samples from the UPZ (I=0.018) and composite UPZ/LPZ (I=0.037) show ionic strength values and major and trace dissolved constituent concentrations that are intermediate between end-member (treated surface water and LPZ samples) values.

Injection of treated surface water into predominantly calcareous aquifer material presents an opportunity to quantify water-rock reactions in an initially dilute solution, and to interpret these reactions as they affect drinking-water quality. Treated-surface-water-quality data collected during storage in the aquifer provide the opportunity to interpret reactions between water and limestone. Treated-surface-water-quality data collected during recovery provide a geochemical tracer to estimate recovery efficiencies, and also can suggest additional (probably non-equilibrium) geochemical reactions that affect drinking-water quality. Most water-quality data were measured during the recovery stage of ASR cycles 4 through 9, and 11 (appendix 2). Water-quality data were collected during ASR cycle 13d to estimate changes during a two-month storage period.

Trends Observed in Recovered Ground-Water Quality

The primary reactions that govern geochemical evolution of injected treated surface water in the SL/BM aquifer during recovery are: (1) increased ionic strength; (2) changing distribution of dissolved carbonate species; and (3) changing calcium carbonate solubility (Mirecki and others, 1995). Trends in water-quality data were interpreted from samples collected early in the recovery cycle (when less than 10 percent of the injectant volume was recovered), through the final samples (when the recovered volume of water was 94 to 109 percent of volume injected; appendix 1).

Samples collected during selected recovery cycles show monotonic increases in ionic strength (fig. 15A). Ionic strength in the final ground-water sample from all recovery cycles ranged from 0.03 to 0.04, similar to ionic strength values in the composite UPZ/LPZ sample. Similar trends were observed in total dissolved solids (TDS) (fig. 15B), sulfate (fig. 15C), and chloride (fig. 15D) concentrations. Samples collected after 99 percent of the injectant water volume was recovered showed sulfate concentrations below that specified by the proposed Federal SMCL of 500 mg/L for sulfate (U.S. Environmental Protection Agency, 1988). The SMCL's for TDS (500 mg/L) and chloride (250 mg/L) were exceeded in samples collected after approximately 30 to 40 percent of the volume was recovered during each ASR cycle. High TDS and chloride concentrations degrade the quality of injected treated surface water only from an aesthetic standpoint.

Trends observed in dissolved inorganic carbon (DIC; $CO_3^{2-} + HCO_3^- + H_2CO_3$) and alkalinity during storage and recovery have practical implications in ASR testing (fig. 16). These geochemical characteristics can indicate whether calcareous aquifer material is either dissolving and enhancing aquifer permeability, or precipitating and reducing aquifer permeability. Alkalinity and DIC concentrations increased monotonically in ground-water samples collected during recovery, although DIC concentrations measured in samples from cycles 9 and 11 were variable (appendix 3). Concentrations of DIC were measured because these data provide a more quantitative measure of carbonate species concentration than do field or lab alkalinity measurements.

Alkalinity values measured in the final sample collected during each ASR cycle usually were similar to that of the composite UPZ/LPZ sample.

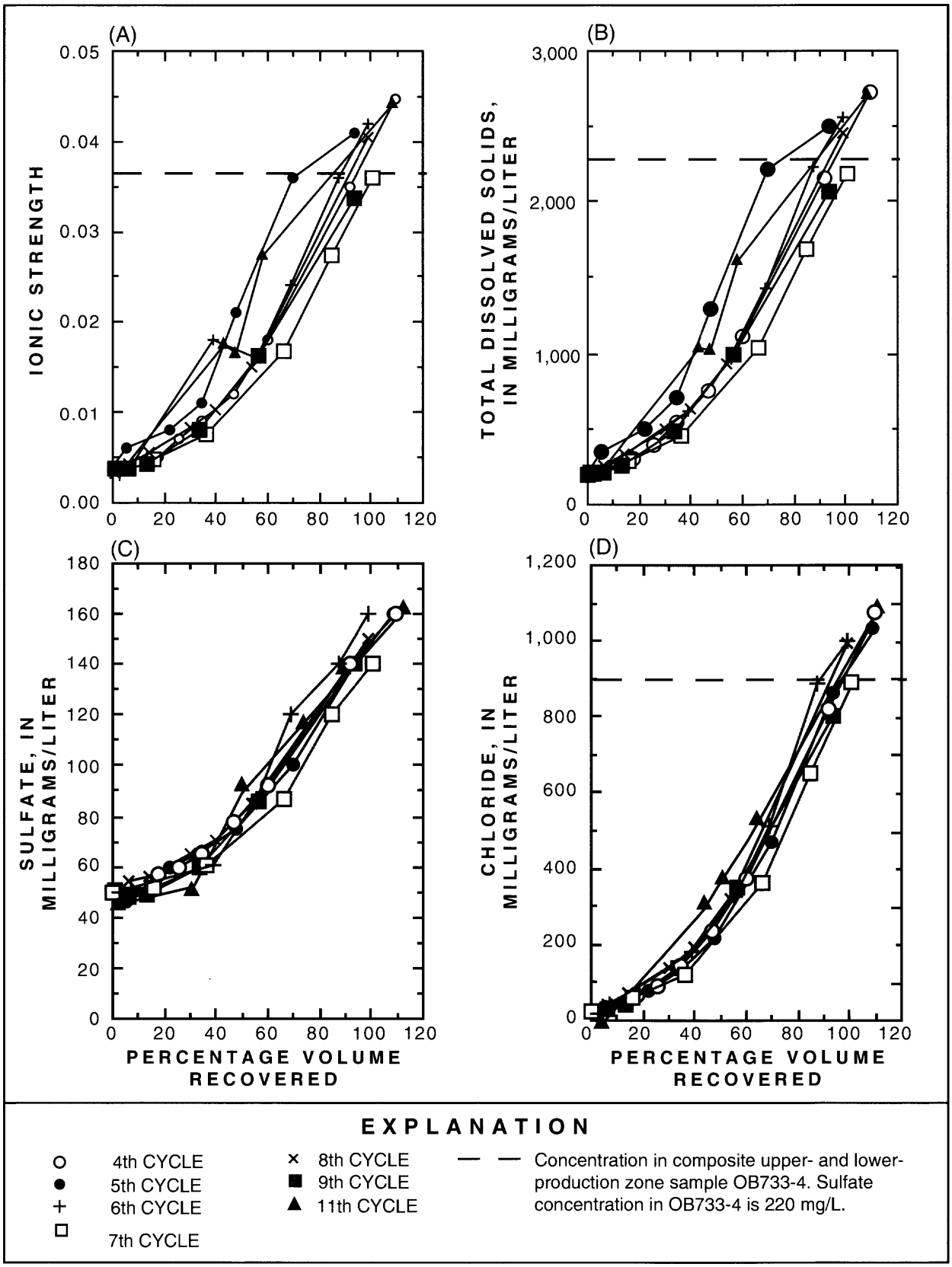

Figure 15. Trends in ionic strength (A), total dissolved solids (B), sulfate concentration (C), and chloride concentration (D) in ground-water samples collected during the recovery phase in aquifer storage recovery cycles 4 through 9 and 11.

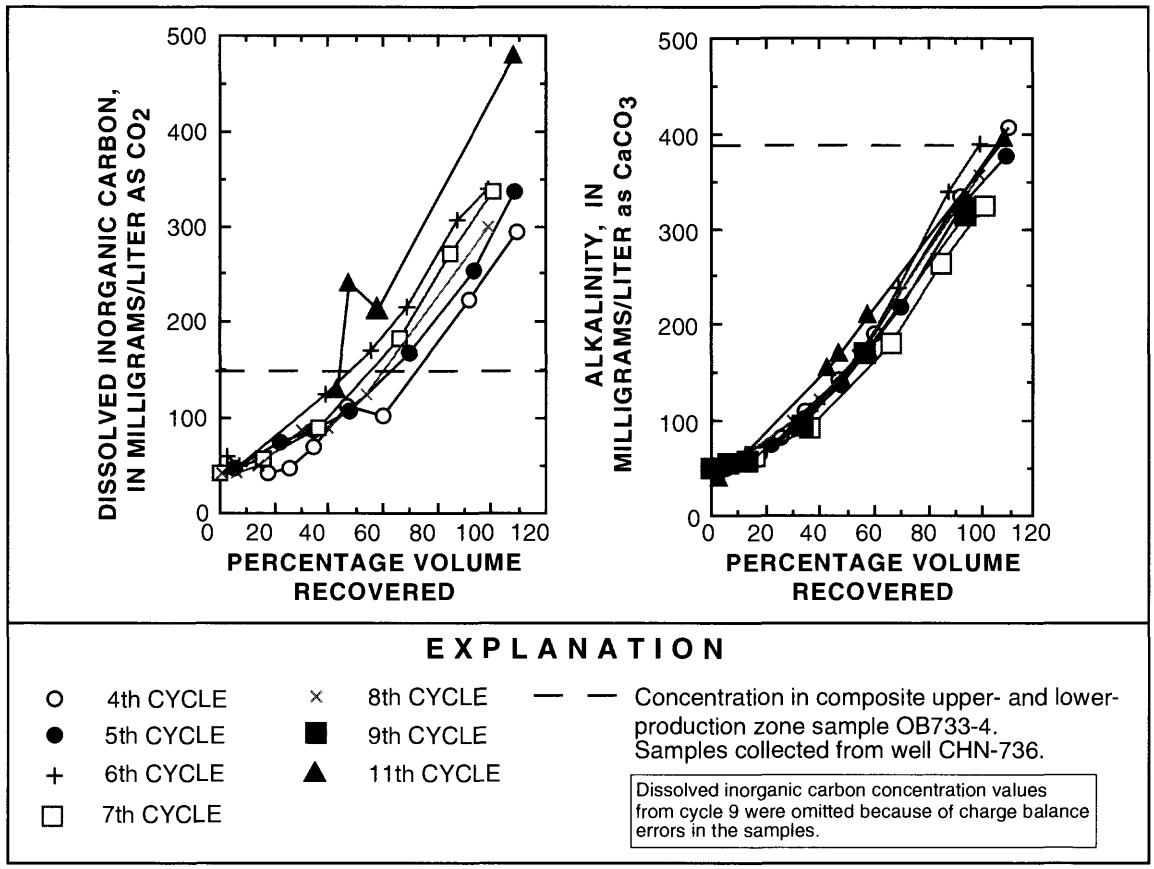

Figure 16. Trends in dissoved inorganic carbon concentrations and alkalinity in ground-water samples collected during the recovery phase of aquifer storage recovery cycles 4 through 9 and 11.

The concentration of DIC measured in the final sample collected during each recovery cycle frequently exceeded that of the composite UPZ/LPZ sample (fig. 16). Samples collected after approximately 70 percent recovery showed DIC values similar to that of the UPZ/LPZ sample (150 mg/L). Increases in DIC and alkalinity can result from dissolution of calcareous aquifer material in the production zones, and (or) mixing of high alkalinity water from the SL/BM aquifer water with treated surface water during recovery. The distribution of dissolved carbonate (CO_3^{2-}), bicarbonate (HCO_3^-), and carbonic acid (H_2CO_3) changed during recovery because these species were contributed from the dissolution of calcareous aquifer material and mixing of waters that had different initial dissolved carbon dioxide (CO_2) concentrations. Mixing of waters that have different carbonate characteristics, especially in contact with limestone, can result in a condition where the resultant mixture is not a linear function of the two compositional end-members (Wigley and Plummer, 1976), making prediction of carbonate species trends problematic.

Dissolution of calcareous aquifer material during each ASR cycle will result from injection of treated surface water that is initially undersaturated with respect to calcite. Calcite saturation indices were calculated from water-quality data to estimate whether calcite dissolved or precipitated during recovery (fig. 17). The saturation index (SI) is a measure of how ion activities of a solution differ from "ideal" ion activities at equilibrium, when that solution is in contact with a pure mineral phase (Drever, 1988). A positive SI value indicates that an equilibrium solution is oversaturated with respect to a mineral, so that mineral will precipitate; a negative SI value indicates that an equilibrium solution is undersaturated with respect to a mineral, so that mineral will dissolve.

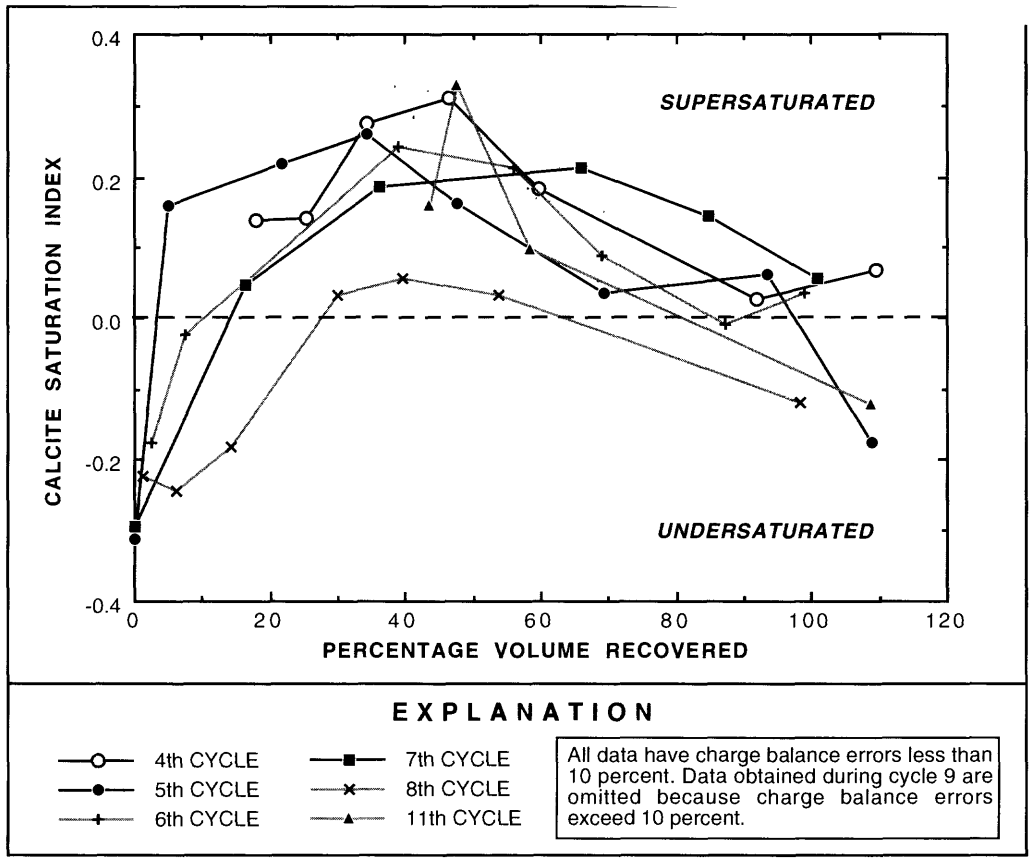

Figure 17. Trends in calcite saturation index in ground-water samples collected during the recovery phase of aquifer storage recovery cycles 4 through 8 and 11.

Calcite saturation indices show that initial ground-water samples collected during each aquifer storage recovery cycle were generally undersaturated (fig. 17). Positive calcite SI values were shown after recovery of approximately 10 percent of treated surface water, suggesting that calcite could precipitate from the supersaturated solution passing through the aquifer. Supersaturated conditions with respect to calcite continued during recovery until nearly 100 percent of the volume was recovered. Precipitation of calcite could reduce permeability of the aquifer, and efficiency of the ASR process.

Positive calcite SI values were calculated for many ground-water samples collected during ASR recovery cycles; however, this condition probably represents one of "apparent" supersaturation. Acceptance of these calcite SI values requires that the ground-water data represent equilibrium conditions between water and aquifer material. In a practical sense, equilibrium conditions are met when water flow velocity is much slower than the reaction rate of calcite precipitation. It is likely that equilibrium conditions are not met during recovery of treated surface water for the following reasons: (1) a flow rate of 130 to 160 gal/min was used to recover the treated surface water; (2) mixing of waters from the two permeable zones within the SL/BM aquifer during recovery; and (3) upconing of Black Creek confining unit water during recovery. Therefore, positive calcite SI values probably represent an "apparent" supersaturation. It is likely that calcite is not precipitated during the dynamic conditions encountered during recovery. This interpretation is supported by physical flow data, which indicates successively faster breakthrough (hence, greater permeability) of injected treated surface water during injection when ASR cycles 4, 6, 9, and 12 are compared (fig. 9). Similar "apparent" supersaturation conditions have been encountered in coupled reaction and transport models

simulating mixing between fresh water and brackish water in coastal aquifers (Sanford and Konikow, 1989).

Concentrations of dissolved oxygen (appendix 4), dissolved hydrogen sulfide and chlorine gases (appendix 5), and dissolved total trihalomethanes (appendix 6) were measured in ground-water samples collected during recovery in selected ASR cycles. Dissolved oxygen concentrations were below saturation values (approximately 8 mg/L at 25 °C) in all samples, indicating that oxygen from the treated surface water was consumed during storage and recovery. Dissolved-oxygen concentrations decreased to 0 mg/L after approximately 10 percent of the volume was recovered (appendix 4). Dissolved hydrogen sulfide gas was measured in samples collected during recovery in ASR cycles 2, 4, 5, and 6 (appendix 5). Increases in hydrogen sulfide concentrations coincident with increases in sulfate concentrations during ASR cycle 4 suggest that water quality was affected simultaneously by several factors including sulfate reduction, and mixing of sulfate-rich waters from the upper- and lower-production zones during recovery.

Concentrations of total trihalomethanes were measured in recovered ground-water samples to determine whether concentrations exceeded the primary USEPA maximum contaminant level (MCL) of 0.1 mg/L. Background trihalomethane concentrations are indicated by analyses of samples having a designation of "PI736" (appendix 6), which are treated-surface water samples collected at the injection well head. Total trihalomethane concentrations were variable, and ranged between 77 and 130 µg/L in four samples of treated-surface water analyzed prior to injection (PI736-13, PI736-44, PI736-55, and PI736-66; appendix 6). Total trihalomethane concentrations generally decreased from these initial values in samples collected during recovery in ASR cycles 2, and 4 through 11 (appendix 6). The maximum concentration measured was 156 µg/L (0.156 mg/L) in cycle 4 (appendix 6), which exceeds the MCL for total trihalomethanes. However, total trihalomethane concentrations decreased to levels below the MCL after approximately 50 to 60 percent of the injected volume was recovered in all ASR cycles.

Trends Observed in Water Quality During Storage

Most of the water quality data presented in this report were collected during recovery in each ASR cycle. Of equal or greater importance is the determination of water-quality changes that resulted from interactions between injected treated-surface water and aquifer material during storage, because these trends have direct implications on the success of ASR. Water-quality data obtained during recovery probably do not represent conditions and reactions occurring in the aquifer, except for conservative ions such as chloride, so these data cannot be used to interpret water-quality changes without ambiguity. Water-quality samples collected during ASR cycle 13 were analyzed to estimate water-quality changes resulting from a 61-d storage period (appendix 3).

Water-quality characteristics measured in ground water samples collected from the open-hole observation well CHN-733 during ASR cycle 13 did not represent water quality in the adjacent production zones of the SL/BM aquifer. This conclusion is supported by two lines of evidence: (1) comparison of specific conductance values measured before and during pumping in cycle 13d, and (2) comparison of specific conductance profiles performed in the observation well on a weekly basis during the storage period of cycle 13.

Specific conductance values measured in observation well CHN-733 decreased abruptly (from 2,560 µS/cm to approximately 700 µS/cm) soon after pumping during recovery was initiated. The decrease in specific conductance values show that water stored in the aquifer was considerably less brackish than water under static conditions in the observation well. Higher specific conductance values that characterized static water in the observation well apparently resulted from mixing of all waters in the open-hole well. Lower specific conductance values (generally less than

700 μS/cm) were characteristic of stored treated surface water in the SL/BM aquifer.

Mixing of aquifer waters in the open-hole well is shown by changing shape of specific conductance profiles measured weekly during the storage period of cycle 13 (fig. 18). Specific conductance profiles showed less definition with depth as the weeks progressed, suggesting that water at depth in the observation well did not represent water in the adjacent permeable zone. Lowest specific conductance values were expected adjacent to zones of high permeability in the SL/BM aquifer, but this structure became less defined as the storage period continued.

Consequently, ground-water samples collected in observation well CHN-733 after the first week of storage (OI733-78 through OI733-82; appendix 3) probably did not represent geochemical conditions in the aquifer, based on their high specific conductance values. These data were not used for interpretation of water-quality changes during storage.

Preliminary estimates of water-quality changes that occurred during storage were interpreted using data from early samples collected during recovery in selected ASR cycles. Samples collected after recovery of one well volume (approximately 1,500 gal for production well CHN-736), but before the effects of upconing of high specific conductance water were observed, provided a qualitative estimate of water-quality changes during storage. Five ground-water samples (one each from cycles 4, 5, 6, 7, and 8) were used for interpretation of injectant storage characteristics. These samples (PR736-15, PR736-23, PR736-30, PR736-37, PR736-49; appendix 2) showed low specific conductance values (less than 550 μS/cm), and were collected after one well volume was pumped from the SL/BM aquifer after storage periods that ranged from 16 hours (hr) to 144 hr (0.7 and 6 d).

Ground-water sample data representing the 0.7- to 6-d storage periods more closely resembled the water-quality characteristics of treated surface water than water from the production zones (fig. 19). Samples collected during storage periods have low ionic strength (less than 0.006), low specific conductance (less than 550 μS/cm), but have higher pH values (8.2 to 8.8) resulting from dissolution of calcium carbonate in the aquifer. Chloride and sulfate concentrations, along with alkalinity and total dissolved solids values, at least doubled during storage. However, concentrations of these water-quality characteristics remained below SMCL's in the selected ground-water samples (appendix 2).

Water-quality changes described in this report occurred after short storage durations. On the basis of these limited data, it is not yet possible to state whether the water-quality characteristics described above represented the maximum degradation of treated surface water that could occur from prolonged storage in the SL/BM aquifer. Further discussion of geochemical trends that occurred during storage and withdrawal is presented in the following section.

Concentrations of dissolved chlorine gas (appendix 5) and total trihalomethanes (appendix 6) were measured in samples collected during ASR cycle 13. The maximum value of dissolved chlorine gas was 4.0 mg/L, measured in the first samples collected during recovery (less than 1 percent volume recovered) and decreased as recovery proceeded. These data indicate that stored water might require disinfection prior to use after storage in the SL/BM aquifer. Total trihalomethane concentrations measured in samples collected from observation well CHN-733 during cycle 13 (18 to 32 μg/L) were below the MCL. Concentrations of dissolved chlorine and trihalomethanes may reflect degassing of volatiles or mixing of waters in the open-hole well.

Geochemical Simulation of Water-Quality Changes During Storage

Water-quality changes that occurred during storage were interpreted using the geochemical model code NETPATH (Plummer and others, 1994), which uses the mass-balance approach to specify geochemical reactions between initial and final wells along a flowpath. In the context of an ASR cycle and for the purpose of this report, the

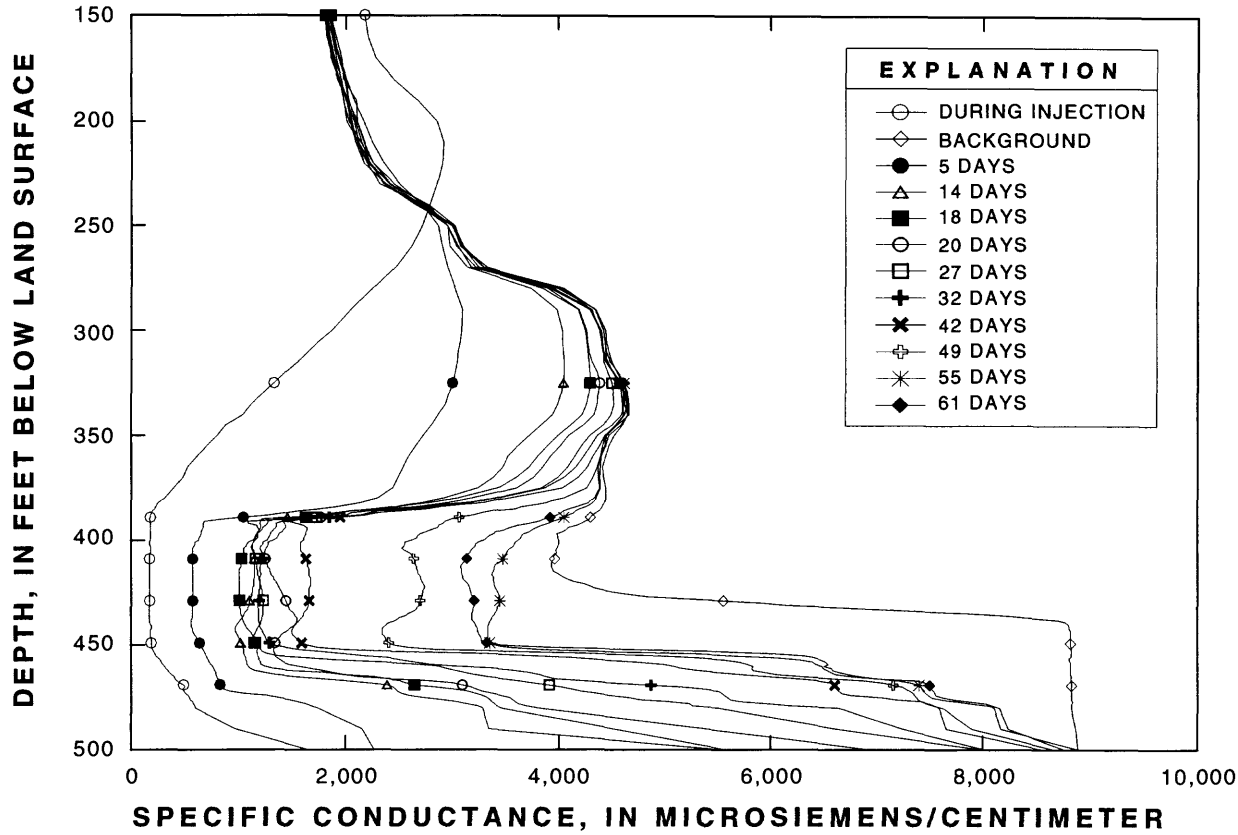

Figure 18. Specific-conductance profiles for observation well CHN-733 over a 61-day storage period during aquifer storage recovery cycle 13d, after injecting 1,045,277 gallons of treated surface water.

"flowpath" is actually the 0.7- to 6-d storage period. Geochemical reactions are inferred between the initial condition (treated surface water; sample PI736-66, appendix 2) and the final condition (samples PR736-15, PR736-23, PR736-30, PR736-37, PR736-49; appendix 2), which together represent the maximum duration of storage during ASR cycles 4 through 8. Groundwater samples representing storage during cycles 9 and 11 were not used in NETPATH, because they (samples PR736-58 and PR736-71) showed charge balance errors of 14 and 46 percent, respectively, indicating an analytical problem. Acceptable charge balance errors (less than 10 percent) were calculated for all other samples used in NETPATH.

The geochemical model that describes changing water quality during storage includes dissolution of calcite, dolomite, gypsum, halite, and a soluble silicate, assumed to be amorphous silica (table 7). Increases in Na^+/Ca^{2+} ratios were interpreted in the context of ion-exchange on clays of the Williamsburg Formation of the Black Mingo Group. Water-quality changes during storage were constrained by lithologic descriptions of core CHN-733, or inferred from detailed mineralogic analyses of similar units in the Clubhouse Crossroads corehole located approximately 25 mi southwest of the ASR site (Gohn and others, 1977).

Calcite and dolomite were chosen as carbonate phases in the model because they approximated the composition of the Santee Limestone in the UPZ. Carbonate phases were forced to dissolve because treated surface water (the initial condition) was undersaturated with respect to calcite and dolomite. Carbon dioxide gas also was included as a phase because it is dissolved in treated surface water in equilibrium with the atmosphere, thus producing carbonic acid that dissolves calcareous aquifer material during storage.

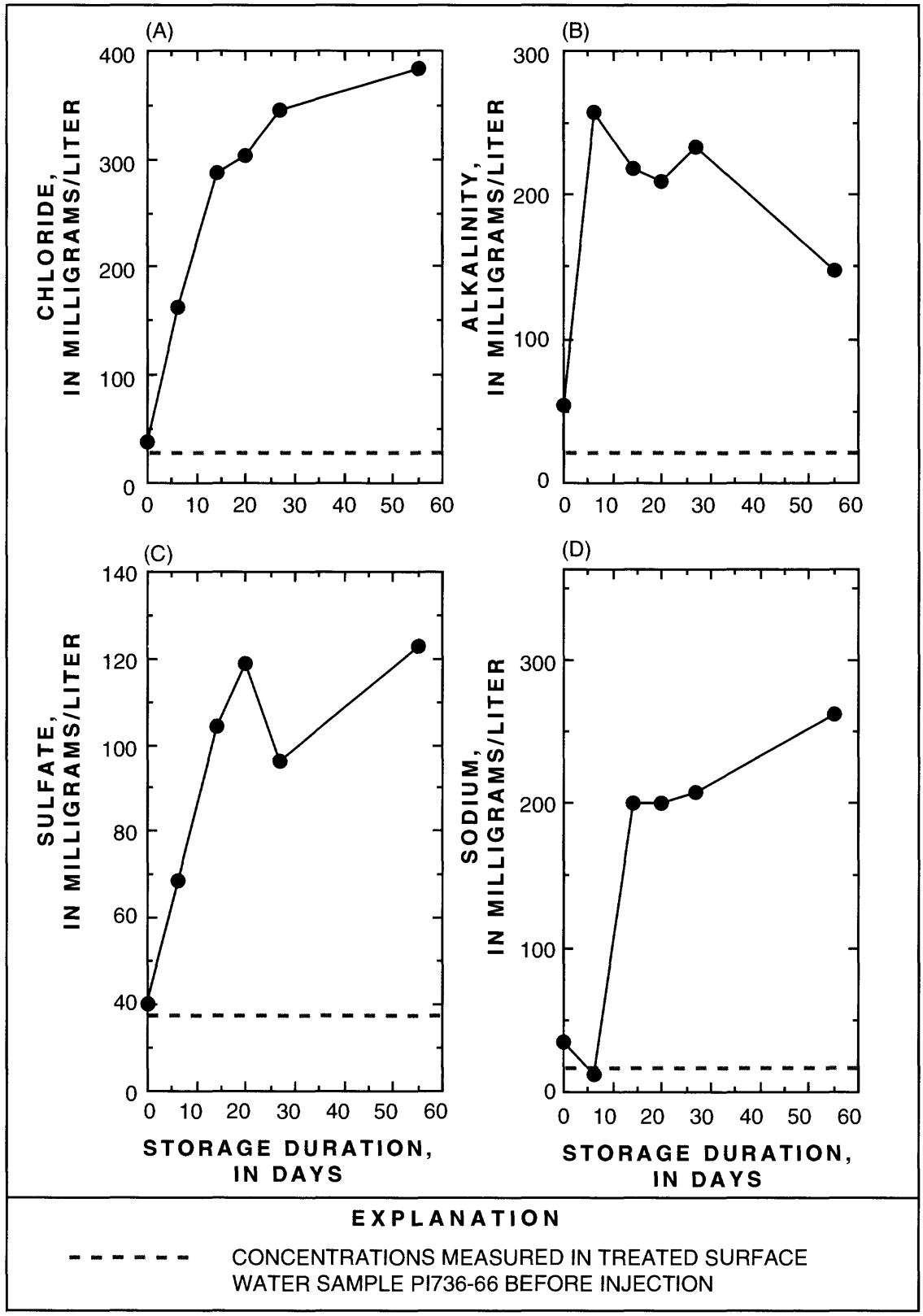

Figure 19. Changes in chloride (A), alkalinity (B), sulfate (C), and sodium (D) concentrations in ground-water samples collected during the storage phase of aquifer storage recovery cycle 13.

Table 7. Simulated[1] mass-transfer reactions that occurred during storage of treated surface water in the Santee Limestone/Black Mingo aquifer, Charleston, South Carolina

[mmol, millimolar; kg, kilogram; CO_2, carbon dioxide; Na^+, sodium]

Sample number (initial)	Sample number (final)	Mass transfer reactions
PI736-66	PR736-15	0.31 mmol calcite dissolves per kg solution
		.02 mmol dolomite dissolves per kg solution
		.22 mmol gypsum dissolves per kg solution
		1.52 mmol halite dissolves per kg solution
		.06 mmol silica dissolves per kg solution
		.18 mmol CO_2 gas ingasses to solution
		.63 mmol Na^+ desorbed from clay
PI736-66	PR736-23	.28 mmol calcite dissolves per kg solution
		.02 mmol dolomite dissolves per kg solution
		.25 mmol gypsum dissolves per kg solution
		.85 mmol halite dissolves per kg solution
		.04 mmol silica dissolves per kg solution
		.32 mmol CO_2 gas ingasses to solution
		.51 mmol Na^+ desorbed from clay
PI736-66	PR736-30	.31 mmol calcite dissolves per kg solution
		.02 mmol dolomite dissolves per kg solution
		.16 mmol gypsum dissolves per kg solution
		.84 mmol halite dissolves per kg solution
		.04 mmol silica dissolves per kg solution
		.32 mmol CO_2 gas ingasses to solution
		.51 mmol Na^+ desorbed from clay
PI736-66	PR736-37	.36 mmol calcite dissolves per kg solution
		.02 mmol dolomite dissolves per kg solution
		.17 mmol gypsum dissolves per kg solution
		1.32 mmol halite dissolves per kg solution
		.08 mmol silica dissolves per kg solution
		.42 mmol CO_2 gas ingasses to solution
		.60 mmol Na^+ desorbed from clay

Table 7. Simulated[1] mass-transfer reactions that occurred during storage of treated surface water in the Santee Limestone/Black Mingo aquifer, Charleston, South Carolina--Continued

[mmol, millimolar; kg, kilogram; CO_2, carbon dioxide; Na^+, sodium]

Sample number (initial)	Sample number (final)	Mass transfer reactions
PI736-66	PR736-49	0.28 mmol calcite dissolves per kg solution
		.01 mmol dolomite dissolves per kg solution
		.19 mmol gypsum dissolves per kg solution
		.87 mmol halite dissolves per kg solution
		.04 mmol silica dissolves per kg solution
		.24 mmol CO_2 gas ingasses to solution
		.45 mmol Na^+ desorbed from clay

[1]Geochemical model (NETPATH) input: Constraints - carbon, sulfur, calcium, magnesium, chloride, and silica; Phases - calcite, dolomite, gypsum, halite, silica, carbon dioxide gas, and sodium/calcium exchange.

It is possible that microbial activity (Chapelle and others, 1987) or organic matter oxidation in the SL/BM aquifer served as an additional source of dissolved carbon dioxide. Gypsum, halite, and amorphous silica were not quantitatively identified in the lithologies at the production zones, but the presence of these mineral phases would not be unusual.

Clay mineralogy of the uppermost Black Mingo Group in the Clubhouse Crossroads corehole consists of kaolinite, illite, and smectite (Gohn and others, 1977). Clays are present in Black Mingo Group lithologies of the core from CHN-733, although their mineralogies are unknown at present. However, it is likely that these clays serve as an exchange surface on which dissolved calcium and magnesium are sorbed, and sodium is released to ground water.

Mass-transfer calculations show that calcite, halite, and gypsum dissolution are the dominant reactions that occurred during storage (table 7). Model results differ only in the magnitude of dissolution of all minerals, or sodium desorption. Calcite dissolution ranges from 0.28 millimolar per kilogram (mmol/kg) of solution to 0.36 mmol/kg of solution, or 24.7 mg/kg to 31.7 mg/kg. Halite dissolution ranges from 0.84 mmol/kg to 1.52 mmol/kg (49.1 mg/kg to 88.8 mg/kg). Gypsum dissolution ranges from 0.16 mmol/kg to 0.25 mmol/kg (21.8 mg/kg to 34.0 mg/kg). Dissolution of halite and gypsum, and sodium desorption are required in this model to account for increases in sodium, chloride, and sulfate concentrations during storage. Mass-transfer values suggest an ingassing of carbon dioxide gas to the ground-water solution. Carbon dioxide could have evolved from bacterial activity in the SL/BM aquifer, or by oxidation of organic matter by dissolved oxygen or chlorine present in treated surface water (appendices 4 and 5).

Geochemical Simulation of Water-Quality Changes During Recovery

The geochemical model code PHREEQE (Parkhurst and others, 1980) simulated mixing during recovery by developing solutions comprised of treated surface water and SL/BM aquifer water. The percentage of SL/BM aquifer water in each model mixture was based on dissolved chloride concentration as a conservative tracer.

The use of chloride as a conservative tracer of mixing should be appropriate because chloride ions are chemically non-reactive in this carbonate aquifer. Chloride concentrations are diminished only by dilution; therefore chloride concentrations will decrease as a result of mixing between injected treated-surface water with native SL/BM aquifer water having higher specific conductance values. Chloride concentrations will increase from influx of high specific conductance water(s) during recovery, and (or) from dissolution of halite in aquifer material. Halite is assumed to be a minor component of the aquifer material.

Chloride concentrations differ significantly among end-member water samples, so mixing models are less ambiguous when chloride is the conservative tracer. Chloride concentration in the composite UPZ/LPZ sample (800 mg/L; OB733-4) is significantly higher than that of treated surface water (11.0 mg/L; PI736-66). During each ASR cycle, chloride concentration of the recovered water was positively correlated to the percent volume recovered (fig. 15). Dissolved chloride concentrations in ground-water samples collected near the end of recovery (80 to 90 percent volume recovered) during ASR cycles 4 through 9 and 11 were similar to the 800 mg/L chloride concentration in sample OB733-4.

The simulated mixing line generated by PHREEQE shows the relation between chloride concentration and percent of SL/BM aquifer water in recovered ground-water samples (fig. 20). The trend of the simulated mixing line is similar in both curve shape and magnitude to the trends of chloride concentrations measured in ground-water samples collected during recovery in ASR cycles 4 through 9 and 11. Because of this similarity, increases in chloride concentration in recovered ground-water samples were interpreted to result from a greater proportion of SL/BM aquifer water in a sample. Least-squares regression of the simulated mixing line resulted in an equation that related chloride concentration to percentage of SL/BM aquifer water in the sample. This equation was used to estimate a maximum percentage of SL/BM aquifer water in ground-water samples recovered during cycles 4 through 9 and 11. Samples collected early during recovery consisted of 1 to 7 percent SL/BM aquifer water. Samples collected at the end of the recovery period often had chloride concentrations exceeding that of the composite SL/BM aquifer data used as an end-member in mixing calculations. Therefore, the calculated percentage of SL/BM water in these samples exceeded 100 percent, suggesting that an additional source of dissolved chloride may exist. Considering simulations of all aquifer storage recovery samples, when 80 to 90 percent of the injectant was withdrawn, ground-water samples consisted of approximately 100 percent of SL/BM aquifer water.

Simulation of a Production-Scale Aquifer Storage Recovery System

A second ground-water flow model was used to determine the feasibility of injecting treated surface water into the SL/BM aquifer at ten potential ASR sites across the Charleston peninsula. The model incorporated the calibrated aquifer and confining unit hydraulic characteristics used to simulate the January 1995 aquifer test and ASR cycle 12 at the pilot-scale ASR site. The objective of this simulation was to determine at what approximate injection rates water could be injected into the SL/BM aquifer using a production-scale ASR system without raising the post-injection potentiometric surface of the SL/BM aquifer above the land-surface altitude of the Charleston peninsula. Existing wells open to the SL/BM aquifer in the Charleston area would become flowing wells under such conditions.

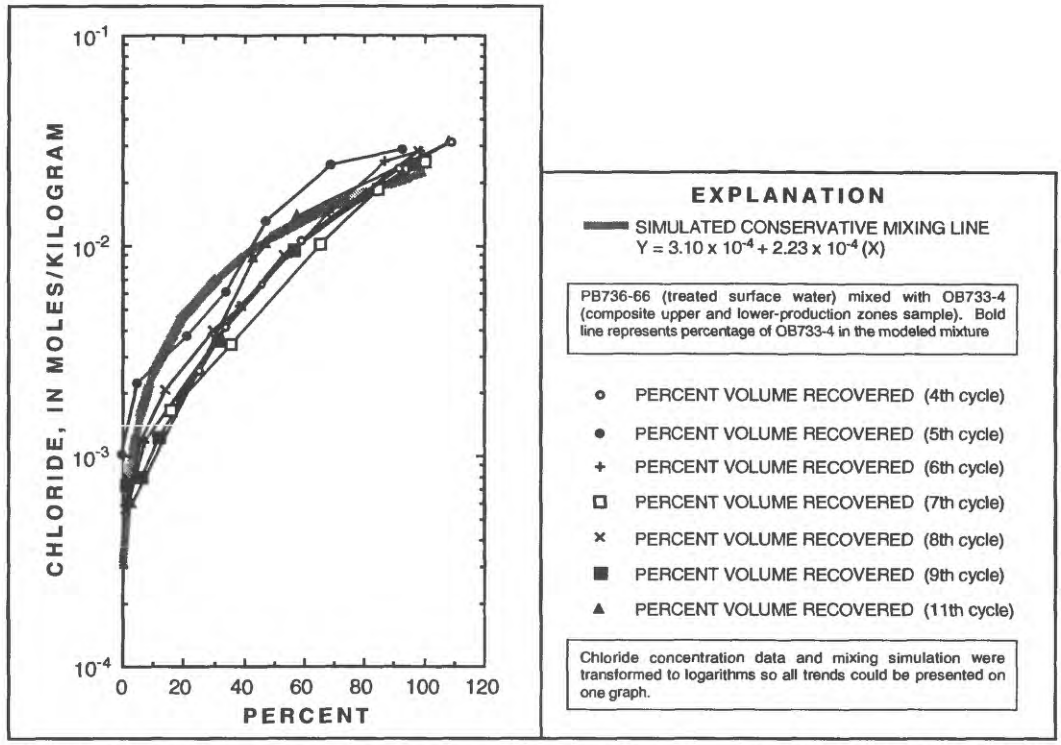

Figure 20. Comparison of a conservative mixing line simulated by PHREEQE with trends in chloride concentration measured in ground-water samples collected during the recovery phase of aquifer storage recovery cycles 4 through 9 and 11.

Production-Scale Model Design

The USGS ground-water flow model MODFLOW (McDonald and Harbaugh, 1988) was used to simulate production-scale ASR operations. The modeled area included the entire Charleston peninsula. Lateral model boundaries were located at sufficient distances from the area of interest to minimize the effects of the boundaries on the water levels at the potential ASR production wells (fig. 21). The model grid used to simulate the pilot-scale ASR test results could not be used, because the overall grid dimensions were too small and the grid cells were too highly discretized in areas not of interest to production-scale ASR operations.

The production-scale model simulated the surficial and SL/BM aquifers using a variably spaced grid of 11,248 cells that represented an area of 115,000 ft by 158,000 ft (fig. 21). The model grid was discretized across the Charleston peninsula with individual cell sizes representing an area of 100 ft by 100 ft. Cell dimensions progressively increased from this most highly discretized region out to the lateral model boundaries by a factor of 1.5, with the exception of the final three rows of cells at the northernmost part of the model. The length of these three rows were equal.

The surficial aquifer was simulated as a source-sink layer with specified-head conditions (H = 0.0 or 10.0 ft). Model cells located offshore, in the Charleston harbor, or in a major river were assigned a value of 0.0 ft. Cells located onshore were assigned a uniform value of 10.0 ft. Because a detailed water table surface was not available for the surficial aquifer in this area, this value of head was used to roughly approximate the elevation of the water table in the surficial aquifer. The SL/BM aquifer was actively simulated as a confined aquifer, which could receive leakage through the overlying confining unit. The confining unit, located between the surficial and SL/BM aquifers, was modeled using a conductance array

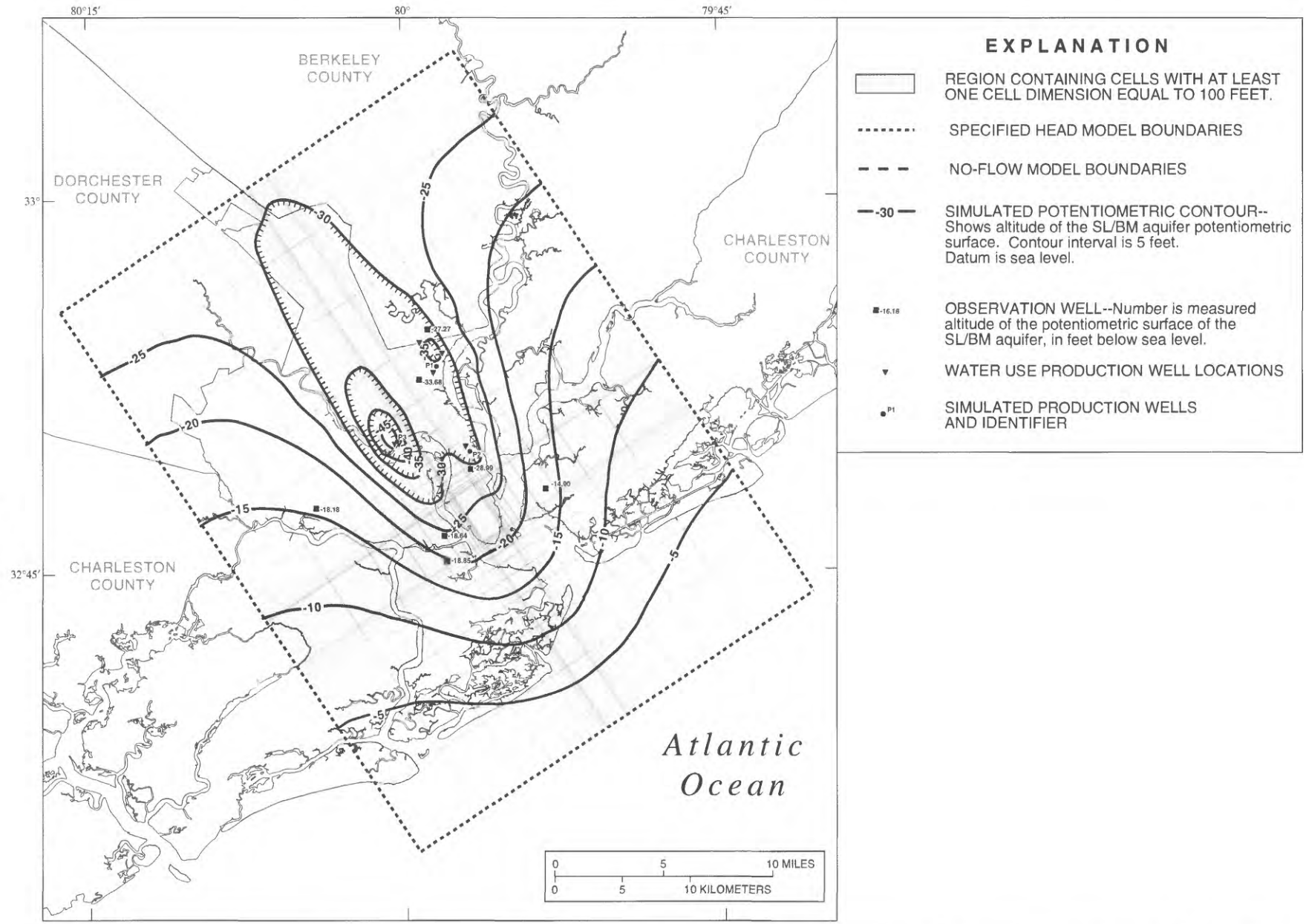

Figure 21. Grid design, location of model boundaries, and simulated October 1996 potentiometric surface of the Santee Limestone/Black Mingo aquifer for the production-scale model, Charleston, South Carolina.

for steady-state simulations and the transient leakage package (Leake and others, 1994) for transient simulations.

The limited number of wells open to or screened in the SL/BM aquifer in the Charleston area prohibited the development of a detailed potentiometric map of this unit. Water-level data from seven wells open to or screened in the SL/BM aquifer were collected in October 1996 (fig. 21). A reversal of the natural seaward hydraulic gradient is evident from these data and from wells located north of the study area (Aucott and Speiran, 1985a; B.L. Hockensmith, S.C. Department of Natural Resources, written commun., 1995). Water-use data for Berkeley, Charleston, and Dorchester counties indicate that at least seven private wells located within the model area were pumping water from the SL/BM aquifer in 1996 (fig. 21; S.C. Department of Health and Environmental Control, written commun., 1996). Pumping rates are relatively constant over an annual period and October 1996 water levels are considered to approximate long term water-level conditions in the SL/BM aquifer.

Aquifer and confining unit hydraulic characteristics derived from the pilot-scale model (table 3) were initially assigned as constant values to corresponding arrays in the production-scale model. The high confining unit vertical hydraulic conductivity assigned directly above the pilot-scale production well was not used for the production-scale simulations. All ASR system wells constructed on the Charleston peninsula probably will be cased through the entire SL/BM confining unit to the top of the SL/BM aquifer and will not penetrate the Black Creek confining unit. Thus, the vertical hydraulic conductivity assigned to the SL/BM confining unit located directly above the location of proposed production-scale wells was set equal to the value assigned to the entire SL/BM confining unit array. This design eliminates two sources of potential leakage at the production-scale wells.

A steady state ground-water flow model was calibrated to the October 1996 water-level data (fig. 21). Specified-head conditions, approximating those observed in October 1996, were assigned to the northern (H = -30 ft) and southern (H = 0 ft) boundaries. No-flow boundary conditions were assigned to the eastern and western boundaries and to the base of the SL/BM aquifer.

Simulation of the October 1996 water levels using the hydraulic characteristics based on the calibration of the pilot-scale model were unsuccessful. Because this was a steady-state simulation and the transient leakage package could not be used to simulate leakage into the SL/BM aquifer, the confining unit was simulated using a vertical conductance array between the two aquifers. The leakage rate across the SL/BM confining unit calibrated in the pilot-scale ASR model allowed too much water to flow into the SL/BM aquifer. A confining unit vertical hydraulic conductivity of 5.0×10^{-5} ft/d produced reasonable results. The necessity of using a lower vertical hydraulic conductivity than the pilot-scale model is expected considering that the assigned head of the surficial aquifer for the pilot-scale model was from 33 to 43 ft lower than the production-scale model.

Calibration of the production-scale model was achieved by adjusting the pumping rates at the simulated production wells such that simulated and observed October 1996 water levels agreed as closely as possible. Several of the wells located within the model area were located within the same or adjacent model cell as another well and, therefore, were simulated as a single well (fig. 21). Initially, the average annual groundwater pumping rates at the resulting three production wells (fig. 21) were based on reported water-use data (S.C. Department of Health and Environmental Control, written commun., 1996); however, the simulated drawdown produced in areas adjacent to these wells, using these pumping rates, were greater than that observed in October 1996. Calibrated pumping rates for these three simulated production wells (P1 to P3) were 15,000 ft^3/d, 11,000 ft^3/d, and 34,000 ft^3/d, respectively. Because of the lack of data that could be used to describe the spatial variability of aquifer and confining unit hydraulic characteristics, the steady-state model was calibrated to

roughly approximate the water levels in the SL/BM aquifer (fig. 21).

The simulated potentiometric response at the lateral model boundaries was evaluated to determine if the assumption of specified-head and no-flow boundaries for the SL/BM aquifer adversely affected simulation results. A maximum simulated head difference of 6.08 ft was produced at the center of the southern model boundary at the end of model calibration. Simulated head differences less than 6 ft were produced at all other model boundaries. This response corresponds well to the assumed flow conditions at the model boundaries (fig. 21) and confirms that the assignment of specified-head and no-flow boundaries did not adversely influence the calibrated model results.

An RMSE value of 1.98 ft was calculated for the calibrated model using the water levels measured at the seven wells in October 1996. A lower RMSE value could have been achieved by varying the hydraulic characteristics across the SL/BM aquifer and overlying confining unit, however, data were not available to support or qualify such efforts. The potentiometric surface simulated by the calibrated steady-state model was used as initial conditions for all transient production-scale simulations.

The volumetric budget for the calibrated production-scale ground-water flow model was compiled for constant head flow into and out of the model, leakage from the surficial aquifer to the SL/BM aquifer, and discharge from wells located within the SL/BM aquifer. Because this was a steady-state simulation, contributions of water from storage in the SL/BM aquifer and confining bed storage were not simulated. Budget results indicate that 51,506 ft^3/d of water leaked from the surficial aquifer to the SL/BM aquifer. Volumetric flow rates of 53,525 and 45,031 ft^3/d flowed into and out of the constant head boundaries of the SL/BM aquifer, respectively. Finally, 60,000 ft^3/d of water was discharged from wells open to the SL/BM aquifer.

Application of the Production-Scale Model

Ten potential ASR sites were chosen in undeveloped areas across the Charleston peninsula (fig. 22) and used as reference sites to compare land-surface altitudes to the results of production-scale simulations. Sites were selected on public property and located near water towers, where possible. Eight observation points (fig. 22), other than the ASR sites, were also located on the model grid and evaluated to determine if the altitude of the simulated potentiometric surface exceeded the land-surface altitude during the simulated injection. Land-surface altitudes at all reference sites were estimated from the USGS Charleston, S.C., 7-1/2 minute topographic map (1958). Topographic contours on the Charleston, S.C., 7-1/2 minute topographic map are shown at intervals of 5 ft. Therefore, the range of accuracy of the estimated land surface altitudes are 1/2 of this contour interval. The observation sites were selected at locations between the proposed ASR injection wells where the cumulative effects of injection and recovery should create the greatest changes in the potentiometric surface, excluding the area directly surrounding the injection wells. Areas directly surrounding the proposed injection well sites will be located in city of Charleston parks and are not known to contain any wells open to the SL/BM aquifer. Areas between the proposed wells are private property and may contain wells open to the SL/BM aquifer.

The calibrated production-scale model was revised to accommodate the computation of storage changes in the SL/BM aquifer and confining unit and was used to simulate injection for a 1-year time period at the ten production-scale ASR sites. The aquifer storage coefficient and confining unit specific storage assigned to all transient production-scale models were the same as those used to simulate the pilot-scale tests (table 3). A total of 50 variably spaced time steps was used for these simulations. The steps were varied so that most occurred early in the 1-year simulation period when the greatest water-level changes were expected to occur. A constant injection rate was assigned at all of the ASR wells.

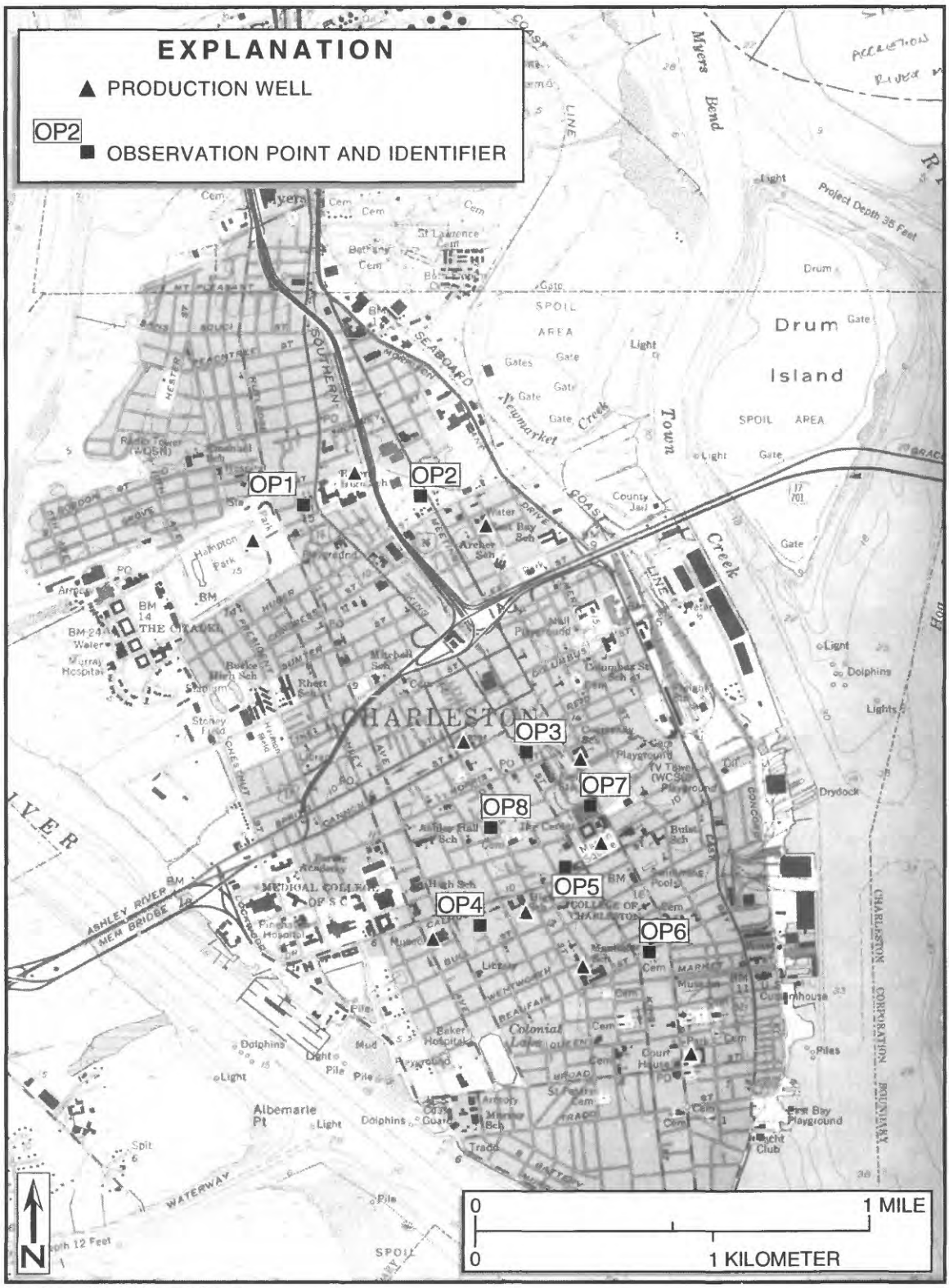

Base from U.S. Geological Survey
Charleston 1:24,000, 1983

Figure 22. Proposed production wells and observation points for the simulated production-scale aquifer storage recovery system across the Charleston peninsula, South Carolina.

Simulation results for the transient production-scale model incorporating the arrays of hydraulic characteristics derived from the calibrated pilot-scale model and using an injection rate of 22 gal/min for each well are listed in table 8, simulation number 5. These results indicate that injection rates higher than 22 gal/min would cause the potentiometric surface of the SL/BM aquifer to exceed land-surface altitude at simulated observation point OP5. Testing combinations of various injection rates at the production-scale ASR sites was beyond the scope of this study. At an injection rate of 22 gal/min, approximately 317,000 gal of water could be injected at ten wells per day, and approximately 116 Mgal of water could be injected during a year.

A volumetric budget for the simulation of injection at the ten production-scale ASR sites for a 1-year time period is presented in table 9. This budget was produced using the hydraulic characteristics derived from the calibrated pilot-scale model (simulation number 5, table 8). The table lists, for each time step, the volumetric flow rates of water that are exchanged within the model through confining bed storage, constant head leakage, aquifer storage, constant head boundaries, or well discharge and recharge. An average volumetric flow rate for the entire year was calculated for each flow component and is listed at the bottom of table 9.

The lack of data regarding the distribution of hydraulic characteristics and potentiometric levels for the SL/BM aquifer limited a comprehensive evaluation of model calibration and required that the sensitivity of the model arrays be tested to determine the possible effects of parameter variability on the simulated potentiometric surface. The hydraulic characteristics and other array values of the calibrated model were increased or decreased by a specific percentage to determine the effects of such changes on the simulated potentiometric surface of the SL/BM aquifer. For this analysis, changes in the potentiometric surface were evaluated at the eight simulated observation points (OP1 to OP8, fig. 22). Because these were predictive simulations and there were no measured water-level data for comparison, RMSE values could not be calculated. Instead, simulated changes in potentiometric-surface altitude at the various observation points were tabulated and graphed according to the specified percentage changes in model arrays.

The sensitivity of the SL/BM aquifer transmissivity and the vertical hydraulic conductivity of the SL/BM confining unit were evaluated separately and in conjunction with one another. The storage coefficient of the SL/BM aquifer and the specific storage of the confining unit were not included in the sensitivity analysis. For the purpose of this study, the sensitivity of model simulations to the transmissivity and lateral anisotropy of the SL/BM aquifer and the vertical hydraulic conductivity of the confining unit were tested by increasing or decreasing respective calibrated values by 25 percent while maintaining all other model input parameters at their calibrated values. Similarly, the sensitivity of model simulations to changes in the specified heads that represent the surficial aquifer was tested by increasing and decreasing the specified head value by 10 ft. The specified head of model cells located offshore, in the Charleston harbor, or corresponding to a major river was not varied for the sensitivity analysis. The resultant potentiometric surface altitudes at the eight observation points are listed in table 8.

In the production-scale model, the SL/BM aquifer is modeled as homogeneous and anisotropic. Results from the sensitivity analysis indicate that, under these assumptions, a SL/BM aquifer transmissivity equal to or greater than 130 ft^2/d is suitable for a combined, long-term injection rate (in ten wells) of 220 gal/min across the Charleston peninsula without causing the potentiometric surface to exceed the land surface altitude at the eight observation points after injecting for one year. The land-surface altitude is exceeded by the simulated potentiometric surface at 1 observation point (OP5) using a vertical hydraulic conductivity of the SL/BM confining unit of 6.25×10^{-5} ft/d; at 5 observation points using an anisotropy factor

Table 8. Simulated water levels at eight observation-point locations using the transient production-scale aquifer storage recovery flow model, Charleston, South Carolina

[ft, foot; ft^2/d, foot squared per day; ft/d, foot per day]

Model parameters					[1]Observation-point locations							
Simulation number	[2]Starting head (ft)	[3]T (ft^2/d)	[4]K_v (ft/d)	[5,6]A	OP1 (11 ft)	OP2 (10 ft)	OP3 (12 ft)	OP4 (8 ft)	OP5 (10 ft)	OP6 (12 ft)	OP7 (12 ft)	OP8 (10 ft)
1	0, 10	98	$3.75x10^{-5}$	15	6.43	6.65	14.86	10.71	16.67	15.39	15.14	16.44
2	0, 10	98	$5.00x10^{-5}$	15	6.55	6.77	14.91	10.77	16.70	15.40	15.18	16.49
3	0, 10	98	$6.25x10^{-5}$	15	6.69	6.90	14.98	10.84	16.75	15.43	15.24	16.55
4	0, 10	130	$3.75x10^{-5}$	15	1.74	1.97	8.42	5.41	9.90	9.05	8.71	9.65
5	0, 10	130	$5.00x10^{-5}$	15	1.88	2.10	8.51	5.51	9.98	9.12	8.79	9.74
6	0, 10	130	$6.25x10^{-5}$	15	2.03	2.25	8.62	5.62	10.08	9.20	8.89	9.85
7	0, 10	162	$3.75x10^{-5}$	15	-1.05	-0.82	4.56	2.23	5.84	5.25	4.85	5.58
8	0, 10	162	$5.00x10^{-5}$	15	-0.91	-0.69	4.66	2.34	5.94	5.33	4.94	5.68
9	0, 10	162	$6.25x10^{-5}$	15	-0.76	-0.54	4.78	2.46	6.04	5.43	5.06	5.80
10	0, 10	130	$5.00x10^{-5}$	11	3.58	4.09	11.61	8.71	13.30	12.13	12.08	12.92
11	0, 10	130	$5.00x10^{-5}$	19	0.77	0.81	6.48	3.44	7.81	7.12	6.64	7.64
12	0	130	$5.00x10^{-5}$	15	1.13	1.37	7.81	4.79	9.29	8.45	8.11	9.03
13	0, 20	130	$5.00x10^{-5}$	15	2.63	2.83	9.21	6.22	10.67	9.78	9.47	10.45

[1]Identification of the observation-point locations, figure 22. (11 ft) - approximate land-surface elevation in feet at each simulated observation point.

[2]Starting head of the surficial aquifer in feet above sea level. If only one number is listed then a uniform starting head value was modeled.

[3]T is transmissivity of the confined aquifer.

[4]K_v is vertical hydraulic conductivity of the confining unit.

[5]A is anisotropy of the confined aquifer.

[6]Anisotrophy factor is the ratio of the transmissivity along a model column to the transmissivity along a model row.

Note: shaded row represents results using the original production-scale model (results prior to sensitivity analysis).

Table 9. Simulated volumetric budget for the transient production-scale model, Charleston, South Carolina

[All units are in cubic feet per day (ft^3/d), except where indicated]

		Inflow					Outflow				
Time step	Total time, days	Confining bed storage	Leakage from surficial aquifer	Storage	Constant head (southern boundary)	Well recharge	Confining bed storage	Leakage to surficial aquifer	Storage	Constant head (northern boundary)	Well discharge
10	0.009	168	51,573	8,000	53,523	42,350	424	0	50,090	45,038	60,000
15	.04	206	51,574	2,930	53,523	42,350	1,152	0	44,378	45,038	60,000
20	.1	213	51,575	1,198	53,523	42,350	3,074	0	40,744	45,038	60,000
25	.5	122	51,575	426	53,522	42,350	5,835	0	37,122	45,038	60,000
30	2	51	51,572	118	53,520	42,350	8,062	0	34,509	45,039	60,000
35	7	29	51,566	19	53,339	42,350	13,425	0	28,838	45,040	60,000
40	26	10	51,555	1	51,073	42,350	21,705	0	18,199	45,085	60,000
45	98	0	51,567	0	44,790	42,350	22,510	0	9,867	46,329	60,000
50	365	0	51,639	0	37,594	42,350	18,035	0	2,613	50,934	60,000
Average		2	51,605	4	41,945	42,350	19,968	0	7,512	48,427	60,000

of 11 for the SL/BM aquifer; and at 2 observation points using the high specified head conditions (0, 20 ft) in the surficial aquifer.

Simulated hydrographs at three observation points located on the Charleston peninsula (OP1, OP3, and OP6) using the original model (simulation 5, table 8), the low aquifer transmissivity/high confining unit vertical hydraulic conductivity model (simulation 3, table 8), and the high aquifer transmissivity/low confining unit vertical hydraulic conductivity model (simulation 7, table 8) were generated (fig. 23). These hydrographs indicate the possible range of geohydrologic conditions under which the potentiometric surface of the confined aquifer would exceed the land-surface altitude at these simulated observation points while injecting at a rate of 22 gal/min at all of the proposed production-scale ASR sites. The sensitivity analysis for horizontal anisotropy indicates that reducing horizontal anisotropy in the SL/BM aquifer, in effect, reduced the average transmissivity of the aquifer. This reduction resulted in higher simulated water levels in the area surrounding the injection wells than those simulated by the original model. Increasing the horizontal anisotropy of the SL/BM aquifer caused the opposite effect.

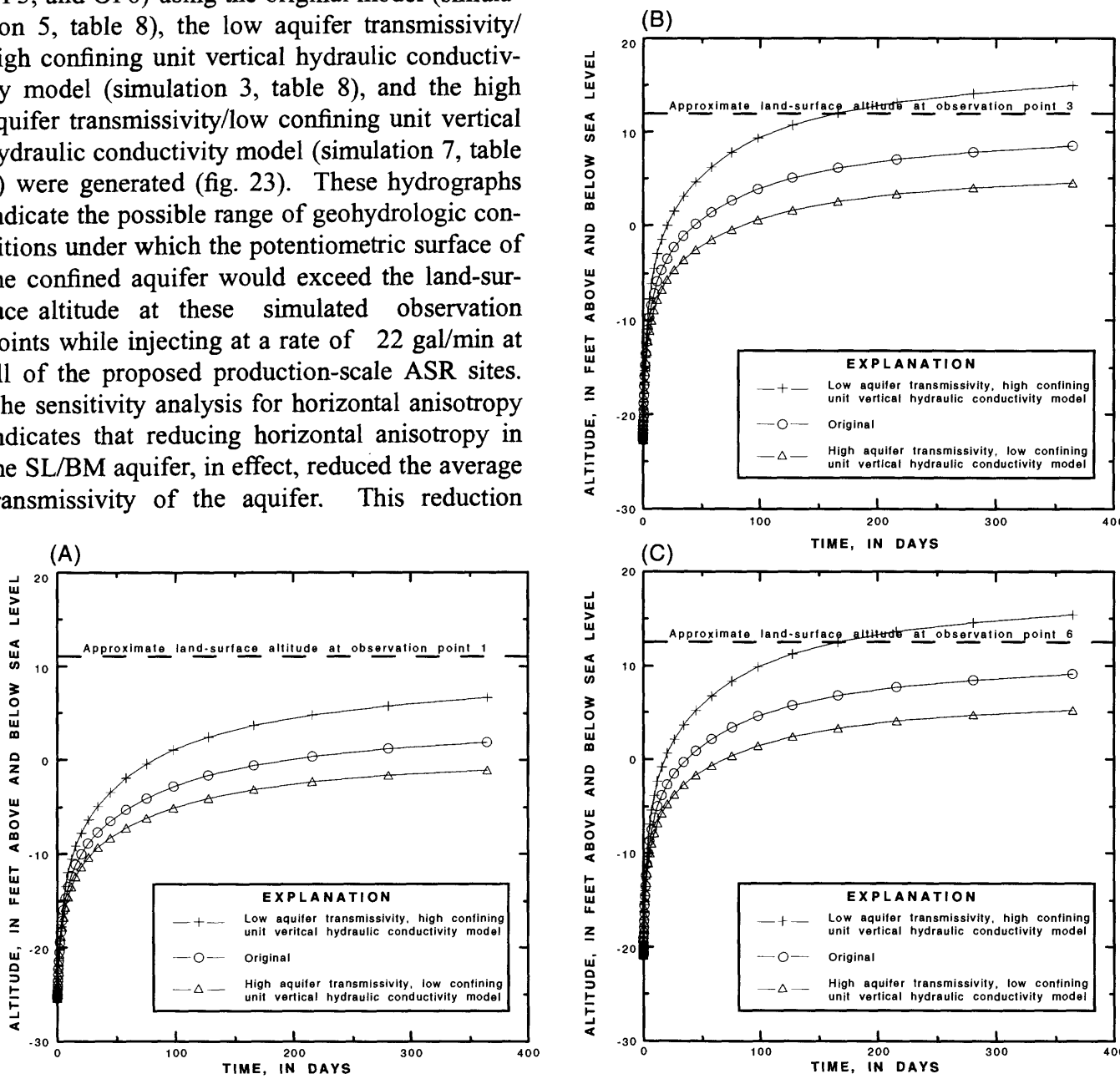

Figure 23. Simulated potentiometric-surface altitude at observation point 1 (A), point 3 (B), and point 6 (C) located on the Charleston peninsula, South Carolina.

An important consideration when planning a production-scale ASR system on the Charleston peninsula is the possible increase in SL/BM aquifer transmissivity over time as a result of the dissolution of soluble minerals within the SL/BM aquifer. Although the maximum possible injection rate at the ASR wells may be limited at first, the effective injection rate perhaps will increase moderately with successive cycles of injection and recovery. To illustrate how an increase in transmissivity could affect allowable injection rates using production-scale ASR wells, a simulation was completed using a transmissivity of 260 ft^2/d for the SL/BM aquifer. All other parameters of the calibrated production-scale model were maintained as previously described. Using an injection rate of 35 gal/min at each production well produced potentiometric levels similar to the original model. This increase in transmissivity would allow an additional 187,000 gal of water to be injected in a day which is equivalent to approximately 68 Mgal of water per year. Although the change in transmissivity over time is unpredictable, model results indicate that an increase in transmissivity can result in an appreciable increase in injection capacity at the production-scale ASR wells.

The heterogeneity of the SL/BM aquifer cannot be evaluated in the Charleston area due to a lack of suitable well data. The uncertainty resulting from this lack of geohydrologic information must be kept in mind when evaluating the results of production-scale ground-water flow model simulations. The purpose of the simulations was to gain an understanding of the possible results of implementing a production-scale ASR program. Based on model simulations and the hydraulic characteristics of the SL/BM aquifer and confining unit, a combined rate of 220 gal/min of water can be injected at ten wells dispersed at various locations on the Charleston peninsula without raising heads above land surface after continually injecting for 1 year. An injection rate of 220 gal/min would result in the storage of 116 Mgal of water per year.

SUMMARY

Aquifer storage recovery technology was evaluated in the city of Charleston, South Carolina, for storing potable water for emergency use. Test wells were installed in the SL/BM aquifer to determine hydrologic and geochemical constraints of applying ASR technology in the Charleston area.

A pilot-scale ASR system was installed and tested to determine the effects of injecting treated surface water into the SL/BM aquifer. The system consisted of a 509-ft deep production/injection well and a 530-ft deep observation well. Water-level and specific conductance data were measured at 5-min intervals at two depths in the observation well (CHN-733). The production well (CHN-736) was equipped with a 10-horsepower submersible pump, injection line, and various sampling ports for injection, recovery, and water-quality sampling.

Tertiary and Quaternary stratigraphy at the ASR site consists of unconsolidated marine clay and sand sediments of the upper Paleocene Black Mingo Group. The Black Mingo Group is unconformably overlain by crystalline biosparruidite of the middle Eocene Santee Limestone. Unconformably overlying the Santee Limestone is the middle-upper Eocene Cross Formation, a white, partially silicified calcilutite. The Cross Formation is unconformably overlain by the upper Eocene to upper Oligocene Cooper Group, a dense olive-green calcarenite/calcilutite. Above the Cooper Group are unconsolidated sands of the Marks Head and Wando Formations.

The SL/BM aquifer consists of the upper 100 ft of the Black Mingo Group and the entire Santee Limestone. At the ASR test site, the aquifer is approximately 70-ft thick with two production zones. Permeability in the upper production zone occurs as carbonate-rock type solution openings in the Santee Limestone from 382 to 396 ft bls. Permeability in the lower production zone occurs in the fracture-dominated, semiconsolidated Black Mingo Group sandstones from 420 to 450 ft bls.

Two aquifer tests were conducted at the pilot-scale test site. The U.S. Geological Survey finite-difference ground-water flow model MODFLOW was used to simulate the January 1995 aquifer test in the SL/BM aquifer. The model simulations considered the surficial aquifer to be a shallow unconfined aquifer, the SL/BM aquifer as a deep confined aquifer, and the Marks Head Formation, Cooper Group, and Cross Formation as a leaky confining unit located between the two aquifers. The model was developed by integrating field-derived initial and boundary conditions into the model and calibrating the model with aquifer-test results. The vertical hydraulic conductivity of the SL/BM confining unit was modeled as $5.0x10^{-4}$ ft/d throughout the layer, except at the location directly above the production well where it was 10,000 ft/d. The transmissivity, storage coefficient, and lateral anisotropy of the SL/BM aquifer were calculated to be 130 ft^2/d, $1.0x10^{-4}$, and 15, respectively.

A sensitivity analysis completed on the calibrated model indicated that the model is most sensitive to variations in transmissivity, storage coefficient, and lateral anisotropy of the confined aquifer. The model is moderately sensitive to variations in the vertical hydraulic conductivity of the confining unit directly above the production well. The model is not very sensitive to variations in the other properties of the confining unit or the initial conditions of the surficial aquifer.

Thirteen cycles of injection, storage, and recovery were conducted at the ASR test site. Variables tested during these cycles were volume of water injected, length of storage time, and injection/recovery rates. Recovery efficiencies were calculated for the amount of water injected and the amount of potable water recovered. Recovery efficiencies generally improved as more water was injected into and recovered from the aquifer. Injection capacity of the aquifer increased over the time of the testing. Injection rates increased from 30 to 100 gal/min and recovery rates increased from 140 to 160 gal/min. The time required for breakthrough of treated surface water at the observation well decreased as the testing progressed. Drawdown and recovery curves changed shape from aquifer tests conducted before and after the injection/recovery testing.

Geochemical data were obtained during storage and recovery in ASR cycles 4 through 9 and 11. These data were interpreted to determine the trends in water-quality changes that occurred during storage and recovery, and possible causes of these water-quality changes. Ground-water samples collected after 0.7- to 6-d storage periods showed water-quality characteristics more closely resembling those of treated surface water than water from the production zones in the SL/BM aquifer. Samples recovered after storage in the aquifer had low ionic strength (less than 0.006) and low specific conductance (less than 550 µS/cm), but had higher pH values (8.2 to 8.8) resulting from dissolution of calcium carbonate in the aquifer. Water-quality characteristics measured in selected ground-water samples indicated that chloride and sulfate concentrations remain below MCL's after 0.7- to 6-d storage periods in the SL/BM aquifer.

The magnitude of water-quality changes that occurred during storage was interpreted using the geochemical model code NETPATH. The dominant geochemical reactions that influenced water quality were dissolution of calcite, halite, and gypsum, and Na^+/Ca^{2+} exchange on clays. Mass-transfer calculations from NETPATH simulations yielded estimates of calcite dissolution that ranged from 0.28 to 0.36 mmol/kg of solution (24.7 mg/kg to 31.7 mg/kg). The magnitude of halite dissolution ranged from 0.84 to 1.52 mmol/kg (49.1 to 88.8 mg/kg). The estimated magnitude of gypsum dissolution ranged from 0.16 to 0.25 mmol/kg (21.8 to 34.0 mg/kg). These data suggest that dissolution of minerals in the SL/BM aquifer enhances aquifer permeability.

Water-quality changes that occurred during recovery were interpreted using the geochemical model code PHREEQE. Using dissolved chloride as a conservative tracer of SL/BM aquifer water, a mixing line was developed from different mixture percentages of SL/BM aquifer water and treated

surface water. Chloride concentrations in simulated mixtures of SL/BM aquifer water and treated surface water were compared to measured chloride concentrations in ground-water samples collected during recovery to estimate the percentage of SL/BM aquifer water in each sample. Samples collected early during recovery consisted of 1 to 7 percent SL/BM aquifer water. Considering simulations of all aquifer storage recovery samples, when 80 to 90 percent of the injectant was withdrawn, ground-water samples consisted of approximately 100 percent of SL/BM aquifer water.

A second ground-water flow model was developed, which used most of the hydrologic properties as the January 1995 aquifer-test model to determine the feasibility of injecting water at 10 ASR sites across the Charleston peninsula. This production-scale model used a uniform vertical hydraulic conductivity of 5.0×10^{-5} ft/d to simulate the SL/BM confining unit. Higher vertical hydraulic conductivities allowed too much leakage to flow into the SL/BM aquifer. Ten sites were chosen across the Charleston peninsula in open areas such as city parks near available city water sources. The effects of implementing this ASR system was modeled at eight observation points interspersed with the ten ASR injection wells. The model allowed a uniform injection rate of 22 gal/min at each of the ten ASR wells without the resultant potentiometric surface exceeding the land-surface altitude at the observation points.

The variability of the SL/BM aquifer transmissivity and the vertical hydraulic conductivity of the confining unit were tested in a sensitivity analysis and the altitudes at the eight observation wells were tabulated. Results from the sensitivity analysis indicated that a transmissivity value equal to or greater than 130 ft^2/d allowed a total injection rate of 220 gal/min in the ten production wells without producing a potentiometric surface that exceeded the land surface altitude. At this injection rate, approximately 116 Mgal of water can be injected into the SL/BM aquifer in 1 year. Additional simulations indicate that increases in transmissivity could accommodate appreciable increases in the injection rates at the simulated ASR wells.

REFERENCES

Abbott, W.A., and Huddleston, P.C., 1980, The Miocene of South Carolina, in DuBar, J.R., DuBar, S.S., Ward, L.W., and Blackwelder, B.W., Cenozoic biostratigraphy of the Carolina outer Coastal Plain: Geological Society of America Field Trip Guidebook 9, p. 208-210.

Aucott W.A., and Newcome R., Jr., 1986, Selected aquifer-test information for the Coastal Plain aquifers of South Carolina: U.S. Geological Survey Water-Resources Investigation Report 86-4159, 30 p.

Aucott, W.A., and Speiran, G.K., 1985a, Potentiometric surfaces of the Coastal Plain aquifers of South Carolina prior to development: U.S. Geological Survey Water-Resources Investigation Report 84-4208, 5 sheets.

Aucott, W.A., and Speiran, G.K., 1985b, Potentiometric surfaces of November 1982 and declines in the potentiometric surfaces between the period prior to development and November 1982 for the Coastal Plain aquifers of South Carolina: U.S. Geological Survey Water Resources Investigation Report 84-4215, 7 sheets.

Bollinger, G.A., 1977, Reinterpretation of the intensity data for the 1886 Charleston, South Carolina earthquake, *in* Rankin D.W., ed., Studies related to the Charleston, South Carolina, earthquake of 1886-A preliminary report: U.S. Geological Survey Professional Paper 1028, p. 17-32.

Campbell, B.G. and Gohn, G.S., 1994, Stratigraphic framework for geologic and geohydrologic studies of the subsurface Cretaceous section near Charleston, South Carolina: U.S. Geological Survey Miscellaneous Field Investigation 2273, 2 sheets.

Chapelle, F.H., Zelibor, J.L., Jr., Grimes, D.J., and Knobel, L.L., 1987, Bacteria in deep coastal plain sediments of Maryland: A possible source of CO_2 to groundwater: Water Resources Research, v. 23, no. 8, p. 1625-1632.

Drever, J.I., 1988, The Geochemistry of Natural Waters, 2nd edition. Prentice Hall, 437 p.

Fronabarger, A.K., Katuna, M.P., and Conlon, K.J., 1995, Biostratigraphic and lithostratigraphic analyses of the Cooper Group (upper Eocene to upper Oligocene) within the lower Coastal Plain of South Carolina: Geological Society of America Abstracts with Programs, v. 27, no. 2, p. 54.

Garza, R., and Krause, R.E., 1992, Water-supply potential of major streams and the Upper Floridan Aquifer in the vicinity of Savannah, Georgia: U.S. Geological Survey Open-File Report 92-629, 49 p.

Gohn, G.S., Higgins, B.B., Smith, C.C., and Owens, J.P., 1977, Lithostratigraphy of the deep corehole (Clubhouse Crossroads Corehole 1) near Charleston, South Carolina: *in* Rankin, D.W., ed., Studies related to the Charleston, South Carolina, earthquake of 1886-A preliminary report: U.S. Geological Survey Professional Paper 1028, p. 59-70.

Hach Company, 1989, Water analysis handbook, Loveland, Colorado, 689 p.

Leake, S.A., Leahy, P.P., and Navoy, S.N., 1994, Documentation of a computer program to simulate transient leakage from confining units using the modular finite-difference ground-water flow model: U.S. Geological Survey Open-File Report 94-59, 70 p.

Lohman, S.W., 1979, Ground-water hydraulics: U.S. Geological Survey Professional Paper 708, 70 p.

McCartan, Lucy, Weems, R.E., and Lemon, E.M., Jr., 1980, The Wando Formation (Upper Pleistocene) in the Charleston, South Carolina area, *in* Contributions to Stratigraphy: U.S. Geological Survey Bulletin 1502-A, p. A110-A116

McDonald, M.G., and Harbaugh, A.H., 1988, A modular three-dimensional finite-difference ground-water flow model: U.S. Geological

Survey Techniques of Water-Resources Investigations, book 6, chap. A1, 586 p.

Meadows, J.K., 1987, Ground-water conditions in the Santee Limestone and Black Mingo Formation near Moncks Corner, Berkeley County South Carolina: South Carolina Water Resources Commission Report 156, 38 p.

Mirecki, J.E., Conlon, K.J., and Campbell, B.G., 1995, Geochemical evolution of injected municipal water during an aquifer storage and recovery project, Charleston, South Carolina: Eos Transactions American Geophysical Union, 76 (17), Spring Meeting Supplement, S123.

Motz, L.H., 1992, Salt-water upconing in an aquifer overlain by a leaky confining bed: Ground Water, v. 30, no. 2, p. 192-198.

Newcome, Roy, Jr., 1993, Pumping tests of the coastal plain aquifers in South Carolina with a discussion of aquifer and well characteristics: South Carolina Water Resources Commission Report Number 174, 52 p.

Park, A.D., 1985, The ground-water resources of Charleston, Berkeley, and Dorchester Counties, South Carolina: South Carolina Water Resources Commission Report Number 139, 145 p.

Parkhurst, D.L, Thorstenson, D.C., and Plummer, L.N., 1980, PHREEQE - A computer program for geochemical calculations: U.S. Geological Survey Water-Resources Investigations Report 80-96, 195 p.

Purvis, J.C., 1989, Hurricane Hugo (1989): South Carolina Water Resources Commission, Columbia, S.C., State Climatology Series Report Number 6-37, 49 p.

Plummer, L.N., Prestemon, E.C., and Parkhurst, D.L., 1994, An interactive code (NETPATH) for modeling NET geochemical reactions along a flow PATH, version 2.0: U.S. Geological Survey Water-Resources Investigations Report 94-4169, 130 p.

Pyne, R.D.G., 1995, Groundwater recharge and wells: a guide to aquifer storage recovery: Lewis Publishers, 376 p.

Reilly, T.E., and Goodman, A.S., 1985, Quantitative analysis of saltwater-freshwater relationships in groundwater systems-a historical perspective: Journal of Hydrology, v. 80, p. 125-160.

Sanford, W.E. and Konikow, L.F., 1989, Simulation of calicite dissolution and porosity changes in saltwater mixing zones in coastal aquifers: Water Resources Research, v. 25 (4), p. 655-667.

Sloan, Earle, 1908, Catalog of mineral localities of South Carolina: South Carolina Geological Survey Bulletin 2, 451 p.

U.S. Environmental Protection Agency, 1988, Secondary maximum contaminant levels (section 143.3 of part 143, national secondary drinking water regulations): U.S. Code of Federal Regulations, Title 40, Parts 100 to 149, p. 608.

U.S. Geological Survey, 1958, Charleston, S.C., quadrangle: 7.5-minute series topographic map, scale 1:24,000, contour interval 5 feet.

Ward, L.W., Blackwelder, B.W., Gohn, G.S., and Poore, R.Z., 1979, Stratigraphic revision of Eocene, Oligocene and lower Miocene formations of South Carolina: Geologic Notes, v. 23, no. 1, p. 2-23.

Weems, R.E., and Lemon, E.M., Jr., 1984, Geologic Map of the Mount Holly quadrangle, Berkeley and Charleston Counties, South Carolina: U.S. Geological Survey Geologic Quadrangle Map GQ-1579, scale 1:24,000.

Wehmiller, J.F., and Belknap, D.F., 1982, Amino acid age estimates, Quaternary Atlantic Coastal Plain: Comparison of U-series dates, biostratigraphy, and paleomagnetic control: Quaternary Research, v. 18, p. 311-336.

Wigley, T.M.L., and Plummer, L.N., 1976, Mixing of carbonate waters: Geochimica et Cosmochimica Acta, v. 40, 989-995.

APPENDIX 1

Volumes of treated surface water recovered during selected aquifer storage recovery cycles

Appendix 1. Volumes of treated surface water recovered during selected aquifer storage recovery cycles

[ASR, aquifer storage recovery; min, minute; gal, gallon; gal/min, gallons per minute; TVI, total volume injected; TVR, total volume recovered]

ASR cycle number	Recovery sample number	Time since start of recovery (min)	Volume recovered (gal)	Percentage recovered	Comments
1	PR736-08	5	650	4	Recovery rate: 130 gal/min
	PR736-09	107	13,910	92	Injection rate: 30 gal/min
					TVI: 15,132 gal
					TVR: 19,014 gal
2	PR736-10	10	1,300	6	Recovery rate: 130 gal/min
	PR736-11	135	17,415	77	Injection rate: 30 gal/min
	PR736-12	190	24,100	107	TVI: 22,492 gal
					TVR: 26,838 gal
4	PR736-14	9	1,260	9	Recovery rate: 130 gal/min
	PR736-15	19	2,660	18	Injection rate: 30 gal/min
	PR736-16	27	3,780	26	TVI: 14,832 gal
	PR736-17	38	5,070	34	TVR: 17,675 gal
	PR736-18	52	6,890	47	
	PR736-19	68	8,840	60	
	PR736-20	105	13,650	92	
	PR736-21	125	16,250	110	
5	PR736-22	6	780	5	Recovery rate: 130 gal/min
	PR736-23	26	3,380	22	Injection rate: 30 gal/min
	PR736-24	41	5,330	34	TVI: 15,535 gal
	PR736-25	57	7,410	48	TVR: 17,847 gal
	PR736-26	84	10,771	69	
	PR736-27	115	14,511	93	
	PR736-28	130	16,900	109	
6	PR736-29	10	1,300	3	Recovery rate: 130 gal/min

Appendix 1. Volumes of treated surface water recovered during selected aquifer storage recovery cycles--Continued

[ASR, aquifer storage recovery; min, minute; gal, gallon; gal/min, gallons per minute; TVI, total volume injected; TVR, total volume recovered]

ASR cycle number	Recovery sample number	Time since start of recovery (min)	Volume recovered (gal)	Percentage recovered	Comments
6	PR736-30	29	3,770	8	Injection rate: 30 gal/min
	PR736-31	150	19,500	39	TVI: 49,966 gal
	PR736-32	215	27,950	56	TVR: 50,362 gal
	PR736-33	265	34,450	69	
	PR736-34	335	43,550	87	
	PR736-35	380	49,400	99	
7	PR736-36	9	1,170	3	Recovery rate: 130 gal/min
	PR736-37	47	6,110	16	Injection rate: 30 gal/min
	PR736-38	105	13,650	37	TVI: 37,355 gal
	PR736-39	190	24,758	66	TVR: 37,998 gal
	PR736-40	245	31,850	85	
	PR736-41	290	37,848	101	
8	PR736-48	8	1,040	1	Recovery rate: 130 gal/min
	PR736-49	42	5,460	6	Injection rate: 30 gal/min
	PR736-50	97	12,610	14	TVI: 88,406 gal
	PR736-51	205	26,650	30	TVR: 89,573 gal
	PR736-52	270	35,100	40	
	PR736-53	365	47,450	54	
	PR736-54	660	87,100	99	
9	PR736-58	11	1,540	1	Recovery rate: 135 gal/min
	PR736-59	75	10,500	7	Injection rate: 40 gal/min
	PR736-60	150	21,000	13	TVI: 160,154 gal
	PR736-61	390	53,900	34	TVR: 191,584 gal
	PR736-62	650	91,000	57	
	PR736-63	1070	149,800	94	

Appendix 1. Volumes of treated surface water recovered during selected aquifer storage recovery cycles--Continued

[ASR, aquifer storage recovery; min, minute; gal, gallon; gal/min, gallons per minute; TVI, total volume injected; TVR, total volume recovered]

ASR cycle number	Recovery sample number	Time sincstart of recovery (min)	Volume recovered (gal)	Percentage recovered	Comments
10					Recovery rate: 140 gal/min
					Injection rate: 18 gal/min
					TVI: 443,302 gal
					TVR: 191,584 gal
11	PR736-71	90	13,500	3	Recovery rate: 150 gal/min
	PR736-72	1,170	176,228	43	Injection rate: 18 gal/min
	PR736-73	1,290	193,500	48	TVI: 405,423 gal
	PR736-74	1,570	236,592	58	TVR: 451,440 gal
	PR736-75	2,940	441,000	109	
12a					Recovery rate: 158 gal/min
					Injection rate: 60 gal/min
					TVI: 88,211 gal
					TVR: 97,202 gal
12b					Recovery rate: 119 gal/min
					Injection rate: 60 gal/min
					TVI: 95,130 gal
					TVR: 105,116 gal
13a					Recovery rate: 160 gal/min
					Injection rate: 60 gal/min
					TVI: 98,795 gal
					TVR: 50,677 gal
13b					Recovery rate: 160 gal/min
					Injection rate: 60 gal/min

Appendix 1. Volumes of treated surface water recovered during selected aquifer storage recovery cycles--Continued

[ASR, aquifer storage recovery; min, minute; gal, gallon; gal/min, gallons per minute; TVI, total volume injected; TVR, total volume recovered]

ASR cycle number	Recovery sample number	Time since start of recovery (min)	Volume recovered (gal)	Percentage recovered	Comments
13b					TVI: 106,597 gal
					TVR: 68,809 gal
13c					Recovery rate: 160 gal/min
					Injection rate: 60 gal/min
					TVI: 101,915 gal
					TVR: 86,761 gal
13d					Recovery rate: 160 gal/min
					Injection rate: 60 gal/min
					TVI: 1,048,120 gal
					TVR: 555,038 gal

APPENDIX 2

Dissolved inorganic constituent concentrations and water-quality characteristics measured in groundwater samples collected during recovery in aquifer storage recovery cycles 4 through 9 and 11

Appendix 2. Dissolved inorganic constituent concentrations and water-quality characteristics measured in ground-water samples collected during recovery in aquifer storage recovery cycles 4 through 9 and 11

[ASR, aquifer storage recovery; °C, degrees Celsius; su, standard units; µS/cm, microsiemens per centimeter; mg/L, milligrams per Liter; $CaCO_3$, calcium carbonate; CO_2, carbon dioxide; --- indicates data missing; NA, not applicable]

ASR cycle number	Sample number	Temperature (°C)	pH (su)	Specific conductance (µS/cm)	Calcium, dissolved (mg/L)	Sodium, dissolved (mg/L)	Magnesium, dissolved (mg/L)	Potassium, dissolved (mg/L)	Chloride, dissolved (mg/L)
4	PR736-15	24.8	8.8	470	15	73	1.8	4.9	65
	PR736-16	24.5	8.8	609	14	110	2.1	5.9	91
	PR736-17	24.5	8.8	857	14	150	2.8	7.5	150
	PR736-18	24.3	8.6	1,180	16	210	3.8	9.8	230
	PR736-19	24.3	8.4	1,720	22	350	6.5	15	380
	PR736-20	24.3	7.8	3,460	35	690	13	25	820
	PR736-21	24.3	7.7	4,380	40	890	17	35	1,100
5	PR736-22	23.5	8.3	352	14	41	1.6	3.2	36
	PR736-23	24.9	8.6	534	14	83	1.8	5.0	79
	PR736-24	24.8	8.6	778	15	140	2.3	6.9	130
	PR736-25	24.7	8.5	1,120	18	200	3.5	9.7	220
	PR736-26	24.5	8.1	2,080	27	390	8.0	16	470
	PR736-27	24.4	7.7	3,510	40	700	16	25	860
	PR736-28	24.3	7.6	4,110	43	760	18	29	1,000
6	PR736-29	25.1	8.2	282	18	32	1.5	3.0	21
	PR736-30	25.3	8.5	377	17	52	1.7	3.9	41

Appendix 2. Dissolved inorganic constituent concentrations and water-quality characteristics measured in ground-water samples collected during recovery in aquifer storage recovery cycles 4 through 9 and 11--Continued

[ASR, aquifer storage recovery; °C, degrees Celsius; su, standard units; µS/cm, microsiemens per centimeter; mg/L, milligrams per Liter; $CaCO_3$, calcium carbonate; CO_2, carbon dioxide; --- indicates data missing; NA, not applicable]

ASR cycle number	Sample number	Temperature (°C)	pH (su)	Specific conductance (µS/cm)	Calcium, dissolved (mg/L)	Sodium, dissolved (mg/L)	Magnesium, dissolved (mg/L)	Potassium, dissolved (mg/L)	Chloride, dissolved (mg/L)
6	PR736-31	25.0	8.4	1,010	18	180	3.3	8.6	180
	PR736-32	24.7	8.2	1,570	22	280	5.4	13	330
	PR736-33	24.6	7.9	2,380	29	450	9.1	19	510
	PR736-34	24.5	7.6	3,580	38	680	15	28	890
	PR736-35	24.4	7.6	4,240	40	810	19	32	1,000
7	PR736-36	25.0	8.2	289	20	32	1.7	3.2	22
	PR736-37	25.5	8.5	438	16	67	1.8	4.6	58
	PR736-38	25.3	8.5	708	16	120	2.5	7.1	120
	PR736-39	24.9	8.1	1,660	26	300	6.1	14	360
	PR736-40	24.7	7.8	2,690	35	500	10	22	650
	PR736-41	24.6	7.6	3,470	40	660	15	28	880
8	PR736-48	24.4	8.3	294	19	30	1.5	2.9	20
	PR736-49	25.1	8.3	385	19	50	1.5	4.2	42
	PR736-50	25.1	8.3	512	18	77	1.9	5.8	73
	PR736-51	25.0	8.3	792	19	130	2.6	8.0	140
	PR736-52	24.9	8.3	1,010	20	170	3.4	9.4	190
	PR736-53	24.8	8.1	1,460	24	260	5.0	13	320

Appendix 2. Dissolved inorganic constituent concentrations and water-quality characteristics measured in ground-water samples collected during recovery in aquifer storage recovery cycles 4 through 9 and 11--Continued

[ASR, aquifer storage recovery; °C, degrees Celsius; su, standard units; µS/cm, microsiemens per centimeter; mg/L, milligrams per Liter; $CaCO_3$, calcium carbonate; CO_2, carbon dioxide; --- indicates data missing; NA, not applicable]

ASR cycle number	Sample number	Temperature (°C)	pH (su)	Specific conductance (µS/cm)	Calcuim, dissolved (mg/L)	Sodium, dissolved (mg/L)	Magnesium, dissolved (mg/L)	Potassium, dissolved (mg/L)	Chloride, dissolved (mg/L)
8	PR736-54	24.4	7.4	3,900	51	740	21	31	990
9	PR736-58	24.1	---	298	20	33	1.7	4.2	26
	PR736-59	24.3	8.4	316	16	39	1.4	4.5	28
	PR736-60	24.3	8.4	382	16	51	1.4	5.3	45
	PR736-61	24.3	8.2	760	21	120	2.5	8.4	140
	PR736-62	24.2	7.9	1,610	29	280	5.5	15	350
	PR736-63	24.1	7.6	3,320	38	630	13	27	810
11	PR736-71	19.8	8.8	278	25	20	2.5	2.7	21
	PR736-72	21.9	8.3	1,500	20	260	4.9	12	310
	PR736-73	21.9	8.2	1,690	23	300	5.9	14	360
	PR736-74	22.2	8.0	2,180	25	390	7.2	17	490
	PR736-75	22.7	7.4	4,450	35	850	17	30	1,100
NA	[1]PI736-66	22.6	7.2	174	18	9.0	1.2	1.5	11
NA	[2]OB733-3	26.0	8.0	1,690	39	280	12	14	310
NA	[3]OB733-4	23.2	8.0	3,450	22	700	17	26	800
NA	[4]PB736-6	24.0	7.9	6,530	40	1,300	32	40	1,700

[1]Treated surface-water sample.
[2]Upper-production zone ground-water sample.
[3]Composite upper-production zone/lower-production zone ground-water sample.
[4]Santee Limestone/Black Mingo aquifer ground-water sample.

Appendix 2. Dissolved inorganic constituent concentrations and water-quality characteristics measured in ground-water samples collected during recovery in aquifer storage recovery cycles 4 through 9 and 11--Continued

[ASR, aquifer storage recovery; °C, degrees Celsius; su, standard units, µS/cm, microsiemens per centimeter; mg/L, milligrams per Liter; $CaCO_3$, calcium carbonate; CO_2, carbon dioxide; --- indicates data missing; NA, not applicable]

ASR cycle number	Sample number	Sulfate, dissolved (mg/L)	Fluoride, dissolved (mg/L)	Silica, dissolved (mg/L)	Iron, dissolved (mg/L)	Strontium, dissolved (mg/L)	Dissolved solids residue at 180 °C (mg/L)	Alkalinity (mg/L as $CaCO_3$)	Inorganic carbon, dissolved (mg/L as CO_2)
4	PR736-15	57	1.4	11	3	73	274	65	41.6
	PR736-16	60	1.5	13	5	92	346	82	48.0
	PR736-17	65	1.7	15	8	120	470	110	69.9
	PR736-18	78	1.9	17	4	160	660	142	112
	PR736-19	92	1.9	20	6	260	994	191	104
	PR736-20	140	1.5	26	7	560	1,950	335	223
	PR736-21	160	1.5	30	6	760	2,440	407	294
5	PR736-22	46	1.0	10	6	56	190	50	48.2
	PR736-23	60	1.2	12	3	75	318	76	76.1
	PR736-24	66	1.6	15	3	100	439	104	86.9
	PR736-25	75	1.7	17	3	150	622	137	108
	PR736-26	100	1.7	22	4	300	1,160	219	168
	PR736-27	140	1.4	28	14	560	1,980	329	254
	PR736-28	160	1.2	30	5	670	2,320	376	338
6	PR736-29	50	1.0	9.7	4	55	171	43	61.3
	PR736-30	51	1.0	10	3	64	221	54	49.6

Appendix 2. Dissolved inorganic constituent concentrations and water-quality characteristics measured in ground-water samples collected during recovery in aquifer storage recovery cycles 4 through 9 and 11--Continued

[ASR, aquifer storage recovery; °C, degrees Celsius; su, standard units, µS/cm, microsiemens per centimeter; mg/L, milligrams per Liter; $CaCO_3$, calcium carbonate; CO_2, carbon dioxide; --- indicates data missing; NA, not applicable]

ASR cycle number	Sample number	Sulfate, dissolved (mg/L)	Fluoride, dissolved (mg/L)	Silica, dissolved (mg/L)	Iron, dissolved (mg/L)	Strontium, dissolved (mg/L)	Dissolved solids residue at 180 °C (mg/L)	Alkalinity (mg/L as $CaCO_3$)	Inorganic carbon, dissolved (mg/L as CO_2)
6	PR736-31	70	1.5	16	4	130	565	119	126
	PR736-32	85	1.7	19	3	200	887	172	170
	PR736-33	110	1.6	23	5	320	1,320	238	216
	PR736-34	140	1.5	28	8	540	2,010	338	307
	PR736-35	160	1.0	33	9	590	2,360	389	340
7	PR736-36	50	1.2	10	5	53	192	50	41.9
	PR736-37	52	1.2	12	3	60	260	68	59.0
	PR736-38	61	1.4	15	3	77	390	93	91.6
	PR736-39	87	1.6	20	3	180	910	181	183
	PR736-40	120	1.5	25	3	320	320	265	271
	PR736-41	140	1.4	24	4	450	1,970	325	338
8	PR736-48	47	1.1	83	86	60	157	46	41.9
	PR736-49	54	1.2	97	3	70	212	57	41.6
	PR736-50	56	1.2	12	3	80	279	69	51.4
	PR736-51	65	1.4	15	3	100	433	101	87.1
	PR736-52	71	1.5	16	81	120	556	123	91.7
	PR736-53	85	1.6	19	35	180	822	169	126

Appendix 2. Dissolved inorganic constituent concentrations and water-quality characteristics measured in ground-water samples collected during recovery in aquifer storage recovery cycles 4 through 9 and 11--Continued

[ASR, aquifer storage recovery; °C, degrees Celsius; su, standard units, µS/cm, microsiemens per centimeter; mg/L, milligrams per Liter; $CaCO_3$, calcium carbonate; CO_2, carbon dioxide; --- indicates data missing; NA, not applicable]

ASR cycle number	Sample number	Sulfate, dissolved (mg/L)	Fluoride, dissolved (mg/L)	Silica, dissolved (mg/L)	Iron, dissolved (mg/L)	Strontium, dissolved (mg/L)	Dissolved solids residue at 180 °C (mg/L)	Alkalinity (mg/L as $CaCO_3$)	Inorganic carbon, dissolved (mg/L as CO_2)
8	PR736-54	150	1.3	34	17	770	2,190	357	298
9	PR736-58	51	.9	9.1	14	65	185	50	106
	PR736-59	48	1.1	9.7	92	60	179	55	160
	PR736-60	49	1.2	11	13	60	218	58	126
	PR736-61	60	1.3	15	18	100	419	95	227
	PR736-62	86	1.4	20	14	210	210	171	335
	PR736-63	140	1.4	29	14	480	1,860	313	---
11	PR736-71	44	1.0	9.2	3	70	152	43	300
	PR736-72	10	2.4	19	12	190	816	158	131
	PR736-73	86	2.4	21	3	220	922	174	240
	PR736-74	100	2.4	22	3	290	1,200	214	214
	PR736-75	160	2.5	30	3	660	2,460	400	480
NA	[1]PI736-66	36	.8	7.4	88	40	112	21	8.5
NA	[2]OB733-3	110	1.2	50	7	530	965	247	---
NA	[3]OB733-4	220	2.3	39	4	640	2,020	393	150
NA	[4]PB736-6	220	.8	44.8	3	1,600	3,760	584	438

[1]Treated surface-water sample.
[2]Upper-production zone ground-water sample.
[3]Composite upper-production zone/lower-production zone ground-water sample.
[4]Santee Limestone/Black Mingo aquifer ground-water sample.

APPENDIX 3

Selected dissolved inorganic constituent concentrations and water-quality characteristics measured in ground-water samples collected during storage in aquifer storage recovery cycle 13d

Appendix 3. Selected dissolved inorganic constituent concentrations and water-quality characteristics measured in ground-water samples collected during storage in aquifer storage recovery cycle 13d

[°C, degrees Celsius; mg/L, milligrams per Liter; $CaCO_3$, calcium carbonate; µS/cm, microsiemens per centimeter; CO_2, carbon dioxide; --indicates data missing or not analyzed]

Sample number	Storage duration (days)	Temperature (°C)	pH, field	pH, lab	Alkalinity (mg/L as $CaCO_3$)	Specific conductance (µS/cm)	Calcium, dissolved (mg/L)	Sodium, dissolved (mg/L)	Chloride, dissolved (mg/L)	Sulfate, dissolved (mg/L)	Fluoride, dissolved (mg/L)	Silica, dissolved (mg/L)	Inorganic carbon, dissolved (mg/L as CO_2)
OB733-76	0.2	20.3	9.2	6.8	54	331	14.5	34.6	38	41.2	0.97	8.0	30.2
OB733-77	6.0	28.5	8.1	8.4	258	625	14.4	12.8	162	68.4	1.5	16	63.8
OB733-78	14.0	22.9	8.2	7.9	218	1,120	16.5	200.0	288	104.5	1.6	19	130.2
OB733-79	20.0	24.7	7.5	8.0	209	1,153	18.0	200.0	303	119.1	1.7	21	135.8
OB733-80	27.0	24.6	8.3	--	234	1,347	11.0	208.0	346	96.3	1.6	19	134.3
OB733-81	42.0	23.3	8.2	--	148	1,140	--	262.0	383	122.9	1.9	21	170.2
OB733-82	55.0	25.8	8.0	--	410	1,490	56.6	817.0	1,002	210.0	3.0	34	333.3

NOTE: All laboratory analyses were performed at the Charleston Commission of Public Works laboratory except for dissolved inorganic carbon measurements, which were performed in the U.S. Geological Survey laboratory in Columbia, South Carolina.

APPENDIX 4

Dissolved oxygen concentrations measured in ground-water samples collected during recovery in aquifer storage recovery cycles 2, 4, 5, 6, 7, 8, and 11

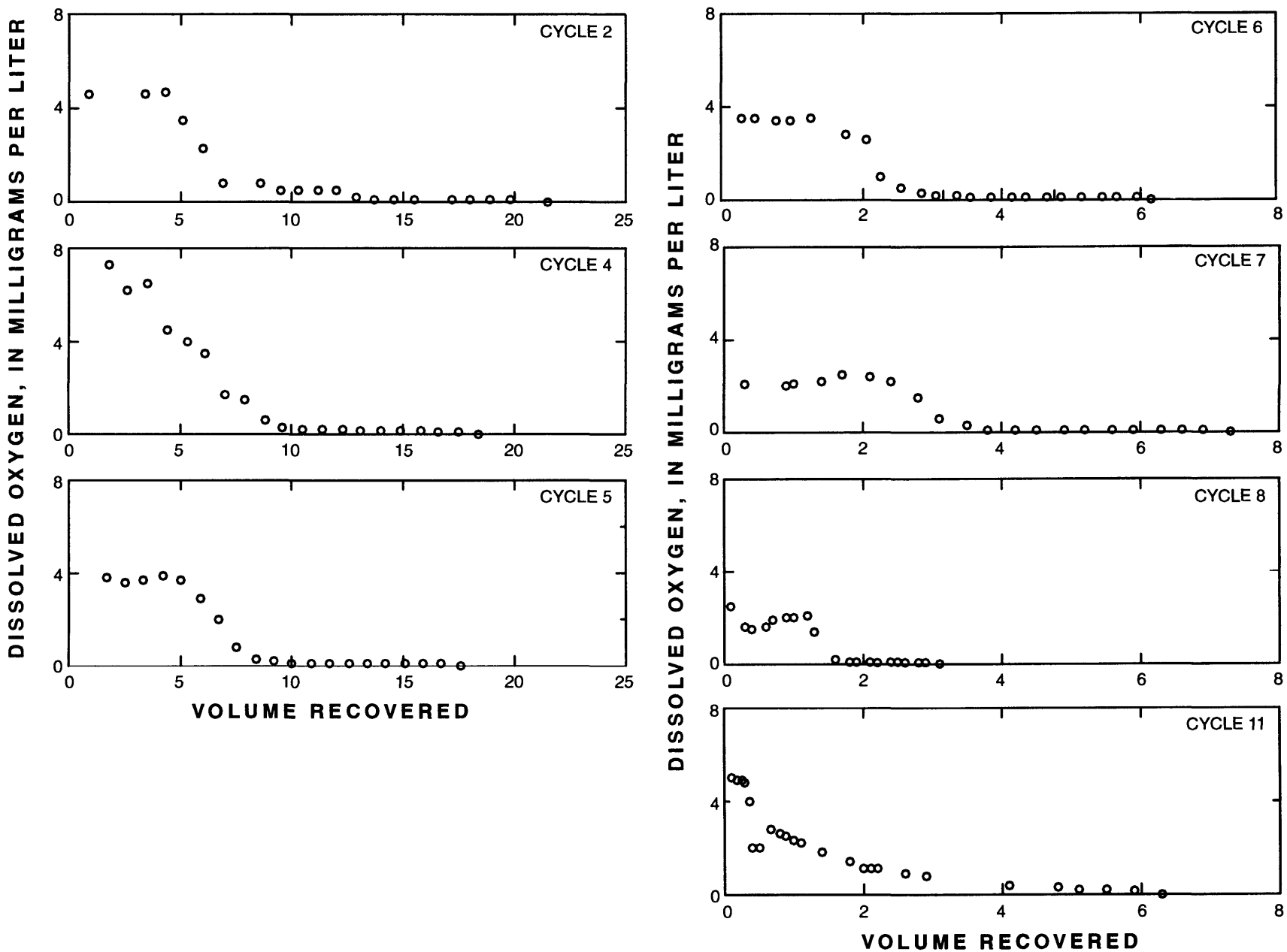

Appendix 4. Dissolved oxygen concentrations measured in ground-water samples collected during recovery in aquifer storage recovery cycles 2, 4, 5, 6, 7, 8, and 11.

APPENDIX 5

Dissolved hydrogen sulfide and chlorine concentrations measured in ground-water samples collected during recovery in aquifer storage recovery cycles 2, 4, 5, 6, 12, and 13

Appendix 5. Dissolved hydrogen sulfide and chlorine concentrations measured in ground-water samples collected during recovery in aquifer storage recovery cycles 2, 4, 5, 6, 12, and 13

[ASR, aquifer storage recovery; min, minute; gal, gallon; mg/L, milligrams per Liter; -- indicates data missing; <, less than]

ASR cycle number	Time since start of recovery (min)	Volume recovered (gal)	Percent volume recovered	Hydrogen sulfide, dissolved (mg/L)	Chlorine, dissolved (mg/L)
2	22	2,860	19	0.318	--
	105	13,650	20	.212	--
4	17	2,210	15	.106	--
	19	2,470	17	.212	--
	36	4,680	32	.200	--
	85	11,050	75	.212	--
	130	16,900	114	.424	--
5	154	20,020	128	.106	--
6	330	42,900	86	.053	--
12a	225	35,550	40	.070	--
12b	35	4,165	4	--	<0.1
	45	5,355	6	--	<.1
13a	5	800	.8	--	4.0
	14	2,240	2	--	1.0
	22	3,520	4	--	.4
	35	5,600	6	--	<.1
13b	3	480	.5	--	3.0
	11	1,760	2	--	1.5
	21	3,360	3	--	.4
	25	4,000	4	.031	--
	29	4,640	5	--	<.1
13c	6	960	.9	--	3.0
	13	2,080	2	--	1.0
	21	3,360	3	--	.4
	35	5,600	6	--	<.1

APPENDIX 6

Dissolved trihalomethane and methane concentrations measured in ground-water samples collected during aquifer storage recovery cycles 2, 4 through 11, and 13

Appendix 6. Dissolved trihalomethane and methane concentrations measured in ground-water samples collected during aquifer storage recovery cycles 2, 4 through 11, and 13

[ASR, aquifer storage recovery; µg/L, micrograms per Liter; mg/L, milligrams per Liter; NA, not applicable; ND, below detection limit of 0.01 mg/L]

ASR cycle number	Sample number	Percent volume recovered	Percent volume injected	Trihalomethane, dissolved (µg/L)	Methane, dissolved (mg/L)
2	PR736-10	6	NA	28	ND
	PR736-11	77	NA	17	ND
	PR736-12	107	NA	11	ND
4	[1]PI736-13	NA	23	130	ND
	PR736-14	9	NA	156	ND
	PR736-16	26	NA	91	ND
	PR736-18	47	NA	111	ND
	PR736-20	92	NA	61	ND
5	PR736-22	5	NA	53	ND
	PR736-23	22	NA	109	ND
	PR736-24	34	NA	85	ND
	PR736-25	48	NA	103	ND
	PR736-26	69	NA	44	ND
	PR736-27	93	NA	52	ND
	PR736-28	109	NA	35	ND
6	PR736-29	3	NA	108	ND
	PR736-30	8	NA	96	ND
	PR736-31	39	NA	76	ND
	PR736-32	56	NA	64	ND
	PR736-33	69	NA	11	ND
	PR736-34	87	NA	39	ND
	PR736-35	99	NA	31	ND
7	[2]OI733-36	NA	95	4	ND
	PR736-36	3	NA	108	ND

Appendix 6. Dissolved trihalomethane and methane concentrations measured in ground-water samples collected during aquifer storage recovery cycles 2, 4 through 11, and 13--Continued

[ASR, aquifer storage recovery; µg/L, micrograms per Liter; mg/L, milligrams per Liter; NA, not applicable; ND, below detection limit of 0.01 mg/L]

ASR cycle number	Sample number	Percent volume recovered	Percent volume injected	Trihalomethane, dissolved (µg/L)	Methane, dissolved (mg/L)
7	PR736-37	16	NA	83	ND
	PR736-38	37	NA	75	ND
	PR736-39	66	NA	59	ND
	PR736-40	85	NA	46	ND
	PR736-41	101	NA	36	ND
8	[2]OI733-42	NA	37	27	ND
	[2]OI733-43	NA	65	49	ND
	[1]PI736-44	NA	65	80	ND
	[2]OI733-45	NA	98	36	ND
	[3]OI733-46	NA	NA	4.3	ND
	PR736-48	1	NA	51	ND
	PR736-49	6	NA	56	ND
	PR736-50	14	NA	133	ND
	PR736-51	30	NA	75	ND
	PR736-52	40	NA	88	ND
	PR736-53	54	NA	45	ND
	PR736-54	99	NA	18	ND
9	[1]PI736-55	NA	76	77	ND
	OI733-56	NA	NA	4.4	ND
	OI733-57	NA	NA	4	ND
	PR736-58	1	NA	63	ND
	PR736-59	7	NA	43	ND
	PR736-60	13	NA	34	ND
	PR736-61	34	NA	25	ND
	PR736-62	57	NA	19	ND

Appendix 6. Dissolved trihalomethane and methane concentrations measured in ground-water samples collected during aquifer storage recovery cycles 2, 4 through 11, and 13--Continued

[ASR, aquifer storage recovery; µg/L, micrograms per Liter; mg/L, milligrams per Liter; NA, not applicable; ND, below detection limit of 0.01 mg/L]

ASR cycle number	Sample number	Percent volume recovered	Percent volume injected	Trihalomethane, dissolved (µg/L)	Methane, dissolved (mg/L)
9	PR736-63	94	NA	4	ND
10	[2]OI733-65	NA	41	47	ND
	[1]PI736-66	NA	47	104	ND
	[4]OB733-67	NA	NA	19	ND
11	[2]OB733-68	NA	38	28	ND
	OB733-69	NA	44	52	ND
	PR736-71	3	NA	96	ND
	PR736-72	43	NA	34	ND
	PR736-73	48	NA	31	N D
	PR736-74	58	NA	25	ND
13d	OS733-77	NA	NA	32	ND
	OS733-78	NA	NA	22	ND
	OS733-79	NA	NA	22	ND
	OS733-80	NA	NA	22	ND
	OS733-81	NA	NA	18	ND

[1]Treated surface water.
[2]Observation well during injection.
[3]Observation well during storage.
[4]Observation well background.